Aus der Medizinischen Klinik und Poliklinik IV der Ludwig-Maximilians-Universität München
Direktor: Prof. Dr. med. Martin Reincke

Role of Atypical Chemokine Receptor 2 in Systemic Lupus Erythematosus and Lupus Nephritis

Dissertation
zum Erwerb des Doktorgrades der Humanmedizin
an der Medizinischen Fakultät der
Ludwig-Maximilians-Universität München

vorgelegt von

Wenkai Xia

aus Jiangyin, China

2023

Mit Genehmigung der Medizinischen Fakultät
der Ludwig-Maximilians-Universität München

Berichterstatter:	Prof. Dr. med. Volker Vielhauer
Mitberichterstatter:	Prof. Dr. Jürgen Bernhagen
	Prof. Dr. Andreas Schober
Dekan:	Prof. Dr. med. Thomas Gudermann
Tag der mündlichen Prüfung:	26.01.2023

Table of contents

Declaration

I hereby declare that all of the present work embodied in this thesis was carried out by me from 09/2018 until 05/2022 under the supervision of Prof. Dr. Volker Vielhauer, Nephrologisches Zentrum, Medizinische Klinik und Poliklinik IV, LMU Klinikum der Universität München. This work has not been submitted in part or full to any other university or institute for any degree or diploma.

Munich, 27.05.2022	Wenkai Xia
Place, date	Signature

Zusammenfassung

Der systemische Lupus erythematodes (SLE) ist eine komplexe Autoimmunerkrankung mit einem breiten Spektrum klinischer und immunologischer Manifestationen, von denen die Lupusnephritis eine der Hauptursachen für Morbidität und Mortalität darstellt. Es ist bekannt, dass Chemokine und Chemokinrezeptoren die Gewebeinfiltration aktivierter Leukozyten vermitteln und auch bei SLE und der Lupusnephritis zu Gewebeentzündung und Organschädigung beitragen. Der atypische Chemokinrezeptor 2 (ACKR2), früher als D6 oder CCBP2 bezeichnet, ist ein Mitglied der Unterfamilie atypischer Chemokinrezeptoren, die keine klassische Signaltransduktion und inflammatorische Zellaktivierung auslösen, sondern als Scavenger-Rezeptoren das Chemokinsystem modulieren, indem sie beispielsweise gebundene Chemokine internalisieren, ihrem intrazellulären Abbau zuführen und damit lokale Chemokinkonzentrationen verringern können.

Angesichts der bekannten Rolle von ACKR2 bei der Begrenzung von lokaler Entzündung in vivo und der vielfältigen Funktionen von ACKR2 bei Ausbildung angeborener und adaptiver Immunantworten wurden in der vorliegenden Arbeit ein möglicher entzündungsbegrenzender Effekt von ACKR2 und eine mögliche Beeinflussung der systemischen Autoimmunität im Verlauf von SLE und Lupusnephritis analysiert. Um funktionelle Effekte von ACKR2 beim SLE zu charakterisieren wurden die Auswirkungen einer Ackr2-Defizienz in C57BL/6 lpr (B6lpr) Mäusen untersucht, die ein etabliertes Mausmodell einer Lupus-artigen Autoimmunerkrankung darstellen. Hierfür wurden Ackr2-defiziente B6lpr-Mäuse (Ackr2-/-B6lpr) durch Kreuzen von Ackr2-defizienten C57BL/6- mit Fas-mutierten (lpr) C57BL/6-Mäusen erzeugt und ihr Phänotyp mit Wildtyp-B6lpr-Mäusen (WT-B6lpr) verglichen.

Nach entzündlicher Stimulation von Glomeruli und tubulointerstitiellem Gewebe, die aus Nieren von WT-B6lpr- und Ackr2-/-B6lpr-Mäusen isoliert wurden, zeigte sich eine vermehrte Produktion des proinfammatorischen Chemokins CLL2 durch Ackr2-defiziente tubulointerstitielle Zellen, nicht jedoch Glomeruli. Dies ist mit einem reduzierten Ackr2-vermittelten Abbau von Chemokinen in der tubulointerstitiellen Gewebefraktion vereinbar. Diese *in vitro*-Daten stehen im Einklang mit der bekannten Expression von ACKR2 in lymphatischen Endothelzellen, die im tubulointerstitiellen Kompartiment, nicht jedoch Glomeruli vorhanden sind und weisen gemeinsam mit einer induzierten Ackr2 mRNA-

Expression in WT-B6lpr-Mäusen auf einen potentiell entzündungsbegrenzenden Effekt von ACKR2 auch im Verlauf der Lupusnephritis hin.

In vivo zeigten Ackr2-/-B6lpr-Mäuse im Alter von 28 Wochen jedoch eine vergleichbare Nierenschädigung im Vergleich zu Wildtyp-B6lpr-Mäusen, wie durch ähnliche Albuminurie, Plasmakreatinin- und Blutharnstoffstickstoffwerte sowie renale mRNA-Expression der tubulären Schadensmarker NGAL und KIM-1 belegt. Entsprechend war die morphometrische Bewertung der Aktivitäts- und Chronizitätsindizes für die Lupusnephritis in beiden Genotypen identisch. Ackr2-/-B6lpr-Mäuse zeigten allerdings eine signifikant höhere renale Infiltration von CD3+ T-Zellen, nicht jedoch Granulozyten, Makrophagen und dendritische Zellen, wie durch Durchflusszytometrie und immunchemische Färbung nachgewiesen wurde. Weitere histologische Analysen ergaben in Übereinstimmung mit den vorangegangenen in vitro-Untersuchungen, dass T-Zellen vermehrt im tubulointerstitiellen Kompartiment von Ackr2-/-B6lpr-Mäusen akkumulierten, während die Leukozytenzahl in Glomeruli bei beiden Genotypen vergleichbar war. Darüber hinaus zeigte die histologische Analyse signifikant vermehrte peribronchiale Leukozyteninfitrate in Ackr2-/-B6lpr-Mäusen. Der Befund ging mit einer signifikant höheren pulmonalen CD3+ T-Zell-Infiltration in der immunhistologischen Auswertung einher.

Der CCL2-Proteingehalt in entzündeten Nieren und Lungen der Ackr2-/-B6 lpr-Mäuse war mit dem Wildtyp vergleichbar, während sich ein signifikant erhöhter CCL2-Plasmaspiegel in Ackr2-/-B6lpr-Mäusen zeigte. Hinsichtlich der systemischen Immunaktivität führte Ackr2-Defizienz zu einer verminderten Aktivierung dendritischer Zellen in Lymphknoten. CD4 T-Zellzahl und Aktivierung waren in Lymphknoten dagegen vergleichbar, in den Milzen jedoch gegenüber WT-B6lpr-Mäusen gesteigert. Die Produktion zirkulierender Lupus-Autoantikörper und das Ausmaß der glomerulären Immunglobulinablagerung wurden durch Ackr2- Defizienz nicht beeinflusst.

Zusammenfassend zeigen die Ergebnisse dieser Arbeit, dass im B6lpr-Mausmodell des SLE eine Ackr2-Defizienz das Ausmaß der systemischen Autoimmunaktivität nicht vermindert. Zudem scheint der *in vitro* nachgewiesene Effekt von Ackr2, in B6lpr-Nieren lokale Chemokinkonzentration begrenzen zu können, in geschädigten Nieren und Lungen der Ackr2-/-B6lpr-Mäuse *in vivo* durch andere Chemokin-abbauende Mechanismen kompensiert zu werden. Die erhöhten CCL2-Plasmaspiegel in Ackr2-/-B6 lpr-Mäusen könnten dagegen über verstärkte Leukozytenmobilisierung aus dem Knochenmark zu der nachgewiesenen

vermehrten tubulointerstitiellen und pulmonalen T-Zell-Infiltration und ihrer vermehrten Akkumulation in der Milz beitragen. Diese führt jedoch bei unbeeinflusster renaler und pulmonaler Entzündung nicht zu einer vermehrten Organschädigung. Während frühere experimentelle Daten darauf hinweisen, dass Ackr2 in der Regenerationsphase nach akuter Nierenschädigung durch Verminderung lokaler Chemokinkonzentrationen renale Entzündung begrenzen und damit die Entwicklung eines chronischen Nierenschadens verhindern kann, scheint diese protektive Effekt bei autoimmunologischer, chronisch anhaltender Gewebeschädigung wie bei der Lupusnephritis keine entscheidende Rolle zu spielen.

Summary

Systemic lupus erythematosus (SLE) is a complex autoimmune disease that presents with a broad spectrum of clinical and immunologic manifestations, of which lupus nephritis is the leading cause of morbidity and mortality. It is known that chemokines and chemokine receptors mediate infiltration of activated leukocytes into inflamed tissue and contribute to tissue inflammation and injury in SLE and lupus nephritis. The atypical chemokine receptor 2 (ACKR2, previously known as D6 or CCBP2) belongs to the subfamily of atypical chemokine receptors. These are non-signaling decoy receptors which do not induce intracellular signaling and cell activation, but modulate the chemokine system, e.g. by internalizing and degrading bound chemokines. This reduces local chemokine concentrations and may exert anti-inflammatory effects.

Given the known function of ACKR2 in limiting inflammation *in vivo* and its multiple roles of ACKR2 in innate and adaptive immune response, potential roles of ACKR2 in reducing inflammation and tissue injury in SLE and lupus nephritis were investigated, as well as effects on systemic autoimmune responses. To characterize functional roles of ACKR2 in SLE, genetic Ackr2 deficiency was introduced into C57BL/6lpr (B6lpr) mice, a well-established murine model of lupus-like autoimmune disease. After generating Ackr2-deficient B6lpr (Ackr2-/-B6lpr) mice by crossing Ackr2-deficient C57BL/6- with Fas-mutated (lpr) C57BL/6 mice their phenotype was compared to wildtype B6lpr (WT-B6lpr) littermates.

Inflammatory stimulation of glomeruli and tubulointerstitial tissue isolated from WT- and Ackr2-/-B6lpr mice lead to increased production of the pro-inflammatory chemokine CCL2 by Ackr2-deficient tubulointerstitial cells, but not glomeruli. These results are consistent with reduced Ackr2-dependent degradation of chemokines in the tubulointerstitial compartment. They correlate with the known expression of ACKR2 in lymphatic endothelial cells, which in kidneys are present in the tubulointerstitium, but not in glomeruli. Together with induced mRNA expression of Ackr2 in WT-B6lpr mice compared to healthy WT controls, these results suggested a potential anti-inflammatory effect of ACKR2 in lupus nephritis.

In vivo, Ackr2-/-B6lpr mice at 28 weeks of age showed similar renal functional parameters as compared with WT-B6lpr mice, as evidenced by similar albuminuria, plasma creatinine and blood urea nitrogen levels, as well as renal mRNA levels of the tubular damage markers NGAL and KIM-1. Consistently, morphometrical assessment of the activity and chronicity indexes for

lupus nephritis were comparable between the two genotypes. However, Ackr2-/-B6lpr mice revealed a significantly higher renal infiltration of CD3+ T cells, but not neutrophils, macrophages or dendritic cells as demonstrated by flow cytometry and immunochemistry staining. Consistent with the previous *in vitro* findings, immunohistochemistry further demonstrated that increased T cells predominantly accumulated in the tubulointerstitial compartment of Ackr2-/-B6lpr mice, whereas leukocyte numbers in glomeruli were comparable to wildtype. In addition, histology analysis showed significantly increased peribronchial lung infiltrates in Ackr2-/-B6lpr mice. This finding correlated with a significantly higher pulmonary CD3+ T cells infiltration as assessed by immunohistochemistry.

CCL2 protein content in inflamed kidneys and lungs of Ackr2-/-B6lpr mice was comparable to WT-B6lpr mice. However, Ackr2-deficient mice demonstrated increased plasma levels of CCL2. Analysis of systemic autoimmune responses revealed a reduction of activated dendritic cells in lymph nodes of Ackr2-deficient B6lpr mice. CD4+ T cell numbers and activation were comparable in lymphatic tissue of Ackr2-/- and WT-B6lpr mice, but increased in Ackr2-/-B6lpr spleens. In addition, Ackr2 deficiency did not affect levels of circulating lupus-associated antibodies and the extent of glomerular immunoglobulin deposition.

In summary, the results of this work demonstrate that Ackr2 deficiency does not significantly inhibit systemic autoimmune reactivity in the murine B6lpr model of SLE. Although *in vitro* tissue culture experiments revealed a capacity of Ackr2 to reduce local chemokine concentrations in the renal tubulointerstitial compartment, this did not translate into increased renal or pulmonary chemokine levels in Ackr2-deficient mice *in vivo*, suggesting compensatory mechanisms for local chemokine degradation in B6lpr mice with lupus nephritis and lung injury. On the other hand, higher CCL2 plasma levels in Ackr2-/-B6lpr mice may mediate increased tubulointerstitial, pulmonary, and spleen T cell infiltration through enhanced mobilization of leukocytes from the bone marrow. However, this did not exacerbate renal or pulmonary inflammation and parenchymal injury in the absence of enhanced local inflammation. Whereas previous reports clearly demonstrate a beneficial effect of ACKR2 in limiting renal inflammation and kidney disease after episodes of acute renal injury with subsequent regeneration, this protective effect is not present in chronic progressive renal damage due to ongoing autoimmune-mediated tissue injury like lupus nephritis.

1. Introduction

1.1. Systemic lupus erythematosus

1.1.1. Brief introduction to systemic lupus erythematosus

Systemic lupus erythematosus (SLE) is a multisystem autoimmune disease that affects 8-180 cases per 100,000 individuals. Its precise etiological mechanisms remain unclear [1]. It is characterized by the loss of T and B cell tolerance to self-antigens, resulting in the activation of both innate and adaptive immunity [2]. Aberrant autoantibody production, immune complex formation and complement activation result in a broad spectrum of clinical manifestations ranging from mild fever and fatigue to life-threatening organ damage. As in other autoimmune diseases, genetic predisposition, epigenetic, hormonal and environmental factors are known contributors to the pathogenesis of SLE [3,4] (Figure 1).

Innate immunity

The innate immune system comprises of a variety of immune cells, including mononuclear phagocytes like macrophages and dendritic cells (DCs), granulocytes and innate lymphoid cells that circulate in blood and provide protection against pathogens or other environmental challenges.

Although the underlying mechanisms of SLE are yet to be defined precisely, dysregulated DC homeostasis has been implicated in SLE. DCs contribute to disease development both as antigen presenting cells (APCs) and as the main source of type I interferon (IFN), suggesting it could be a potential therapeutic target in the treatment of SLE [5-7].

Dysregulation of macrophages has been recently identified as another key feature in SLE pathogenesis. It seems that impaired macrophages have reduced ability to clear apoptotic cell debris which results in persistent exposure of nuclear self-antigens to adaptive immune cells [8]. Moreover, abnormal M1/M2 macrophage polarization is also involved in adaptive immune activation and tissue damage during SLE [9,10].

Adaptive immunity

The function of autoreactive B cells and T cells are well-studied in SLE (Figure 2). Several studies have demonstrated that defective B cell tolerance for self-antigens will result in the generation and activation of autoreactive B cells, contributing to SLE [11,12]. In addition, B cell survival, proliferation and differentiation are also affected by altered signaling through B cell receptor, B cell activating factor receptor and toll-like receptors (TLRs) [13]. Similarly, T cell subsets are critically involved in regulating B cell responses and organ inflammation in SLE [14,15].

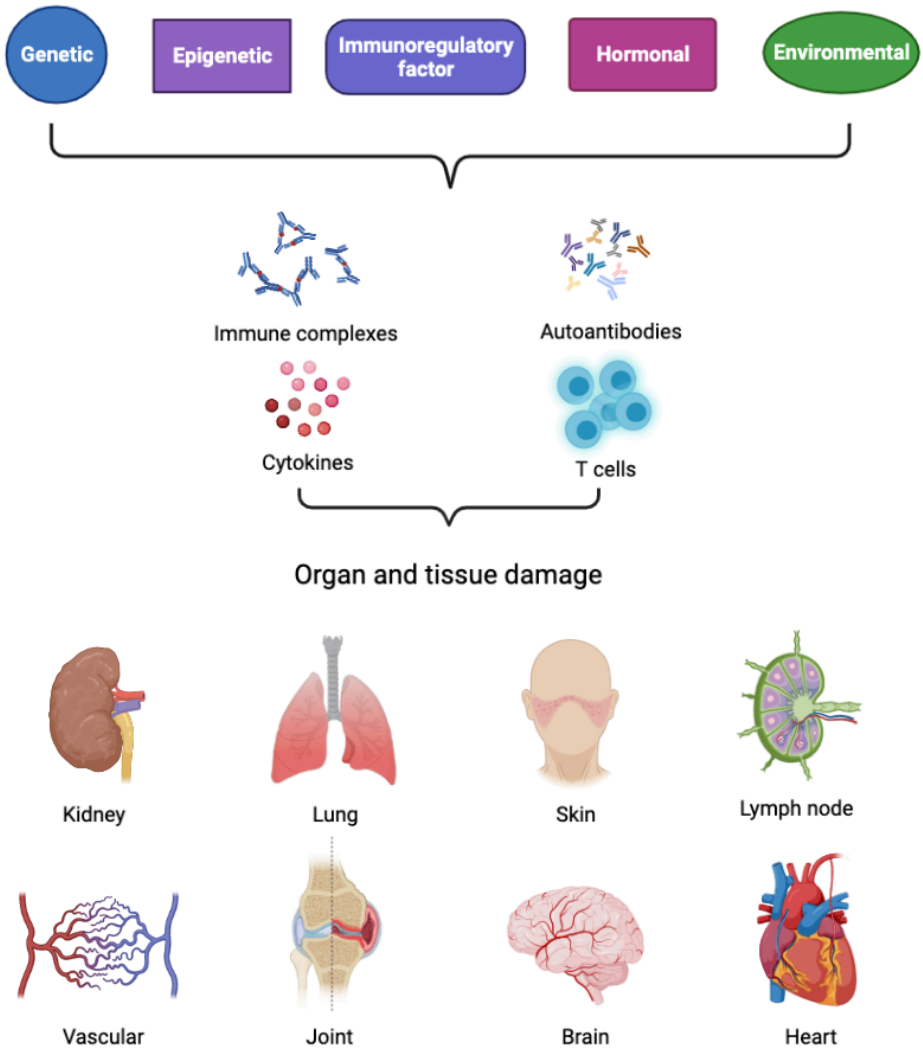

Figure 1: Overview of the pathogenesis of systemic lupus erythematosus. Genetic, epigenetic, hormonal, environmental and immunoregulatory factors have impact on the immune system either sequentially or simultaneously. These pathogenic factors promote the generation of autoantibodies, immune complexes, inflammatory cytokines and T cells, which all contribute and aggravate inflammation and thus result in various tissue and organ damage.

Various immune cells participate in the production of pathogenic autoantibodies. B cells are well-understood participants in SLE pathogenesis, via the differentiation into pathogenic B cells and plasma cells and subsequent generation of autoantibodies, but the role of T cells remains uncertain. Recent evidence in a mouse model and in humans demonstrate that B cells could not trigger SLE pathogenicity without the assistance of the helper T lymphocytes [16,17]. In patients with SLE, treatment with rituximab against CD20 resulted in a lack of significant clinical benefits [18,19]. Therefore, T cells may possess a key role in the development and progression of SLE and lupus nephritis.

Autoantibodies are central players in the development of lupus nephritis. They bind to the abundant nuclear and cellular antigens, leading to the formation of immune complexes and deposition of immune complexes in glomeruli [20]. Impaired clearance of immune complexes may be associated with genetic polymorphisms of Fc receptors and autoantibodies to C1q and C3b [21,22]. In addition to activating complement, intraglomerular immune complexes can initiate intrarenal inflammation and injury by engaging leukocyte Fc receptors [23]. Complement-mediated renal injury, especially activation of the alternative pathway, has been observed in human and murine lupus nephritis [24,25].

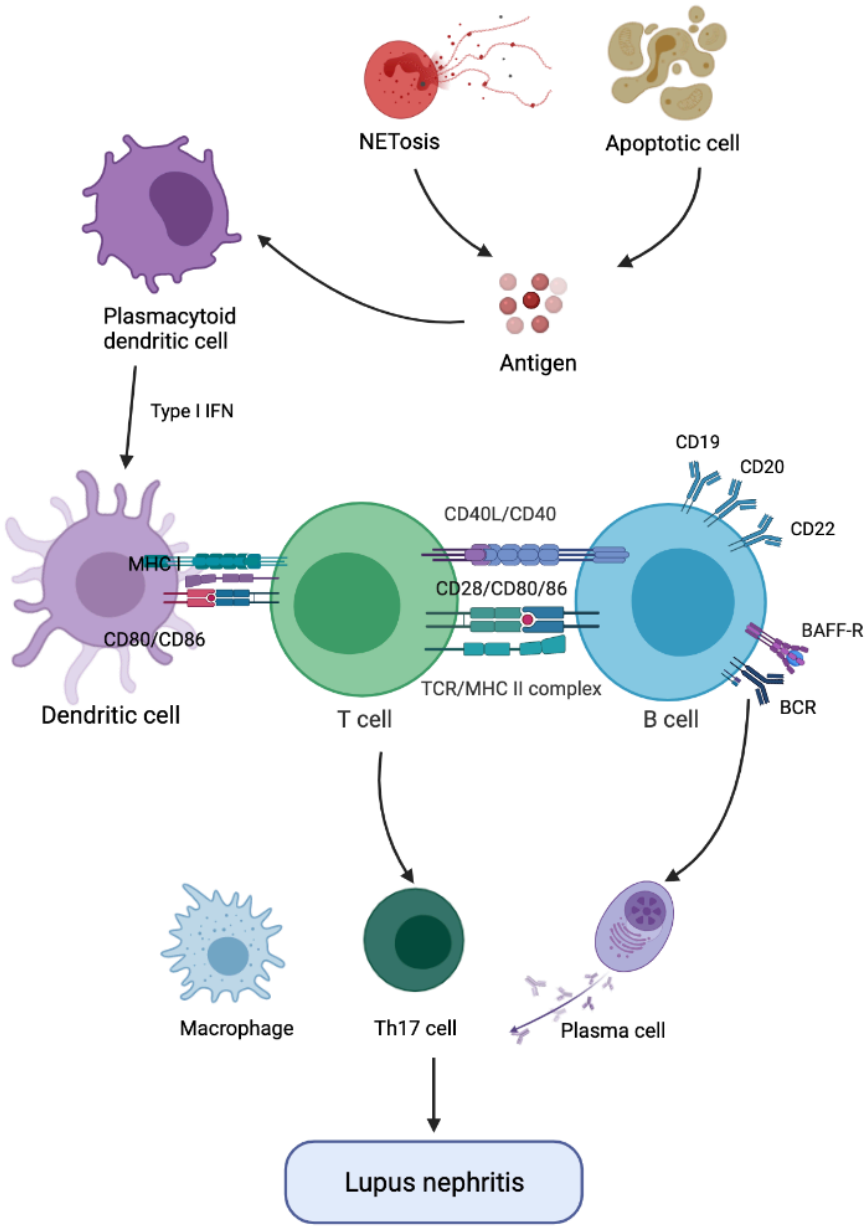

Figure 2: Cellular contributions to the development of lupus nephritis. Apoptotic cells and neutrophils form the apex of the pathogenetic cascade leading to systemic lupus erythematosus and lupus nephritis. They are involved in the generation of critical ligands to produce type I interferons (IFNs). Neutrophils are particularly prominent in mediating organ damage. They release neutrophil extracellular traps (NETs), a major source of nucleic acid antigens, through NETosis. A wide variety of cells produce type I IFNs, but mainly plasmacytoid dendritic cells produce the increased level of these inflammatory cytokines. Apoptotic debris can also promote inflammatory cytokine production, which is involved in the recruitment of immune cells into inflamed tissues. Mature dendritic cells can activate autoreactive T cells. B cells and T cells are both involved in autoreactivity, with B cell-derived plasma cells persistently producing antibodies and with T helper 17 cells driving the expression of IL-17 to induce kidney injury. BAFF-R, BAFF receptor; MHC, major histocompatibility complex; TLR, Toll-like receptor; NET, neutrophil extracellular trap.

1.1.2. Lupus nephritis

Lupus nephritis (LN) is an immune complex-mediated glomerulonephritis and remains one of the most common manifestations of SLE. In many cases, LN is typically discovered by the examination of urine and results in the diagnosis of SLE. Risk factors for patients with SLE to develop LN include male sex, younger age and white ethnicity. Kidney biopsy is currently used to establish the diagnosis of LN, and to correctly classify LN into six distinct classes which has therapeutic and prognostic implications (Table1). Although the role of the first kidney biopsy is well established, the role of a second biopsy within the disease course is still controversial. Previous studies have shown a striking discrepancy between clinical manifestations and histologic findings [26,27]. Thus, further research is needed to validate the utility of repeated biopsies for guiding personalized lupus treatment based on clinical and pathologic features and molecular biology. A recent study using single-cell RNA sequencing observed that gene expression profiles of immune cells in urine highly correlated with the gene signature of kidney immune cells, which could make it possible that invasive biopsy would be replaced by urine tests in the future [28]. Clearly, early and accurate diagnosis of LN is of vital importance for prompt initiation of treatment. LN is generally treated with anti-inflammatory and immunosuppressive drugs, such as corticosteroids, antimalarials, cyclophosphamide and mycophenolic acid derivates. However, despite increased treatment options, conventional treatments are not uniformly effective against LN, and up to 50% of patients may relapse [29,30]. Furthermore, at least 10% of patients with LN develop ESRD within decades from the initial event, and drug-induced toxicity is particularly concerning. Undoubtedly, recent therapeutic advances only achieved modest progress in improving outcomes in patients with LN, which highlights the urgent need for improved and optimized approaches to LN management.

Table 1: The 2003 International Society of Nephrology/Renal Pathology Society (ISN/NPS) classification of LN [31]

Classification category	Histology	Clinical features
I: minimal mesangial LN	Mesangial immune deposits by immunofluorescence, but normal glomeruli by light microscopy	Asymptomatic
II: mesangial proliferative LN	Purely mesangial hyper cellularity or mesangial matrix expansion	Microhematuria or non-nephrotic proteinuria
III: focal LN	Active or inactive focal, segmental, or global endocapillary or extracapillary glomerulonephritis involving < 50% of all glomeruli, typically with focal subendothelial immune deposits, with or without mesangial alterations	Hematuria, proteinuria, hypertension, nephritic syndrome
IV: diffuse LN	Active or inactive focal, segmental, or global endocapillary or extracapillary glomerulonephritis involving ≥50% of all glomeruli, typically with focal subendothelial immune deposits, with or without mesangial alterations	Most common and sever form of LN, nephritic syndrome, high dsDNA and low C3, especially in active disease
V: membranous LN	Global or segmental subepithelial immune deposits or their morphologic sequelae by light microscopy or immunofluorescence or electron microscope, with or without mesangial alternations	Nephritic syndrome with normal renal function, hypertension
VI: advanced sclerotic LN	≤90% of glomeruli globally sclerosed without residual activity	Progressive renal failure with proteinuria and normal urinary sediment

1.1.3. Mouse models of SLE and lupus nephritis

Animal models of human disease have long been employed in an effort to define pathogenic mechanisms as well as to test therapeutic agents. Several murine models were also established for SLE and LN.

In the last four decades, spontaneous or induced mouse models of lupus were developed. Classic models of spontaneous lupus include NZB/NZW F1 strains, the NZM strains, the BXSB/*Yaa* strains and the MRL/*lpr* mouse model of SLE. Induced mouse models include the chronic graft-versus-host disease (cGVHD) models and the pristane-induced lupus model (Table 2). As science and technology progressed, gene knockout techniques, transgenic techniques and humanized mouse models have been extensively used to investigate a specific gene or molecule in the pathogenesis of lupus. Most of these models present a subset of symptoms akin to those observed in human lupus, namely, autoantibody over-production, immune complexes formation, lymphoid activation, and lupus nephritis. However, none of current lupus model is fully representative of human lupus, both in clinical features, genetics and underlying mechanisms. Due to the fact that SLE is so heterogeneous in humans not one inbred mouse model can manifest the entire clinical spectrum of human lupus [32,33]. Despite their distinct limitations, mouse model of lupus contributed significantly to our understanding of the etiology of lupus and the development of new therapies for the disease.

Table 2: Overview over spontaneous and induced mouse models of lupus

Strain	Generation	Sex bias	Autoantibodies	Main clinical manifestation
NZB/NZW F1	New Zealand Black crossed with New Zealand White	Female	ANA, anti-dsDNA, rheumatoid factor, ubiquitin, gp70 anticardiolopin	Splenomegaly, lymphadenopathy, glomerulonephritis, vasculitis, synovitis and leukopenia
NZM 2410/2328	Backcross between NZB/NZW F1 and NZW followed by brother and sister mating	2410 Female; 2328 Both	Overlap with NZB/NZW F1	Splenomegaly, lymphadenopathy and glomerulonephritis
BXSB/Yaa	Backcross C57BL/6 female and SB/Le male	Male	ANA, anti-dsDNA, cryoglobulin, gp70	Splenomegaly, lymphadenopathy, glomerulonephritis and cerebritis
MRL/lpr	Intercrossing four different strains of mice (LG, B6, AKR and C3H)	Both	ANA, anti-dsDNA, anti-Sm, anti-Ro and anti-La	Splenomegaly, lymphadenopathy, glomerulonephritis, vasculitis, arthritis, skin rash and cognitive dysfunction
B6/lpr	lpr mutation in Fas gene on B6 background	Female	ANA, anti-dsDNA, anti-Sm, anti-histone, rheumatoid factor	Splenomegaly, lymphadenopathy and glomerulonephritis
Pristane induced	Intraperitoneally injection of pristane	Female	Anti-RNP, anti-dsDNA, anti-Sm, anti-histone	Glomerulonephritis; anemia, arthritis and serositis
Graft versus host disease (GVHD)	Injection of donor lymphocytes to a semiallogenic recipient	Female	Auto Ab	Immune complex nephritis, proteinuria
Resiquimod induced	Topical application to the ear	Female	Anti-dsDNA	Glomerulonephritis and dilated cardiomyopathy
Anti-GBM induced	Intravenous injection of anti-GBM serum	Both	-	Glomerulonephritis

1.2. Chemokines and chemokine receptors

Chemokines and their receptors are known to play a crucial role in orchestrating the movements of circulating leukocytes in response to physiological and pathological stimuli, resulting in innate and adaptive immune responses and contributing to the pathogenesis of many human diseases including SLE (Figure 3). Approximately 50 chemokines are classified into CC, CXC, CX3C and XC subfamilies based on the nature of a specific cysteine motif [28]. Chemokines guide cell migration by binding to their specific cell surface-expressed receptors which belong to the subfamily of class A G-protein-coupled receptors (GPCRs). Thus far, 10 CCR family members, 7 CXCR family members in addition to CX3CR1 and XCR1 chemokine receptors have been identified [34]. Pharmacological modulation of chemokine receptors has been of great interest, and considerable effort has been devoted to developing antagonists that modulate inflammation and immunity. However, subsequent research has clearly shown that the chemokine/chemokine receptor system is even more complex, with many receptors sharing overlapping ligand specificity, formation of receptor homo- and heterodimers and the description of "atypical" receptors with anti-inflammatory properties. Therefore, a much more comprehensive understanding of its function is required it to be precisely targeted in specific diseases.

1.2.1. The functional role of chemokines and chemokine receptors

Many studies thus far have noted that the biological activity of the chemokine network is by no means limited to cell migration, and leukocytes trafficking in particular (Figure 3). As reviewed elsewhere, a wide variety of cellular and tissue responses can be induced by the activation of chemokine receptors on leukocytes, including proliferation, differentiation, angiogenesis, degranulation, and tumor metastasis [35-37]. Moreover, several chemokines and chemokine receptors may have direct antimicrobial activities to reduce infection [38]. Additionally, a variety of non-leukocytic cell types, including epithelial cells, endothelial cells, neurons, and mesenchymal cells can express chemokine receptors and respond to a wide range to chemokines [39-42]. For example, many CXC chemokines are involved in angiogenesis with the ELR motif showing positive or negative angiogenic activity [43,44]. Interestingly, adipocytes express chemokine receptors and respond to chemokines. This can upregulate inflammatory genes and impair insulin-dependent uptake of glucose inducing insulin resistance. More recently, accumulating studies have identified chemokines and chemokine receptors as important mediators in the initiation or progression of cancer [45-48]. Tumor cells of non-

leukocytic origin infiltrate the tumor microenvironment and provide a secondary source of chemokines that affect tumor growth, angiogenesis, and metastasis [49,50]. Taken together, these innovative findings may provide a scientific rationale for the development of novel therapeutic strategies that target chemokines as well as their receptors in a broad variety of human diseases

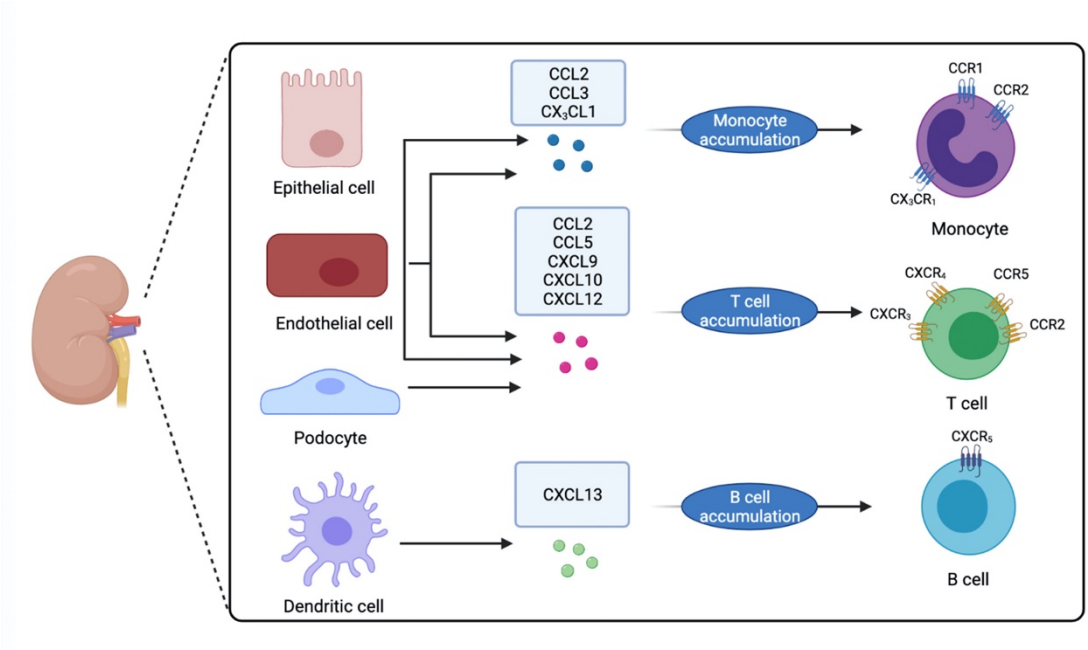

Figure 3: Involvement of chemokines and chemokine receptors in systemic lupus erythematosus. In patients with SLE, renal epithelial and endothelial cells release the chemokines CCL2, CCL3 and CX_3CL1 that facilitate monocyte recruitment through CCR1, CCR2 and CX3CR1, respectively. Renal epithelial, endothelial cells and podocytes also release inflammatory chemokines that promote T cell recruitment via CCR5, CXCR3 and CXCR4. Renal dendritic cells produce CXCL13 that promote B cell recruitment through CXCR5. CCL, CC chemokine ligand; CCR, CC chemokine receptor; CX_3CL, CX_3C chemokine ligand; CX_3CR, CX_3C chemokine receptor; CXCL, CXC chemokine ligand; CXCR, CXC chemokine receptor.

1.2.2 Chemokines and chemokine receptors as therapeutic targets in lupus nephritis

Chemokines and chemokine receptors have been recognized in the last few years as therapeutically targetable mediators of renal leukocytes recruitment and subsequent injury in LN. In MRL/lpr mice, treatment with a small molecule CCR1 antagonist reduced numbers of renal T cells and monocytes/macrophages. This was associated with a reduced amount of proliferating and apoptotic cells in renal infiltrates, less tubular atrophy, and augmented interstitial fibrosis [51]. However, CCR1 blocking did not change glomerular IgG deposits and

circulating anti-dsDNA IgG, suggesting a direct role of the CCR1 antagonist in preventing glomerular macrophages and T cells recruitment, but not systemic autoimmune activity. Furthermore, CCR1 antagonist administration was effective in improving LN in NZB/W F1 mice, as demonstrated by ameliorated glomerular pathology and reduced proteinuria [52].

In lupus-prone mice, expression of CCL2 and its receptor CCR2 was found to be upregulated in the kidney during progressive LN. Using CCL2 deficient mice, studies have shown that CCL2 mostly mediates glomerular infiltration of macrophages and not T cells, and CCL deficiency lead to less proteinuria and reduced glomerular injury, i.e. glomerulosclerosis, hypercellularity, and crescent formation [53,54]. Moreover, CCL2 deficiency resulted in a substantial reduction in interstitial infiltration of both macrophages and T cells. This was associated with less tubulointerstitial injury including tubular atrophy and apoptosis [53,55]. In addition, a non-redundant role for CCR2 in LN was demonstrated in CCR2-deficient MRL/lpr mice [56]. CCR2-deficient animals developed less lymphadenopathy, a reduced systemic T cell response, and reduced lesion scores associated with less renal infiltration of T cells and macrophages. Together, these results suggest a direct function of the CCL2/CCR2 axis in mediating LN development. As interference with CCL2/CCR2 network had the most beneficial effects in terms of injury and inflammation in several renal disease models [57-59], blocking the activity of CCL2/CCR2 in lupus-prone mice was examined as a promising potential therapeutic approach. Similar to CCL2/CCR2 knockout MRL/lpr mice, CCL2 and CCR2 antagonist experiments resulted in a survival benefit with reduced LN in treated mice. This was associated with reduced recruitment of T cells and macrophages into the glomerular and tubulointerstitial compartments [56,60-63].

The critical role of CXCL12 and CXCR4+ cells in the pathogenesis of LN was also investigated by studies with anti-CXCL12 neutralizing antibodies in NZB/W F1 mice and CXCR4 antagonists in B6, SleYaa lupus-prone mice [64,65]. Renal pathology, including proteinuria, deposition of immune complex, and renal inflammation was significantly reduced in the treated mice compared to controls. Systemic autoimmune responses such as the level of circulating autoantibodies and activated T cells in the spleen and lymph nodes were reduced as well, suggesting the involvement of CXCL12/CXCR4 in the development of LN both locally in the kidneys and systemically in lymphoid tissues of lupus-prone mice.

The advent of lupus-prone mice allowed researchers to perform mechanistic studies to better understand LN pathogenesis. A common concern and criticism of mechanistic studies done in mice is that mice and human immune systems differ in a variety of areas and thus make it

difficult to translate mechanistic insights gained from mouse studies to clinical trials [66]. Therefore, it is necessary to understand the similarities and differences between lupus-prone murine models and SLE patients in the functional contribution of chemokines and chemokine receptors to disease pathology. For example, CXCL9 is preferentially used in lupus-prone mice whereas CXCL10 appears to be predominately expressed in the kidney of SLE patients [67,68].

Several commercially developed chemokine receptor antagonists were reported to fail in clinical trials and did not reach their expectations in treating lupus [69-71]. SLE targets the joints, hearts, kidneys, skin, and many other organs. It is difficult to identify tissue-specific chemokines or chemokine receptors critical for the development of lupus. Systemically blocking a chemokine or chemokine receptor may cause a variety of negative side effects other than disease remission, such as the increased risk of cancer and infection [71]. However, targeting chemokines or chemokine receptors may still be a promising therapeutic option in treating lupus. Further studies are warranted to investigate the complicated chemokine and chemokine receptor system, with new compounds and therapeutic interventions designed to target chemokine and chemokine interactions more specifically. This has the potential to reduce off-target effects and adverse reactions previously observed for monoclonal antibodies and immunosuppressive drugs.

1.2.3 Atypical chemokine receptors

Atypical chemokine receptors (ACKRs) are a group of structural decoy chemokine receptors involved in a variety of physiologic and pathologic contexts. The ACKR family currently consists of four members, AKCR1 (DARC), ACKR2 (D6), ACKR3 (CXCR7) and ACKR4 (CCRL1). These receptors are mainly expressed by immune cells, vascular and lymphatic endothelial cells and some tumor cells. Following the discovery of four ACKRs, two other candidate ACKRs, ACKR5 (CCRL2) and ACKR6 (PITPNM3) have been identified to date and await functional confirmation [72,73]. ACKRs were found to bind to chemokines with high affinity, but do not induce cell migration because of their structural inability to couple to G proteins. This characteristic is in contrast to canonical chemokine receptors, which have the canonical G protein-activating DRYLAIV motif. Below, biology of four ACKRs will be reviewed.

ACKR1

ACKR1, also known as the Duffy antigen receptor for chemokines (DARC), was discovered in the 1990s. It binds more than 20 CC and CXC inflammatory chemokines [74]. From the structural perspective, it lacks the entire DRYLAIV consensus motif in the second intracellular loop and has no more than 25% homology with G protein-coupled receptors (GPCRs) [75]. ACKR1 is expressed on erythrocytes, postcapillary venular endothelial cells and kidney epithelial cells [76]. After binding and internalization of chemokines, it not only scavenges chemokines, but can function as an intracellular chemokine transporter and translocate bound chemokines to specific cell surface areas of polarized cells for presentation to leucocytes.

Accumulating evidence demonstrated that ACKR1 expressed by erythrocytes negatively regulates the bioavailability of circulating chemokines. It was reported that individuals lacking ACKR1 expression on erythrocytes were characterized by a higher concentration of circulating chemokines in the blood. In contrast, ACKR1 expressed by endothelial cells modulates chemokine internalization and transcytosis, thereby promoting the presentation of chemokines to the luminal surface of vascular endothelial cells and mediating pro-inflammatory functions.

Indeed, ACKR1 was found to be upregulated in various models of inflammatory conditions. Reduced neutrophil recruitment was found in Ackr1 knockout (KO) mice in a model of acute lung injury induced by acid and was associated with lung protection [77]. ACKR1 also controls inflammatory responses in models of acute kidney injury (AKI) induced by ischemia or lipopolysaccharide (LPS) [78]. After bone fracture, Ackr1 KO mice exhibited reduced macrophage infiltration and pro-inflammatory cytokine expression, promoting cartilage formation [79]. ACKR1 was expressed by the aorta and was associated with a pro-inflammatory phenotype that induced excessive production of chemokines (CCL2 and CXCL1) and increased atherosclerotic lesion size [80]. Additionally, it was found that ACKR1 expression on endothelial cells was essential for neutrophil recruitment to the inflamed synovium in rheumatoid arthritis [82]. More recently, it appeared that ACKR1 could functions as a tumor suppressor in several models, for example by scavenging angiogenic chemokines and inhibiting tumor vascularization [83-86].

ACKR3

ACKR3, originally known as receptor dog cDNA 1 (RDC 1) or CXCR7, was first described as an orphan GPCR that binds CXCL12 and CXCL11 [87]. In contrast to other chemokine receptors that are characterized by having the canonical DRYLAIV motif, it contains the sequence DYRLSIT and interacts with CXCL12 monomers in extracellular loops two and three using a unique N-terminal binding site [88,89]. ACKR3 acts as a scavenger receptor that promotes CXCL12 internalization, but also causes activation of the β-arrestin pathway in tumor cells, and modulates CXCR4 expression by forming heterodimers with CXCR4 [90,91].

ACKR3 continuously recycles between the cell membrane and the endosomal compartment, which likely depends on the presence of ligands. Ligands act as agonists for ACKR3 internalization which concurs with degradation of CXCL12 and CXCL11, thus supporting a role for ACKR3 as a scavenging receptor [92]. Previous studies using zebrafish models have also demonstrated the importance of ACKR3 in regulating cellular populations during embryogenesis [93]. Data from Ackr3-deficient mice correlated with those observed in Cxcr4 KO mice, showing defects in cardiovascular and nervous system development, but not hematopoiesis [94,95].

ACKR3 has proven to be an important receptor in a variety of pathophysiological conditions. In relation to endothelial cells, ACKR3 is expressed in umbilical veins and aorta. Loss of endothelial Ackr3 impaired vascular homeostasis and cardiac remodeling after myocardial infarction, suggesting an important role of ACKR3 in promoting endothelial proliferation and angiogenesis [96]. Additionally, ACKR3 is induced in pulmonary epithelial cells during pulmonary inflammation, such as acute lung injury induced by lipopolysaccharide inhalation, and it favors the circadian oscillations of CXCL12 via its scavenging activity [97]. Evidence for a function of ACKR3 in neuronal migration has come from rodent studies that confirmed its role in neuronal and astrocyte development during neurological diseases [98,99]. It should be noted that ACKR3 is also expressed by renal vesicles and podocytes, and it is upregulated by renal progenitors during acute kidney injury, which are important cells for renal regeneration [100]. Furthermore, a pivotal role for ACKR3 in the development and progression of cancers has emerged [101-103]. It has therefore been highlighted as a potential target for therapeutic intervention.

Similarly to CXCR4, ACKR3 has been identified as a relevant factor in several autoimmune diseases, including inflammatory bowel disease [98], rheumatoid arthritis [104] and

experimental autoimmune encephalitis (EAE) [105]. In these contexts, ACKR3 is associated with a pro-inflammatory phenotype by enhancing angiogenesis and leukocyte extravasation.

ACKR4

ACKR4, previously known as CCX-CXR, CCRL1 or CCR11, is expressed on thymic endothelial cells and keratinocytes as well as on lymphatic endothelial cells, astrocytes and bronchial cells. Of note, the DRY-based motif in human ACKR4 is altered to DRYVAVT sequence. ACKR4 has emerged as an important regulator of homeostatic chemokines. It was found to bind the novel chemokine ligand CCL22 in addition to CCL19, CCL21, CCL25 and CXCL13, and regulated their bioavailability both *in vitro* and *in vivo* without initiating cell migration [106-109].

By controlling chemokine bioavailability, ACKR4 was shown to regulate DC migration into lymphatics and T cells areas of lymph nodes. ACKR4 is best known for its role in maintaining functional gradients of CCL19 and CCL21 to drive migration of CCR7 expressing DCs to the subcapsular sinus of draining lymph nodes during the initiation phase of the adaptive immune response [109,110]. In addition, a role of ACKR4 in regulating early activated B cell differentiation has been proposed. It was shown that ACKR2 reduces early proliferation of B cells, and by this reduces their numbers for subsequent differentiation. Consistently, Ackr4 KO mice demonstrated enhanced plasma blast and germinal center B cell responses in a CCL19- and CCL21-dependent manner [111]. Studies on ACKR4 in tumor progression are still controversial. Emerging evidence suggested its protective role in several cancer models [112,113], but it was also involved in epithelial-mesenchymal transition and metastasis [114,115]. Furthermore, studies with Ackr4-deficient mice in an EAE model demonstrated that defects in homeostatic chemokine clearance can lead to accelerated disease onset, which may be attributed to excessive Th17 responses [116].

1.3. The atypical chemokine receptor 2

1.3.1 Pathophysiology

ACKR2 is composed of an N-terminal domain that contains several acidic amino acids and sulfated moieties, which are important for ligand recognition [117,118]. Similar to other members of the ACKR family, ACKR2 was found to bind to chemokines with high affinity but does not induce cell migration because of its structural inability to couple to G proteins. This characteristic is in contrast to canonical chemokine receptors such as CCR1, CCR2, and CXCR4, which have the canonical DRYLAIV motif.

ACKR2 has been described as being expressed on parenchymal cells and leukocyte populations, including trophoblasts in the placenta [119], innate-like B cells [120], T cells [121], DCs [122] and alveolar macrophages [123]. Further analysis has demonstrated that ACKR2 is mainly expressed by lymphatic endothelial cells in resting tissues [124]. However, not all lymphatic vessels express ACKR2, suggesting that ACKR2 is regulated by lymphatic endothelial cells, but the mechanism of this regulation is not fully understood.

Although an interaction between ACKR2 and CCL2 is involved in the majority of described inflammatory disorders, this interaction is not exclusive. ACKR2 has been shown to interact with multiple additional chemokines, such as CCL4, CCL5, CCL7, CCL8, CCL11 and CCL12. After ligand binding, ACKR2 can activate a β-arrestin-dependent pathway that increases its plasma membrane localization to optimize receptor internalization and recycling to the cell membrane following endosomal degradation of bound chemokines [125,126] (Figure 4). ACKR2 promotes the resolution of inflammation by scavenging almost all inflammatory CC chemokines, and Ackr2-deficient mice exhibit exaggerated inflammation due to a lack of chemokine clearance and increased accumulation of immune cells [127].

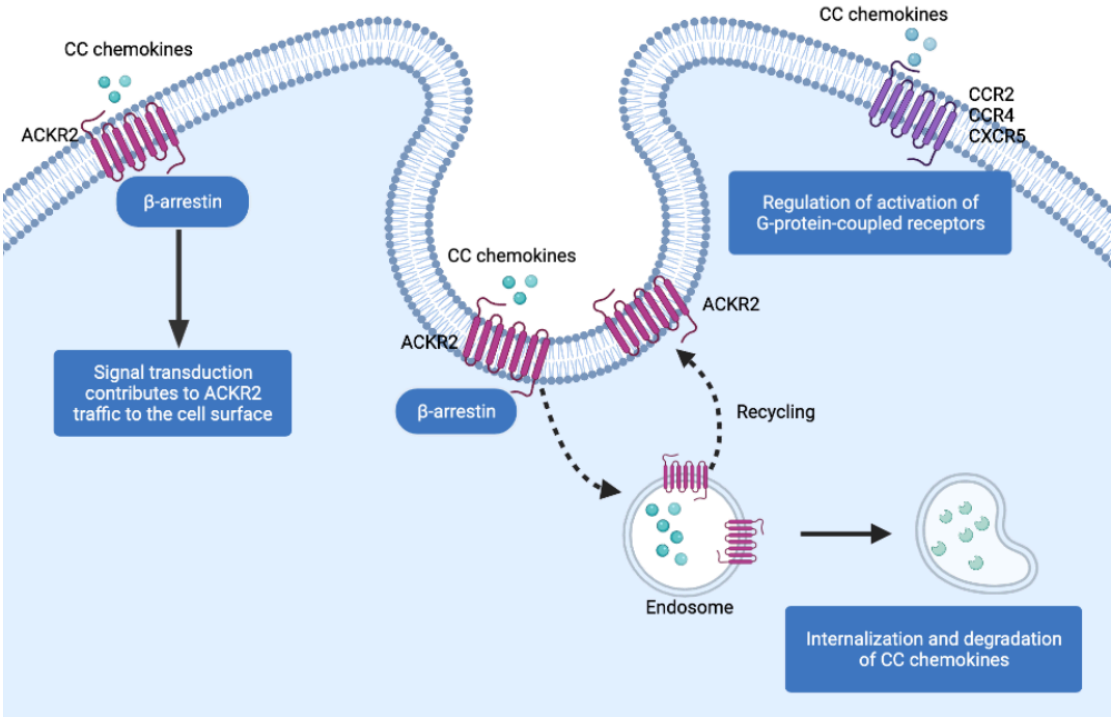

Figure 4: Cellular functions of ACKR2. Atypical chemokine receptor 2 (ACKR2) persistently traffics from and to the cell surface and signaling induced by chemokines via ACKR2 can stimulate its trafficking. ACKR2 regulates the internalization and degradation of chemokines which are captured on the cell surface, followed by ACKR2 recycling to the cell surface. ACKR2 constitutively modulates β-arrestin and activation of co-expressed conventional chemokine receptors, including CCR1, CCR4 and CXCR5. CCR, CC chemokine receptor; CXCR, CXC chemokine receptor.

A role of ACKR2 in the context of autoimmune disease is also debated. Ackr2-deficient mice were shown to be resistant to EAE [128] and have enhanced immunosuppressive activity in a model of graft-versus-host disease [129]. This protection was explained by impaired DC migration from the chemokine-rich site of immunization leading to reduced T cell priming and/or increased mobilization of myeloid-derived suppressor cells. Importantly, using four models of autoimmune disease, Hansel et al. subsequently showed that Ackr2 deficiency may not affect T cell priming but enhances T cell polarization towards a Th17 phenotype [130].

Finally, ACKR2 could function as a tumor suppressor gene by reducing local concentrations of inflammatory chemokines and subsequent leukocyte infiltration into precancerous

inflammatory lesions, which has been shown using inflammation-dependent cancer models of colon [131] and breast cancer [132]. Of note, Ackr2 deletion was found to result in profoundly impaired metastatic development in spontaneous models of metastasis, indicating that the ACKR2 expression by the host can affect tumor progression and metastasis [133].

1.3.2 Role of Ackr2 in kidney disease

ACKR2 in acute kidney injury

Acute kidney injury (AKI) induced by ischemia reperfusion injury (IRI) results in tubular cell apoptosis and necrosis, accompanied by an influx of inflammatory and fibrogenic cells into the renal interstitium [134,135], which underlies the progression from AKI to chronic kidney disease (CKD). Moritz et al. [136] investigated the potential of ACKR2 as a therapeutic target in an IRI rodent model, which is also used to study renal fibrosis in mice. Compared to sham-operated mice, renal ACKR2 levels were significantly increased after IRI and were localized to lymphatic endothelial cells in the tubulointerstitium but not to glomeruli. At 24 h after bilateral IRI, a lack of Ackr2 had no obvious effects on renal function or structural parameters, but enhanced the accumulation of CD11c+F4/80+ mononuclear phagocytes in ischemic kidneys. *In vivo* evidence demonstrated that increased renal CCL2 levels in Ackr2-deficient mice were associated with worsened tubular damage and infiltration of CCR2-expressing macrophages in postischemic kidneys on day 5, but these effects were more prominent on week 5 after IRI, suggesting that increased tubulointerstitial CCL2 levels may enhance CCL2-CCR2-dependent recruitment of inflammatory monocytes during the recovery and regeneration phase after IRI.

The progression from AKI to CKD is characterized by interstitial fibrosis. Whether impaired renal chemokine clearance could exacerbate renal fibrosis in Ackr2-deficient mice 5 weeks after IR was further investigated. Ackr2 deficiency enhanced fibrosis in postischemic kidneys, as revealed by increased levels of pro-inflammatory chemokines and CCR2-expressing fibroblasts in these kidneys when compared to wildtype. Thus, in addition to limiting ongoing inflammation, ACKR2 may directly reduce fibrotic tissue remodeling after renal IRI by limiting CCL2-dependent fibrocyte recruitment into postischemic kidneys.

ACKR2 in immune complex-mediated glomerulonephritis

Increased production of CCL2 critically contributes to immune complex-mediated glomerulonephritis and has been shown to correlate with excessive renal infiltration of monocytes/macrophages and T cells [137,138]. Similarly, in renal biopsies of patients with proliferative glomerulonephritis increased expression of CCL2 and macrophage infiltration have been detected [139].

Bideak et al. [140] investigated the function of ACKR2 in murine autologous nephrotoxic nephritis, which is a well-established model of a T cell-dependent progressive immune complex glomerulonephritis. ACKR2 was prominently expressed in lymphatic endothelial cells in the tubulointerstitial area. The researchers found that ACKR2 was critical in limiting tubulointerstitial accumulation of $CD4^+$ T cells and macrophages, which are important mediators of kidney injury, mainly by degrading the chemokine CCL2. Notably, a lack of Ackr2 accelerated fibrotic remodeling in mice with autologous NTN, as revealed by significantly increased expression of matrix components and prominent tubulointerstitial accumulation of α-SMA^+ myofibroblasts in Ackr2-deficient mice. Interestingly, Ackr2 deletion resulted not only in exacerbated renal inflammation due to increases in local chemokine levels, but also reduced accumulation of activated renal DCs in draining lymph nodes and subsequent T cell activation. This could potentially dampen nephritogenic T cell responses, but did not result in reduced inflammatory renal injury in Ackr2-deficient kidneys. Thus, ACKR2 limits renal inflammation during progressive immune complex-mediated glomerulonephritis and prevents secondary tubulointerstitial fibrosis, a hallmark of CKD progression. Therefore, ACKR2 is expected to be a potential therapeutic target for immune complex-mediated glomerulonephritis.

ACKR2 in aristolochic acid-induced nephropathy

Previous studies have reported that the acute phase of aristolochic acid-induced nephropathy (AAN) is followed by persistent tubulointerstitial inflammation, which results in fibrosis and development of CKD [149,150]. A similar study demonstrated that progressive peritubular accumulation of macrophages and T cells facilitated the transition of the tubular necrosis phase to the tubulointerstitial fibrosis phase [151].

In this model recent evidence has shown significantly exacerbated impairments in renal function and tubular injury in Ackr2-deficient mice, which were associated with excessive tubulointerstitial leukocyte infiltration and increased renal expression of inflammatory mediators. More importantly, it was demonstrated that ACKR2 decreased renal expression of extracellular matrix molecules and prevented fibrotic remodeling and CKD progression in this AAN model. This data together with the previous findings in the immune complex-mediated glomerulonephritis model suggest a common role of ACKR2 in limiting persistent inflammation and fibrotic remodeling following acute injury [136].

ACKR2 in unilateral ureteral obstruction

Unilateral ureteral obstruction (UUO) is a classic rodent model of obstructive nephropathy associated with progressive tubulointerstitial fibrosis. Prominent tubulointerstitial accumulation of CCL2 and the concomitant recruitment of $CCR2^+$ leukocytes and fibrocytes also occur during progressive renal injury in UUO after complete ureter ligation [152,153]. Thus, it was hypothesized that ACKR2 could also play a key role in reducing fibrotic remodeling in the UUO model due to its CCL2 scavenging activity, given its localization in the tubulointerstitial compartment [136,140]. However, a subsequent experiment demonstrated that Ackr2 deletion did not affect tubular injury, inflammation, or progressive fibrosis in the UUO model, despite elevated renal CCL2 levels and increased numbers of inflammatory monocytes in Ackr2-deficient mice at day 14 after UUO [136]. Possible underlying mechanisms could be the persistent and progressive injury in this non-reversible UUO model. The absence of a regenerative repair phase following an acute episode of initial injury may limit the potential of ACKR2 to reduce ongoing inflammation and facilitate regeneration.

ACKR2 in diabetic nephropathy

Diabetic nephropathy (DN) is a leading cause of CKD worldwide. Elevated expression of pro-inflammatory chemokines and increased infiltration of inflammatory leukocytes contribute to the development and progression of DN [141,142]. Previous studies have shown that inhibiting renal inflammation by scavenging chemokines or blocking chemokine receptors can reduce renal damage in DN [143,144].

By binding and internalizing chemokines ACKR2 is implicated in limiting inflammation in the pathogenesis of common metabolic disorders, such as obesity [145] and diabetes [146]. In contrast, it was recently demonstrated in a mouse model of DN that Ackr2 deletion reduced diabetic albuminuria and suppressed the development of DN [147]. Mechanisms to explain this renoprotective effect of Ackr2 deletion in the context of DN are unclear. In renal biopsies of patients with DN, expression of ACKR2 in tubules and interstitial cells dramatically increased, while ACKR2 staining was absent in glomeruli, suggesting that the direct effects of ACKR2 should be limited to the tubular and interstitial compartments in DN [147].

Unexpected protection induced by Ackr2 deletion was also observed in several other disease models, including dextran sulfate-induced colitis [121], allergen-induced airway disease [148], and spinal cord inflammation [128]. Therefore, considering ACKR2 only as an anti-inflammatory scavenger was overly simplistic. Chemokine scavenging properties of ACKR2 may not only alter the function of pro-inflammatory leukocytes but could also limit anti-inflammatory activity of certain leukocyte subsets leading to complex functional roles of ACKR2 depending on the pathological condition.

ACKR2 in sepsis

Sepsis is a life-threatening organ dysfunction due to a dysregulated host response to infection. Early data from experimental models indicated a central role for chemokines in recruiting neutrophils to vital organs, leading to multiple organ failure including AKI [154,155]. Previous studies have shown that ACKR2 is directly involved in the resolution of inflammation by removing and degrading inflammatory CC chemokines [156,157]. Increased renal expression of CCL2 was detected in the kidney in a sepsis model of cecal ligation and puncture (CLP) [158]. Although neutrophil migration to the peritoneal cavity and bacterial load were comparable between wildtype and Ackr2-deficient mice, increased renal chemokine levels, neutrophil infiltration and exacerbated kidney functional impairment was observed in Ackr2-deficient mice, thus raising the possibility that ACKR2 could be a promising target in sepsis.

Table 3: Phenotype summary of ACKR2 knockout mice in different kidney disease models

Disease model	Time points	Inflammation	Fibrosis	Cell infiltrates	Histology	Renal function
IRI	bilateral 24h	←	←	Leukocytes ← Neutrophils ← CD11c+F4/80+ ↑ T cells ←	←	←
	unilateral 5d	worse	←	Leukocytes ↑ CD11c+F4/80+ ↑ CD11c+F4/80- ← T cells ←	←	worse
	unilateral 5w	worse	worse	Leukocytes ↑ CD11c+F4/80+ ↑ CD11c+F4/80- ← T cells ↑	worse	worse
NTN	14d	worse	worse	Leukocytes ↑ CD3 T cells ↑ CD4 T cells ↑ CD11c+ ↑ F4/80+ ↑ CD8 T cells ←	worse	worse
AAN	14d	worse	worse	CD3 T cells ↑ F4/80+ ↑	worse	worse
UUO	7d and 14d	←	←	Leukocytes ← CD11b Ly6C^{high} ← CD3 T cells ↑ CD11c+F4/80- ↑	←	←
DN	2,4,6 months	better	better	Leukocytes ↓ CD3 T cells ↓	not examined	better
Sepsis	1d	worse	not examined	Neutrophils ↑	not examined	worse

IRI, ischemic reperfusion injury; NTN, nephrotoxic serum nephritis; AAN, aristolochic acid nephropathy; UUO, unilateral ureteral obstruction; DN, diabetic nephropathy.

Challenges for the development of ACKR2 targeting therapies in kidney diseases

ACKR2 was first described in 1997 as a chemokine receptor, and since then a number of studies characterized its physiological and pathological roles. Emerging evidence has demonstrated its diverse functions in various rodent organs, tissues and cells. This project focuses on the role of ACKR2 in kidney disease and its role in protecting against inflammation and renal fibrosis. As Ackr2 deficiency has been implicated in the progression and severity of CKD-associated tubulointerstitial inflammation and fibrosis, ACKR2 is expected to be a pivotal therapeutic target in this setting. While the conventional pharmaceutical approach would be to develop chemokine receptor antagonists, in the case of atypical receptors, small molecule inducers of ACKR expression or activity would be helpful. Such inducers might affect intracellular pathways that enhance or stabilize ACKR expression or capitalize on our increasing knowledge on the mechanism of cell surface mobilization of these receptors.

Notably, the expression of ACKR2 specifically in the tubulointerstitial compartment was associated with its renoprotective role in various models of kidney diseases. Further in-depth studies are warranted to examine whether ACKR2 will exhibit similar beneficial effects in renal disease with different underlying inflammatory mechanisms and chronicity. Thus, the role of ACKR2 in other glomerular or tubular diseases and the involved pathways need to be further investigated.

2. Hypothesis

The knowledge and data summarized so far suggest that

ACKR2 could preserve renal function by limiting renal inflammation and fibrosis following acute episodes of renal injury

In particular, previous work showed that Ackr2 deficiency resulted in aggravated renal inflammation and fibrosis in immune complex-mediated glomerulonephritis. In this context, the structural and functional changes were attributed to increased tubulointerstitial chemokine levels, leukocyte infiltration and fibrosis. Thus, it was hypothesized that in a mouse model of LN, an autoimmune-mediated immune complex glomerulonephritis, ACKR2 could also limit renal inflammation and fibrotic remodeling in a similar manner.

Of note, results in the autologous nephrotoxic nephritis mouse model also suggested that next to anti-inflammatory and anti-fibrotic functions of ACKR2 in glomerulonephritis, ACKR2 may support migration of renal DCs into regional lymph nodes and subsequent activation of nephritogenic T cells. Thus, ACKR2 may also facilitate systemic autoimmune responses in SLE, despite its anti-inflammatory local effects in the kidney.

Therefore, the underlying hypotheses to be investigated in this work were as follows:

1. Deficiency of Ackr2 in lupus-prone B6/lpr mice may increase inflammatory organ injury due to reduced chemokine scavenging, including lupus nephritis.

2. Deficiency of Ackr2 may alter systemic autoimmune responses in lupus-prone mice, potentially reducing cellular und humoral autoimmune activity and subsequent tissue injury.

To address these questions Ackr2-deficent B6/lpr mice were generated and their spontaneous phenotype was characterized in comparison to wildtype B6/lpr littermates. This included analysis of kidney and lung injury, as well as systemic autoimmune activity in the two genotypes.

3. Materials

3.1 Mouse strains

C57BL/6J Wild type	Charles River Laboratories, Sulzfeld, Germany
C57BL/6J Ackr2-/-	Provided by Dr. Massimo Locati, Humanitas Clinical and Research Center, Rozzano, Italy
C57BL/6lpr/lpr	Charles River Sulzfeld, Germany

3.2 Equipment

Balance

Analytic Balance, BP 110 S	Sartorius, Göttingen, Germany
Mettler PJ 3000	Mettler-Toledo, Greifensee, Switzerland

Cell Incubators

Type B5060 EC-CO2	Heraeus Sepatech, Munich, Germany

Centrifuges

Heraeus, Minifuge T	VWR International, Darmstadt, Germany
Heraeus Biofuge primo	Kendro Laboratory Products GmbH, Hanau, Germany
Heraeus Sepatech Biofuge A	Heraeus Sepatech, Munich, Germany

ELISA-Reader

Tecan, GENios Plus	Tecan, Crailsheim, Germany

ELISA washer

Microplate-Washer ELx50	Biotek, Bad Friedrichshall, Germany

Homogenizer

Ultra Turra T25 basic	IKA GmbH, Staufen, Germany

Real-time-PCR

LightCycler480	Roche Diagnostics, Mannheim, Germany

Spectrophotometer

Beckman DU® 530	Beckman Coulter, Fullerton, CA, USA
Nanodrop 1000	Thermo Fisher Scientific, Wilmington, DE, USA

TaqMan Sequence Detection System

ABI prism ™ 7700 sequence detector	PE Biosystems, Weiterstadt, Germany

Flow cytometer

FACSCanto II	BD Biosciences, Heidelberg, Germany

Other equipment

Cryostat RM2155	Leica Microsystems, Bensheim, Germany
Cryostat CM 3000	Leica Microsystems, Bensheim, Germany
Microtome HM 340E	Microm, Heidelberg, Germany
pH meter WTW	WTW GmbH, Weilheim, Germany
Thermomixer 5436	Eppendorf, Hamburg, Germany
Vortex Genie 2™	Bender & Hobein AG, Zürich, Switzerland
Water bath HI 1210	Leica Microsystems, Bensheim, Germany

3.3 Chemicals and materials

Chemicals

Acetone	Merck, Darmstadt, Germany
Bovine Serum Albumin	Roche, Mannheim, Germany
DEPC	Sigma-Aldrich, St. Louis, USA
DMSO	Merck, Darmstadt, Germany
EDTA	Calbiochem, San Diego, USA
EDTA-Dikalium 0,2M	neoLab, Heidelberg, Germany
Ethanol	Merck, Darmstadt, Germany
Eosin	Sigma, Deisenhofen, Germany
Formalin	Merck, Darmstadt, Germany
FACS Clean	BD Biosciences, Heidelberg, Germany
FACS Flow	BD Biosciences, Heidelberg, Germany
FACS Rinse	BD Biosciences, Heidelberg, Germany
HCl (5 N)	Merck, Darmstadt, Germany
Magnesium chloride·6H2O	Merck, Darmstadt, Germany
Potassium chloride	Merck, Darmstadt, Germany
Potassium phosphate monobasic	Merck, Darmstadt, Germany
Sodium acetate	Merck, Darmstadt, Germany
Sodium azide	Roth, Karlsruhe, Germany
Sodium chloride	Merck, Darmstadt, Germany
Sodium citrate	Merck, Darmstadt, Germany
Sodium dihydrogen phosphate	Merck, Darmstadt, Germany
Sodium hydrogen carbonate	Merck, Darmstadt, Germany
SSC (Saline-sodium citrate Buffer)	Sigma, Deisenhofen, Germany
Tris	Roth, Karlsruhe, Germany
Tissue Freezing Medium	Leica, Nussloch, Germany
Trypan Blue	Sigma, Deisenhofen, Germany
Tween 20	Sigma-Aldrich, Steinheim, Germany
Oxygenated water	DAKO, Hamburg, Germany
Xylol	Merck, Darmstadt, Germany

Antibodies for immunohistochemistry

anti-F4/80	Serotec, Oxford, UK
anti-CD3	Serotec, Oxford, UK
anti-ER-HR3	Dianova, Hamburg, Germany
anti-Ly6G	BioRad Laboratories Inc., California, USA
anti-α-SMA	Abcam, Cambrdge, UK

Antibodies for FACS

Rat anti-mouse CD45-APC (Clone 30-F11)	BD Pharmingen, Heidelberg, Germany
Rat anti-mouse CD3e-FITC Alexa 488 (Clone 145-2C11)	BD Pharmingen, Heidelberg, Germany
Rat anti-mouse CD4-APC Alexa 647 (Clone RM4-5)	BD Pharmingen, Heidelberg, Germany
Rat anti-mouse CD8a-Cy5-PE (Clone 53-6.7)	BD Pharmingen, Heidelberg, Germany
Rat anti- mouse F4/80-APC (Clone C1:A3-1)	AbD Serotec, Düsseldorf, Germany
Rat anti-mouse CD69- PE (Clone H1.2F3)	BD Pharmingen, Heidelberg, Germany
Rat anti-mouse CD25-PerCP.Cy5.5 (Clone PC61)	BD Pharmingen, Heidelberg, Germany
Rat anti-mouse/human B220-PerCP (Clone RA3-6B2)	BD Pharmingen, Heidelberg, Germany
Rat anti-mouse MHC-II-PE (Clone I-A/b)	BD Pharmingen, Heidelberg, Germany
Rat anti-mouse CD21-FITC (Clone 7G6)	BD Pharmingen, Heidelberg, Germany
Rat anti-mouse CD23-PE (Clone B3B4)	BD Pharmingen, Heidelberg, Germany
Rat anti-mouse CD11b-PerCP (Clone M1/70)	BD Pharmingen, Heidelberg, Germany
Rat anti-mouse CD11c-FITC (Clone HL3)	BD Pharmingen, Heidelberg, Germany
Rat anti-mouse CD138-APC (Clone 281-2)	BD Pharmingen, Heidelberg, Germany
Rat anti-mouse Ly6G-FITC (Clone 1A8)	BD Pharmingen, Heidelberg, Germany
Rat anti-mouse Ly6C-FITC (Clone RB-8C5)	BD Pharmingen, Heidelberg, Germany

Enzyme-linked immunosorbent assays (ELISAs)

Total IgG, IgG1, IgG2a/c, IgG3	BethyLabs, Montgomery, USA
Smith antigen	Immunovision, Springdale, USA
dsDNA	Metabion, Martinsried, Germany
Histone	USB, Cleveland, USA

RF IgG	Jackson Immunoresearch, West Grove, USA
HRP-goat-anti-mouse IgG	Rockland, Gilbertsville, USA
Poly-L-lysine	R&D Systems, Minneapolis, USA
Mouse Albumin	Bethyl Laboratories, TX, USA
Mouse CCL2	BD OptEiA, San Diego, CA, USA
TMB Substrate Reagent Set	BD Biosciences, San Diego, USA
Creatinine FS	DiaSys Diagnostic System, GmBH, Holzheim, Germany
Urea FS	DiaSys Diagnostic System, GmBH, Holzheim, Germany

Cell culture

RPMI-1640 medium	GIBCO/Invitrogen, Paisley, UK
Fetal Bovine Serum (FCS)	Biochrom KG, Berlin, Germany
ITS, Insulin, Transferrin, Selenium	Roche Diagnostics, Mannheim, Germany
Collagenase	Roche Diagnostics, Mannheim, Germany
Penicillin/Streptomycin (100x)	PAA Laboratories GmbH, Cölbe, Germany
HEPES Buffer Solution	ThermoFisher Scientific, Massachusetts, USA
PBS	PAA Laboratories GmbH, Cölbe, Germany
Trypsin / EDTA	PAA Laboratories GmbH, Cölbe, Germany

Miscellaneous

Needles	BD Drogheda, Ireland
Nunc Maxisorp ELISA plate	Nunc, Wiesbaden, Germany
Pipette tips 1-1000 µl	Eppendorf, Hamburg, Germany
Pre-separation filters	Miltenyi Biotec, Bergish Gladbach, Germany
Plastic histosettes	NeoLab, Heidelberg, Germany
Syringes	Becton Dickinson GmbH, Heidelberg, Germany
Tissue culture dishes Ø 100 x 20 mm	TPP, Trasadingen, Switzerland
Tissue culture dishes Ø 35 x10 mm	TPP, Trasadingen, Switzerland

Tissue culture flasks 150 cm^2	Becton Dickinson, Franklin Lakes, NJ, USA
Tubes 15 and 50 mL	TPP, Trasadingen, Switzerland
Tubes 1.5 and 2 mL	TPP, Trasadingen, Switzerland

RNA isolation

RNeasy Mini Kit	Qiagen GmbH, Hilden, Germany
RNase-Free DNase Set	Qiagen, Hilden, Germany
RNase-free-Spray	Gene Choice, Frederick, USA

cDNA synthesis

5x First strand Buffer	Invitrogen, Karlsruhe, Germany
25 mM dNTPs	GE Healthcare, München, Germany
0,1 M DTT	Invitrogen, Karlsruhe, Germany
Hexanucleotide	Roche, Mannheim, Germany
linear Acrylamid	Ambion, Darmstadt, Germany
Superscript II	Invitrogen, Karlsruhe, Germany
RNAsin	Promega, Mannheim, Germany

RT-PCR

10x PE-Puffer	Finnzymes, Espoo, Finnland
1,25 mM dNTPs	Metabion, Martinsried, Germany
25 mM $MgCl_2$	Fermentas, St. Leon-Rot, Germany
SYBR Green Dye detection	Applied Biosystems, Norwalk, USA
Taq DNA- Polymerase	New England BioLabs, Ipswich, USA
qPCR Primers	Metabion, Martinstried, Germany

Table 4: Primer sequences

Gene	Forward sequence	Reverse Sequence
18s	5'-GCAATTATTCCCCATGAACG-3'	5'-AGGGCCTCACTAAACCATCC-3'
Ackr2	5'-CTTCTTTTACTCCCGCATCG-3'	5'-TATGGGAACCACAGCATGAA-3'
Arg-1	5'-AGAGATTATCGGAGCGCCTT-3'	5'-TTTTTCCAGCAGACCAGCTT-3'
CCL2	5'-CCTGCTGTTCACAGTTGCC-3'	5'-ATTGGGATCATCTTGCTGGT-3'
CCL5	5'-CCACTTCTTCTCTGGGTTGG-3'	5'-GTGCCCACGTCAAGGAGTAT-3'
CCR2	5'-GGGCATTGGATTCACCAC-3'	5'-CCGTGGATGAACTGAGGTAA-3'
CXCL10	5'-GGCTGGTCACCTTTCAGAAG-3'	5'-ATGGATGGACAGCAGAGAGC-3'
CTGF	5'-AGCTGACCTGGAGGAAAACA-3'	5'-CCGCAGAACTTAGCCCTGTA-3'
Fizz-1	5'-CCCTTCTCATCTGCATCTCC-3'	5'-CTGGATTGGCAAGAAGTTCC-3'
Fibronectin	5'-GGAGTGGCACTGTCAACCTC-3'	5'-ACTGGATGGGGTGGGAAT-3'
IFNγ	5'-ACAGCAAGGCGAAAAAGGAT-3'	5'-TGAGCTCATTGAATGCTTGG-3'
IL-1 β	5'-TGGACCTTCCAGGATGAGGACA-3'	5'-GTTCATCTCGGAGCCTGTAGTG-3'
IL-10	5'-ATCGATTTCTCCCCTGTGAA-3'	5'-TGTCAAATTCATTCATGGCCT-3'
IL-12	5'-TTGAACTGGCGTTGGAAGCACG-3'	5'-CCACCTGTGAGTTCTTCAAAGGC-3'
iNOS	5'-AGGGTCTGGGCCATAGAACT-3'	5'-TGAAGAAAACCCCTTGTGCT-3'
KIM-1	5'-TCAGCTCGGGAATGCACAA-3'	5'-TGGTTGCCTTCCGTGTCTCT-3'
Laminin	5'-CATGTGCTGCCTAAGGATGA-3'	5'-TCAGCTTGTAGGAGATGCCA-3'
MSR-1	5'-CCTCCGTTCAGGAGAAGTTG-3'	5'-TTTCCCAATTCAAAAGCTGA-3'
MRC-1	5'-ATATATAAACAAGAATGGTGGGCA-3'	5'-TCCATCCAAATGAATTTCTTATCC-3'
NGAL	5'-AATGTCACCTCCATCCTG-3'	5'-ATTTCCCAGAGTGAACTG-3'
Procollagen 1	5'-ACATGTTCAGCTTTGTGGACC-3'	5'-TAGGCCATTGTGTATGCAGC-3'
Procollagen 4	5'-GTCTGGCTTCTGCTGCTCTT-3'	5'-CACATTTTCCACAGCCAGAG-3'
TNFα	5'-CCACCACGCTCTTCTGTCTAC-3'	5'-AGGGTCTGGGCCATAGAACT-3'
TNFR1	5'-CTTCATTCACGAGCGTTG-3'	5'-ATGGATGTATCCCCATCA-3'
TNFR2	5'-GTCTTCGAACTGCAGCTG-3'	5'-AGATCTGGCACTCGTACC-3'
α-SMA	5'-ACTGGGACGACATGGAAAAG-3'	5'-GTTCAGTGGTGCCTCTGTCA-3'
TLR-7	5'-GTGATGCTGTGTGGTTTGTCTGG-3'	5'-CCTTTGTGTGCTCCTGGACCTA-3'
TLR-9	5'-GCTGTCAATGGCTCTCAGTTCC-3'	5'-CCTGCAACTGTGGTAGCTCACT-3'
Ifit1	5'-CAAGGCAGGTTTCTGAGGAG-3'	5'-GACCTGGTCACCATCAGCAT-3'

3.4 Solutions

Anesthesia mixture

Isoflurane	Harvard Anesthesia System, UK

FACS-Buffer

500 ml D-PBS + 1 g BSA + 0.5 g NaAzide

Paris-Buffer, pH 7.4

2.4228 g Tris-HCl
7.31 g NaCl
0.7456 g KCl
0.8203 g Na acetate
0.9 g D-glucose
1000 mL ddH2O

10x HBSS (Hank´s balanced saline solution) with Ca, Mg, pH 7.4

4 g KCl
0.6 g KH_2PO_4
80 g NaCl
0.621 g $Na_2HPO_4 \cdot 2H_2O$
3.5 g $NaHCO_3$
1.4 g $CaCl_2$
1.0 g $MgCl_2 \cdot 6H_2O$
1.0 g $MgSO_4 \cdot 7H_2O$
10 g D-Glucose
1000 mL ddH_2O

10x HBSS (Hank´s balanced saline solution) without Ca, Mg

4 g KCl
0.6 g KH_2PO4

80 g NaCl
0.621 g $Na_2HPO4 \cdot 2H_2O$
1000 mL ddH_2O

DNase stock solution (1 mg/mL)

DNase (Type IV) 15,000 U/6 mg, Sigma-Aldrich, Steinheim, Germany
Reconstitute 6 mg of DNase with 6 ml of 50 % glycerol solution

50% (w/v) glycerol solution in 20 mM Tris/HCl, pH 7.5, 1 mM MgCl2

2.4228 g Tris-buffer in 100 mL H_2O, pH 7.4
15 g Glycerol 100 % + 30 mL Tris-buffer
0.0952 g $MgCl_2$

Collagenase/DNAse solution

10 mg Collagenase
1 ml DNase-stock (1 mg/ml)
9 ml 1x HBSS (with Ca, Mg)
Prewarmed in water bath at 37°C

Collagenase solution

10 mg Collagenase
10 ml 1x HBSS (with Ca, Mg)
Prewarmed in water bath at 37°C

2 mM EDTA

100 µl of 0.2 M EDTA solution + 10 ml 1x HBSS
Prewarmed in water bath at 37°C

TAC Buffer, pH 7.2

50 mM Tris Buffer
450 mL 0.83% NH_4Cl

10x PBS, pH 7.4

80 g NaCl
14.2 g Na_2HPO_4
2 g KCl
2.7 g KH_2PO_4
1000 mL H_2O

Tris-NaCl/ 0.05 % Tween-Buffer, pH 8.0

6.06 g Tris
8.18 g NaCl
1000 mL H2O
0.05 % Tween 20
Coating-Buffer
1.59 g Na_2CO_3
2.93 g $NaHCO_3$
1000 mL H2O

4. Methods

4.1 Animal studies

All mice were kept in poly-propylene cages under normal housing conditions with a 12 hours light/dark cycle and unlimited access to water and food ad libitum. All experimental procedures were performed according to the regulations of the Deutsches Tierschutzgesetz and the European Directive 2010/63/EU.

4.1.1 Generation of Ackr2-/-B6lpr/lpr mice

Ackr2-deficient mice were originally obtained from the laboratories of Dr. Massimo Locati (Humanitas Clinical and Research Center, Rozzano, Italy) bred on a C57BL/6J background. C57BL/6lpr/lpr mice were purchased from Charles River Laboratories and backcrossed with Ackr2-/- mice. The first generation of offspring were heterozygous for both Ackr2 and the lpr mutation and again mated with each other. Homozygous mice of the F2 generation were born at expected Mendalian ratios and were further crossbreed for the planned phenotype analysis.

4.1.2 Plasma, urine and tissue collection

Blood samples were collected at the end of the study period. Samples were collected in micro centrifuge tubes containing EDTA. Plasma was separated by centrifugation at 5500 g for 5 minutes and stored at -20℃ for further measurements. Urine samples were collected at monthly intervals and stored -20℃ for further analysis. At the end of study, mice were sacrificed and organ weights of lymph nodes and spleens were determined. Kidney, lung, lymph node and spleen were harvested for histology analysis, flow cytometry, protein and RNA analysis.

4.2 Genotyping

For genotyping of mice, DNA samples were first isolated from the tip of the mouse tail. Gene sequences were amplified by PCR and finally were evaluated in gel electrophoresis.

Genotyping was performed as follows:

Genomic DNA isolation: Tissue was placed in lysis buffer containing proteinase K at 55℃ under constant shaking for 3 hours until complete lysis was achieved. Incubation was stopped for 45 minutes at 85℃ to achieve complete heat inactivation of proteinase K. The genomic DNA was eluted with a DNA kit as instructed by the manufacturer.

PCR: For lpr genotyping, 1 µl of the isolated DNA sample was mixed with 1 µl of each diluted Fas forward, Fas reverse and lpr reverse primers and a master mix of 2.5 µl of 10x PE buffer, 4.0 µl of 1.25 mM dNTPs, 5 µl of PCR optimizer, 0.2 µl of Taq polymerase and 9.3 µl of H_2O to a total volume of 25 µl. The master mix with ddH_2O instead of added primers served as a negative control. For Ackr2 genotyping, WT, heterozygous and homozygous mice were examined with respective primers.

Gel electrophoresis: The obtained PCR products were evaluated using agarose gel electrophoresis. The agarose gel was prepared by boiling 3 g of agarose in 150 ml 0.5x TBE buffer, adding 7.5 ul ethidium bromide. The DNA fragments were separated by electrophoresis according to length and were visualized under UV light (Figure 5).

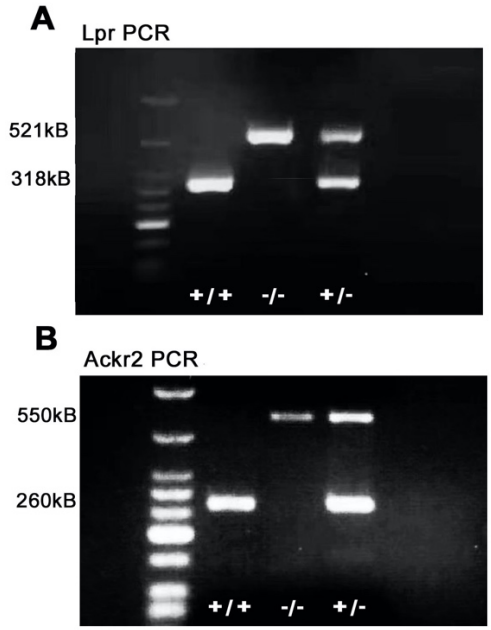

Figure 5: Genotyping of mice. (A) The length of the DNA fragment can be characterized using the length standard in the left lane. The 521 kB band indicates the lpr genotype. The wild type is indicated by the band of 318 kB. (B) A solitary band at 260 kB indicated a wildtype and a 550 kB band indicated an Ackr2 knockout genotype. The presence of both bands suggests a heterozygous genotype.

4.3 Urinary albumin to creatinine ratio

Urinary albumin

Urinary albumin levels were determined by an albumin ELISA kit from Bethyl laboratories following the manufacturer ‘s instructions. In brief, the NUNC ELISA plate was coated with 100 µl capture antibody diluted in carbonate bicarbonate coating buffer (pH 9.6) and incubated overnight at 4°C. On the next day the plate was washed 3 times with washing buffer and blocked with blocking solution for 1 hour at room temperature. After blocking, the plate was washed 3 times with washing buffer followed by addition of standards and diluted samples into the respective wells, with subsequent incubated for 2 hours. Each well was washed again 3 times and incubated with diluted HRP-conjugated detection antibody for 1 hour. After incubation, the plate was washed 10 times and tetramethylbenzidine (TMB) reagent was added and incubated in the dark to develop color followed by addition of 100 µl of 2 N H_2SO_4. The absorbance was read at 450 nm after the addition of stop solution, with a reference wavelength of 620 nm using a spectrophotometer.

Urinary creatinine, plasma BUN and creatinine determination

Urinary creatinine and plasma creatinine levels were determined with a Creatinine FS kit based on Jaffe´s enzymatic reaction. Urine samples were diluted 10 times with ddH_2O whereas plasma samples were used undiluted. The standard samples in recommended concentrations were prepared using the stock solution provided in the kit. Working reagent was prepared by mixing 4 parts of reagent 1 (R1, sodium hydroxide) and 1 part of reagent 2 (R2, picric acid). Subsequently, 10 µl of undiluted sample and standard were added to a 96-well plate with flat bottom plate (Nunc maxisorb plate). 200 µl of working reagent was added to each well, and after 1 minute of incubation, the absorbance of the reaction mixture was read immediately at 492 nm using an ELISA plate reader. The absorbance was measured again after 1 minute (A1) and 2 minutes (A2) of additional incubation. The change in absorbance (Δ A) was defined as:

Δ A = [(A2 – A1) sample or standard] – [(A2 – A1) blank].

Creatinine concentration of samples was calculated as follows:

Creatinine (mg/dl) = ΔA sample /ΔA standard * Concentration of standard (mg/dl)

Plasma BUN levels were tested using the Urea FS kit from DiaSys Diagnostic System. Plasma samples and prepared standard were added to a 96-well plate followed by immediate addition of 200 µl working reagent. The reaction mixture was incubated for 1 minute before measuring the absorbance at 360 nm, and again after 1 minute (A1) and 2 minutes (A2) using an ELISA plate reader. The change in absorbance (Δ A) was calculated as:

Δ A = [(A1 – A2) sample or standard] – [(A1 – A2) blank].

BUN concentrations of samples were calculated as follows:

Urea (mg/dl) = ΔA sample /ΔA standard * concentration of standard (mg/dl)

BUN (mg/dl) = Urea (mg/dl) * 0.467.

Urinary albumin to creatinine ratio (UACR)

Urinary albumin to creatinine ratios were calculated using albumin content of each sample (mg/dl) divided by its creatinine concentration (mg/dl), and were expressed in mg/mg creatinine.

4.4 Histology and immunohistochemistry

Tissues harvested from all mice were placed in plastic histocassettes and immediately fixed in 10% formalin overnight. On the next day formalin-fixed tissues were processed with an automatic tissue processor (Leica). Tissues were dehydrated by incubating in a series of increasingly concentrated ethanol baths, followed by xylene to remove ethanol. Subsequently, histocassettes were removed from the tissue processor and tissues were embedded in hot liquid paraffin and solidified. These blocks were cooled down and later cut into 2-µm sections for subsequent staining or immunohistochemistry. The sections were deparaffinized using xylene followed by incubation in a graded serious of ethanol (100%, 95%, 80% and 50%) and rinsed with phosphate buffered saline (PBS). Periodic acid-Schiff (PAS) staining was performed following routine protocols.

4.5 Immunohistochemistry

All immunohistochemistry staining was performed on 2 µm thick paraffin-embedded sections. Prior to antibody staining, the sections were incubated in a H_2O_2 and methanol mixture (20 ml 30% H_2O_2 and 180 ml methanol) to block endogenous peroxidases, followed by washing with PBS twice. To avoid non-specific binding and background staining, sections were pre-incubated in 10% goat serum for 10 minutes. The following primary antibodies were used: rat anti-Ly6B (dilution 1:100, clone7/4, BIO-RAD, CA, USA) for neutrophils, anti-CD3 (1:100, clone 500A2, BD) for T cells, and anti-F4/80 (1:50, clone CI:A3-1, BIO-RAD, CA, USA) and anti-ER-HR3 (1:50, clone ER-HR3, DPC Biermann, Bad Nauheim, Germany) for monocytes/macrophages. Anti-mouse smooth muscle actin (1:100, clone 1A4, Dako, Carpinteria, CA) was used to stain myofibroblasts. Negative controls were performed by incubation with respective isotype antibodies instead of primary antibody. After incubation, the sections were washed in PBS and labelled with secondary antibodies for 30 minutes. Subsequently, sections were stained with 3'3'diaminobenzidine (DAB) and counterstained with methyl green followed by washing with alcohol to remove excess stain and xylene.

Histopathological evaluations

The severity of renal lesions was assessed using the activity and chronicity indices as described for human lupus nephritis [159]. The following index was used analyzing PAS-stained renal sections:

Activity index (0-24)		Chronicity index (0-12)	
Glomerular proliferation	(0-3) ×2	Glomerular sclerosis	(0-3)
Cellular crescents	(0-3) ×2	Fibrous crescents	(0-3)
Karyorrhexis /fibrinoid necrosis	(0-3)	Tubular atrophy	(0-3)
Leukocyte infiltration	(0-3)	Interstitial fibrosis	(0-3)
Hyaline deposits	(0-3)		
Interstitial inflammation	(0-3)		

The severity of lung lesions was accessed in PAS-stained sections using an established semi-quantitative method [160].

Score	Lung peribronchiolar leukocyte infiltration
0	None
1	3 cell layers in >50% of bronchi
2	3-6 cell layers in >50% of bronchi
3	> 6 cell layers in >50% of bronchi

4.6 Cytokine and SLE autoantibody ELISAs

Cytokines

Cytokine levels in plasma samples from mice or supernatants of *in vitro* cell stimulation experiments were determined using ELISA kits according to the manufacturer's instructions. NUNC ELISA plates were coated with capture antibody in coating buffer and placed overnight at 4°C. The plate was washed 3 times with washing buffer and blocked with reagent diluent for a minimum of 1 hour at room temperature. After blocking the plate was washed 3 times. 100 µl

of samples and standards diluted in appropriate diluent were added per well and incubated for 2 hours at room temperature. This was followed by washing for 3 times. Subsequently, HRP-conjugated detection antibody was added to each well and incubated for 1 hour. The plate was washed again for 3 times and incubated with freshly prepared TMB substrate solution in the dark for 20 minutes. The reaction was stopped with 2 N H_2SO_4 and absorbance was determined at the specified wavelength of 410 or 450 nm using a spectrophotometer.

Total IgG and isotype plasma levels

Quantification of plasma levels of IgG and its isotypes was performed with commercially available ELISA kits (Bethyl Labs, Montgomery, TX, USA) using the following antibodies: anti-mouse IgG, IgG1, IgG2a, IgG2b, IgG2c and IgG3. First, the NUNC maxisorp 96-well flat bottom ELISA plate was incubated with diluted antibody for 1 hour at room temperature. After incubation, the plate was washed 5 times and was blocked with blocking solution for 30 minutes. After blocking, diluted samples and standard were transferred to assigned wells and were incubated for 1 hour. After washing the plate 5 times, wells were incubated with HRP detection antibody for 1 hour. The plate was then developed by adding TMB substrate to each well at room temperature in the dark for 15 minutes. The reaction was stopped by adding 2 N H_2SO_4, and absorbance was read at 450 nm.

Anti-dsDNA antibody levels

For the detection of dsDNA antibodies in mouse plasma, plates were coated with 100 µl of poly-L-lysine for 1 hour at room temperature. After washing the plate for 3 times with washing buffer, sample wells were coated with dsDNA (1 µg/ml) in SSC buffer. For standard samples, wells were coated with total IgG antibody (1 µg/ml) with coating buffer. The plate was washed 5 times and 200 µl of assay diluent was added to each well and incubated for 30 minutes. Standard dilutions and samples were pipetted into appropriate wells and incubated for 1 hour. After washing the plate with washing buffer, 100 µl of secondary antibody was added and incubated for 1 hour at room temperature. Five final washing steps were followed by TMB substrate solution incubation in the dark for 15 minutes. The reaction was stopped with 2 N H_2SO_4 and absorbance was measured at 450 nm.

Anti-histone antibody levels

NUNC ELISA plates were coated with 100 µl of histone solution (10 µg/ml) in coating buffer overnight at 4 ℃. On the next day the plate was washed 5 times with washing buffer and non-specific binding was blocked with blocking solution for 90 minutes. Following washing, the standard and samples were added into the respective wells and incubated at room temperature for 1 hour. Subsequently, the plate was washed 10 times and the HRP-conjugated secondary antibody was added. After washing the plate for 3 times, TMB substrate solution was added to each well to develop color in dark. The reaction was stopped by addition of 2 N H_2SO_4. The plate was read using an ELISA reader with a wavelength of 410 nm.

Rheumatoid factor levels

Plasma rheumatoid factor levels were quantified using a commercial ELISA kit (FUJIFILM, Wako, Japan) according to the instruction manual. Briefly, plates were coated with diluted capture antibody overnight at 4 ℃. The 96 well plates were washed for 3 times and tap dried on blotting paper. Samples and standard were diluted in required dilution and added in respective wells and incubated for 2 hours at room temperature on a shaker. The plates were washed for 3 times and then coated with TMB substrate in the dark without covering for 20 minutes. The reaction was stopped with 2 N H_2SO_4 and absorbance was measured at 450 nm within 30 minutes.

Anti-Sm antibody levels

The NUNC ELISA plate wells were coated with Smith antigen at a dilution of 1:250 overnight at 4 ℃. Serum samples were applied at dilutions of 1:25 to 1:50. A horseradish peroxidase-conjugated goat anti-mouse IgG was used as detection antibody at a dilution of 1: 50,000 in assay diluent. 100 µl of TMB substrate solution was added and incubated for 15 minutes in the dark followed by the addition of 2 N H_2SO_4 to stop the color reaction. The absorbance was measured at 450 nm within 30 minutes.

4.7 RNA expression analysis

RNA isolation

Tissue samples from each mouse were preserved in RNA later immediately after tissue harvest and stored at -20℃. Total RNA was isolated from tissues using PureLink RNA Mini Kit. In brief, tissues were placed in 600 µl lysis buffer containing 1% β-mercaptoethanol and homogenized with an electric homogenizer at 14,500 rpm for 30 s. The supernatants collected after centrifugation at 5000 g for 5 minutes were mixed gently with an equal amount of 70% ethanol. The whole mixture was then transferred to RNA columns and processed for RNA isolation as instructed by the kit's protocol. Isolated RNA was stored at -80℃ for long-term storage. The RNA was quantified and purity was determined by spectrophotometric measurement of optical density (OD) at 260 nm and 280 nm using 2 µl of RNA sample. 260/280 nm OD ratios were calculated for each sample. Values of 2.0±0.2 were considered to be of acceptable quality. If necessary, RNA integrity was additionally checked by denaturing RNA gel electrophoresis. Electrophoresis was run at approximately 80 volts using running buffer for 1 hour. The gel was visualized by UV lamp and documented.

cDNA synthesis and real-time RT-PCR

The isolated RNA samples were transcribed into cDNA using SuperScript II reverse transcriptase. For a reaction size of 22.45 µl, RNA samples were diluted in RNAse-free diethylpyrocarbonate (DEPC)-treated water to a concentration of 66.67 ng/µl in 15 µl and added to RNase-free tubes. A master mix was prepared with reagents containing 4 µl of 5x first strand buffer, 0.4 µl of 25 mM dNTP, 0.215 µl of hexanucleotide, 1 µl of 0.1 M dithiothreitol (DTT), 0.5 µl of 40 U/µl RNasin, 0.25 µl of 15 µg/ml linear acrylamide, 0.435 µl of SuperScript II reverse transcriptase or ddH_2O in case of cDNA-free controls. The cDNA synthesis reaction was carried out at 42 °C in a thermal shaker incubator for 90 min. The reaction was stopped by incubating at 85°C for 5 minutes to inactivate the reverses transcriptase. The cDNA sample was either directly used for real-time RT-PCR analysis or was stored at -20°C until use.

The synthesized cDNA samples were diluted in a 1:10 ratio with RNase-free water for the real-time RT-PCR. 2 µl of diluted cDNA samples was placed in a 96-well PCR reaction plate, mixed with 10 µl SYBR-Green mastermix, 0.6 µl forward and reverse primers of the specific genes, respectively, 0.16 µl of TaqMan polymerase and 6.64 µl of ddH_2O. The plate was sealed,

centrifuged briefly and placed in the LightCycler® 480. The protocol for RT-PCR were as follows: The first incubation was carried out for 5 minutes at 95℃ to guarantee complete denaturation of cDNA. Subsequently, the template was amplified for 45 cycles, each cycle comprising 15 seconds of incubation at 95℃ followed by 1 min incubation at 65℃. All samples were performed in duplicate, and negative controls contained no template cDNA. 18S rRNA was used as a housekeeper gene for normalization. The CT values were recorded using the LightCycler® 480 software and the results were evaluated with respect to the respective housekeepers.

4.8 Flow cytometry

Preparation of murine spleen and lymph node cells

Spleens and lymph nodes were isolated from mice of all groups. Tissues were placed in pertri plates containing 2-3 ml of ice-cold PBS. Subsequently, they were minced into fine pieces using forceps. Cell suspensions were passed through a 70 µm cell strainer and were carefully transferred to a 15 ml Falcon tube, followed by centrifugation at 400 g at 4℃ for 5 minutes. For spleen cells the supernatant was discarded and the pellet was resuspended in pre-warmed red blood cell (RBC) lysis buffer (0.3 M NH_4Cl), with subsequent incubation at 37°C for 5 minutes. After centrifugation at 400 g the pellet was washed with ice-cold PBS followed by centrifugation at 400 g for 5 minutes. Tissue was resuspended in cold PBS and passed through 70 µm cell strainers. After centrifugation, supernatants of spleen cell suspensions were discarded and the pellets of spleen cells and previously obtained lymph node cells were resuspended in ice-cold FACS buffer until further analysis.

Preparation of murine kidney cells

Kidneys were isolated from mouse and mechanically disrupted in pertri plates containing 2-3 ml of chilled Paris buffer. The tissue pieces were transferred into a Greiner tube filled with 10 ml Paris buffer using a syringe without cannula. Following centrifugation at 400 g, the supernatant was poured off and the pellet was resuspended in 10 ml ice-cold HBSS (with Ca, Mg) solution. After centrifugation and aspirating the supernatant, the cell suspension was incubated in digestion buffer (collagenase + DNAse I in HBSS) at 37°C for 20 min with occasional mixing in a water bath, followed by centrifugation at 400 g at 4℃ for 5 minutes.

The pellet was incubated in 5 ml of 2 mM EDTA in HBSS (without Ca, Mg) at 37°C for 20 min to stop the digestion. After centrifugation the supernatant was transferred to pre-cooled Greiner tubes and was kept on ice. The remaining pellet was incubated again in collagenase solution at 37°C for 20 min. The suspension was subsequently passed through 19-gauge, 26-gauge and 30-gauge needles to break up remaining cell clusters and combined with the previous supernatant stored in the Greiner tube. After centrifugation, the supernatant was removed and the pellet was dissolved in FACS buffer and filtered through a 70 µm cell strainer followed by resuspension in 10 ml PBS. The cell suspension was centrifuged again at 400 g at 4℃ for 5 minutes and was resuspended in FACS buffer until further analysis.

Analysis of cell populations in spleen, lymph node and kidney

The cell pellet obtained was resuspended in FACS buffer and non-specific binding sites on the cell surface were blocked with a mixture of 5 µl of rat serum and 5 µl of mouse serum added to 100 µl of cells. Then, cell suspensions were stained with different antibodies to detect various cell populations (Table 5). Isotype controls were also used to compensate for the spectral overlap of the fluorochromes. Flow cytometric acquisition was performed on BD FACSCanto II (BD Biosciences, Heidelberg, Germany), and the raw data were analyzed using Cellquest software (BD Biosciences).

Table 5: Various leukocyte populations with the respective surface markers

T lymphocytes	CD45-PE, CD3-FITC, CD4-APC, CD8-PerCP
Activated T lymphocytes	CD3-FITC, CD4-APC, CD8-PerCP, CD69-PE
Regulatory T lymphocytes	CD3-FITC, CD4-APC, CD25-PerCP
Mature B lymphocytes	B220-PE, IgM-APC, IgD-FITC
Marginal zone/Follicular B lymphocytes	B220-FITC, CD21-APC, CD23-PE
Activated B lymphocytes	CD45-APC, B220-PE, CD19-PerCP, CD69-FITC
Plasma cells	B220-FITC, K light chain-PE, CD138-APC
Dendritic cells	CD45-FITC, CD11c-PE, CD4-APC, CD8-PerCP
Myeloid dendritic cells	CD11c-APC, CD40-FITC, MHC Ⅱ-PE
Macrophages	CD45-APC, CD11b-PerCP, F4/80-FITC, MHC Ⅱ-PE
Granulocytes	CD45-APC, CD11b-PerCP, CD11c-PE, Ly6G-FITC
Inflammatory macrophages	CD45-APC, CD11b-PerCP, CD11c-PE, Ly6C-FITC

4.9 In vitro experiments

Magnetic cell sorting technique for compartment-specific isolation of renal cells

For separation of kidney tissue compartments the paramagnetic isolation method according to Takemoto et al. was used [161]. Briefly, anesthetized mice were sacrificed by cervical dislocation. The abdominal wall and chest were cut open by a longitudinal incision to expose liver and heart. After cutting open the inferior vena cava below the right cardiac atrium, the left cardiac ventricle was punctured. Using a pressure-controlled perfusion device filled with 40 ml of pre-warmed PBS and 200 µl of blocked Dynabeads, the beads were slowly injected into the left cardiac ventricle. Successful perfusion was indicated by pale discoloration of kidneys and liver. After completion of perfusion, organs were harvested, kidneys were minced into 1 mm^3 pieces and digested with collagenase A (1 mg/ml dissolved in HBSS) for 30 minutes at 37°C. Under these conditions, Bowmann`s capsule of glomeruli and tubulointerstitial tissue is digested, but the glomerular tuft with embolized paramagnetic Dynabeads within glomerular capillaries remains intact. The digested tissue was gently pressed through a 100 µm cell strainer and transferred into a 15 ml tube placed in the magnetic particle concentrator. Tissue was washed 5 times to obtain a pure glomerular fraction retained in the tube due to embolized paramagnetic Dynabeads in the intact glomeruli. The first wash contained tubular fragments and tubulointerstitial cells, the second wash contained predominantly tubular fragments. After 3 further washes a purity of 95%-98% of the isolated glomerular fraction was achieved when analyzing tissue fragments under the microscope (Figure 6).

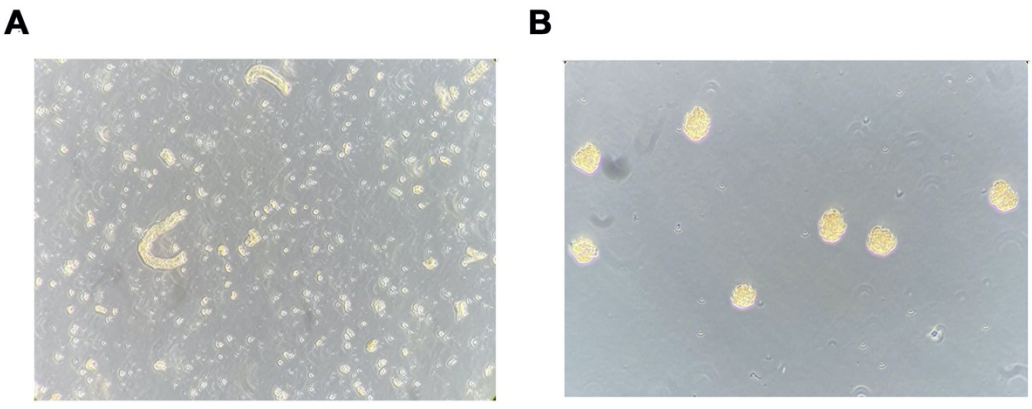

Figure 6: Microscopic view of separated renal tissue compartments after perfusion with magnetic beads. (A) Tubulointerstitial fraction. (B) Glomerular fraction.

In vitro stimulation of glomeruli and tubulointerstitial tissue

Separated tissue compartments were cultured in Roswell Park Memorial Institution (RPMI) 1640 medium supplemented with 15% fetal calf serum (FCS), 15 mM HEPES, 0,66 U/ml insulin and 100 U/ml penicillin containing 100 µl streptomycin. Plates were incubated in a 37℃ incubator for 24 hours. After incubation the media was separated from the tissue pellet by centrifuging it at 400 g for 5 minutes. The pellet was suspended with FCS/PS free RPMI-1640 and the number of glomeruli was counted under the microscope using a Neubauer chamber after suitable dilution. A total of 12,500 glomeruli and 100 µl tubulointerstitial cell suspensions standardized to a protein content of 0.5 mg/ml were stimulated with recombinant murine TNF (50 ng/ml) or PBS for 24 hours at 37℃. After centrifugation the supernatant was collected and stored at -20℃ until ELISA measurement.

Bradford protein assay

Protein content of the tubulointerstitial tissue samples were determined using the Bradford assay. Briefly, 10 µl each of tubulointerstitial sample and serial dilutions of standard was added into the respective wells, 200 µl Bradford reagent was mixed with the samples and then incubated at room temperature for at least 5 minutes. The absorbance was read at 595 nm using a spectrophotometer.

4.10 Statistical analysis

All statistics were performed using Prism 8.0 software (GraphPad Software, San Diego, CA). Illustrations were created with Biorender (https://biorender.com/). Data are presented as mean ± SD. Prior to statistical analysis, data were checked for the Shapiro-Wilk normal distribution test and homoscedasticity test (equality of variance). For more than two datasets, the normally distributed and homoscedastic datasets were tested for statistical differences by one-way analysis of variance (ANOVA). The *post hoc* Tukey test was applied for multiple comparisons. Nonnormally distributed datasets were tested for statistical significance by Kruskal-Wallis test and *post hoc* Dunn test for multiple comparisons. A p value < 0.05 was considered as statistical significance.

5. Results

5.1 Ackr2-dependent chemokine scavenging in tubulointerstitial tissue of B6 lpr kidneys and increased renal Ackr2 expression in B6lpr mice with lupus nephritis

The potential ability of ACKR2 to limit renal inflammation and injury in lupus nephritis of B6lpr mice was first explored *in vitro* using glomeruli and tubulointerstitial tissue isolated from WT-B6lpr and Ackr2-/-B6lpr mice. Untreated glomeruli and tubulointerstitial tissue of both genotypes showed minimal and comparable secretion of the pro-inflammatory chemokine CCL2 into supernatants. Inflammatory stimulation with TNF-α for 24 hours increased production of CCL2 by Ackr2-deficient tubulointerstitial cells, but not glomeruli (Figure 7). These results are consistent with reduced Ackr2-dependent degradation of chemokines in the tubulointerstitial compartment. The restriction of ACKR2 effects to the tubulointerstitial tissue fraction also correlates with the known parenchymal expression of renal ACKR2 in the interstitial lymphatic endothelium, which is not present in glomeruli.

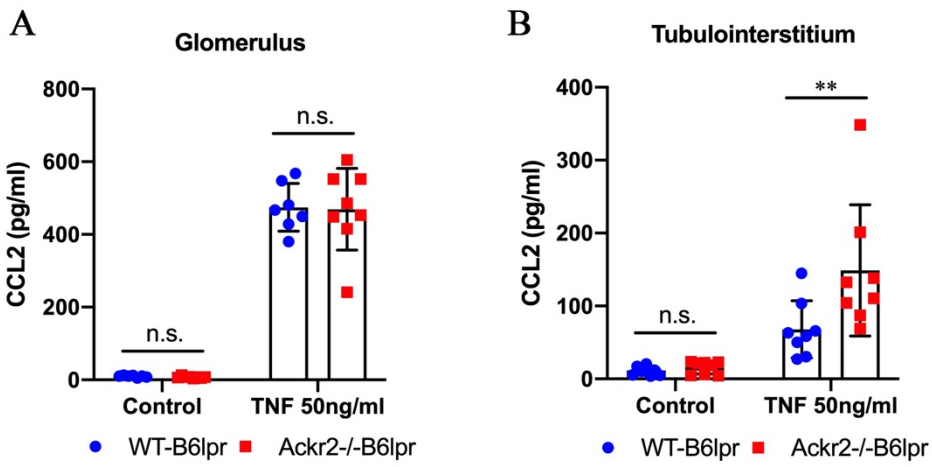

Figure 7: Compartment-specific CCL2 release in renal tissue isolated from WT- and Ackr2-/-B6lpr mice. Glomeruli (25,000/ml) and tubulointerstitial tissue (standardized using protein content analysis) were isolated and stimulated with 50 ng/ml TNF for 24 hours in cell culture. Supernatants were collected to determine CCL2 concentration. Concentration of CCL2 in unstimulated (Control) and TNF-stimulated (A) glomerular and (B) tubulointerstitial tissue of WT- and Ackr2-/-B6lpr mice are shown. $^{**}p<0.01$; n.s. not significant.

Furthermore, mRNA expression analysis demonstrated that renal Ackr2 expression was induced by 4.3-fold in female WT-B6lpr mice at week 28 of age compared to age-matched healthy B6 WT controls without the lpr mutation. No expression was detected in Ackr2-/- mice (Figure 8).

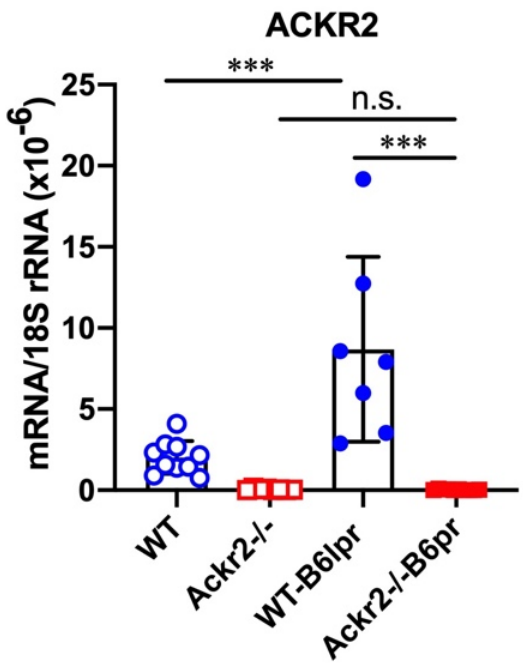

Figure 8. Ackr2 mRNA expression in B6lpr mice at week 28 of lupus nephritis. mRNA expression levels of Ackr2 were determined in wildtype (WT) and Ackr2-/- control mice, and WT-B6lpr and Ackr2-/-B6lpr mice. ***$p<0.001$; n.s. not significant.

Together, these results suggested a potential anti-inflammatory effect of ACKR2 in lupus nephritis, and exacerbated renal injury when ACKR2 activity is blocked or genetically absent. As no specific ACKR2 antagonists are currently available this was further investigated *in vivo* by comparing the spontaneous phenotype of female Ackr2-deficient B6lpr mice with WT littermates until week 28 of age.

5.2 Effects of Ackr2 deficiency on survival rate and body weight of B6lpr mice

Female WT-B6lpr and Ackr2-/-B6lpr mice were followed-up for 28 weeks to characterize spontaneous development of their lupus-like autoimmune phenotype and inflammatory organ injury. Age-matched female WT and Ackr2-/- B6 mice without the lpr mutation served as controls.

Mouse survival rate was determined throughout the experiment. Two out of 15 mice died in the WT-B6lpr group and one mouse out of 16 mice died in the Ackr2-/-B6lpr group until week 28, while all WT and Ackr2-/- control mice without the lpr mutation survived until week 28. Mortality was not significantly different between the WT-B6lpr group and the Ackr2-/-B6lpr group, with a p=0.47 (Figure 9A).

Body weight was monitored every 4 weeks (Figure 9B). Although the body weight of all strains continued to increase progressively during 28 weeks, healthy WT mice had a lower body weight than the other three groups. However, at 28 weeks of age Ackr2-/-B6lpr mice had similar body weights compared to their WT-B6lpr counterparts, indicating that Ackr2-deficiency had no effect on body weight in lupus-prone B6lpr mice.

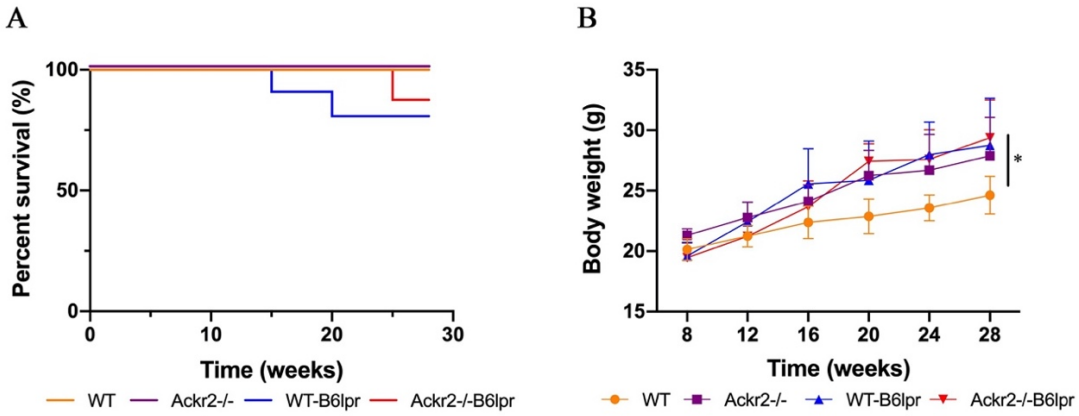

Figure 9: Effect of Ackr2 deficiency on survival rate and body weight. (A) Kaplan-Meier survival curves. Kaplan-Meier survival curves were compared with Mantel-Cox test. N=10 in wildtype (WT) group, N=8 in Ackr2-/- group, N=15 in WT-B6lpr group and N=16 in Ackr2-/-B6lpr group. (B) Body weight. *p<0.05.

5.3 Effect of Ackr2 on renal function and injury in B6lpr mice

To evaluate excretory kidney function in WT-B6lpr and Ackr2-/-B6lpr mice plasma creatinine and blood urea nitrogen (BUN) levels were measured. At the age of 28 weeks, mice of both genotypes showed no statistically significant differences in plasma creatinine and BUN levels, and these were also comparable to WT and Ackr2-/- control mice without the lpr mutation (Figure 10A). Albuminuria as a functional marker of glomerular injury was measured in spot urine samples of WT-B6lpr and Ackr2-/-B6lpr mice at regular intervals until week 28. Albuminuria was expressed as urine albumin to urine creatinine ratios. WT- and Ackr2-/-B6lpr mice displayed a normal range of albumin to creatinine ratios (ACR) until the end of the study (Figure 10B, C).

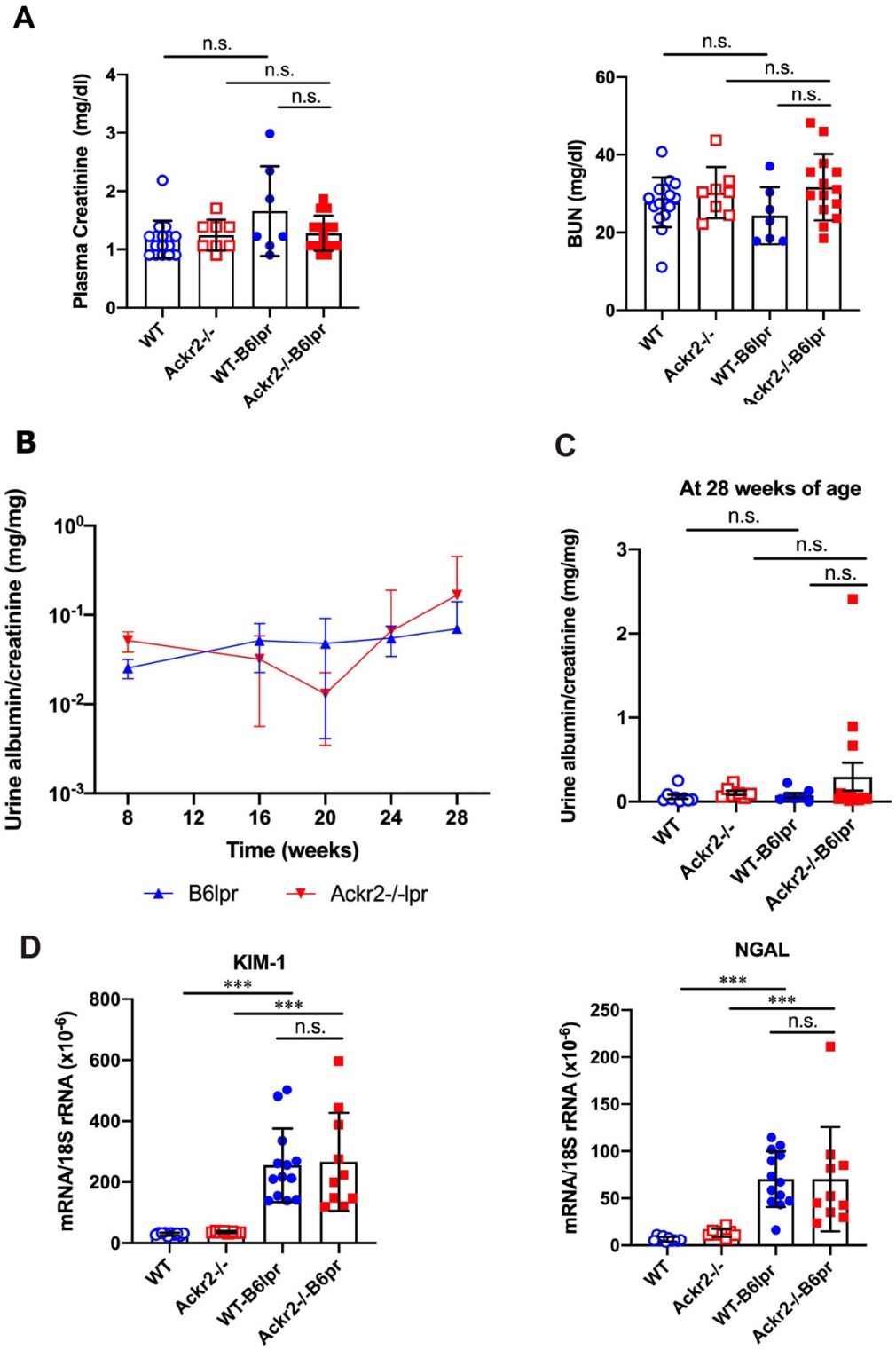

Figure 10: Effect of Ackr2 deficiency on renal functional parameters and injury. (A) Plasma creatinine and BUN levels at 28 weeks of age. (B) The concentration of albumin and creatinine in spot urine were measured by ELISA and Jaffe method, respectively, and albuminuria was quantitated by calculating the urinary albumin to creatinine ratio (UACR). (C) UACR at 28 weeks of age. (D) Kidney mRNA expression of the tubular injury markers KIM-1 and NGAL was measured by real-time quantitative PCR. BUN, blood urea nitrogen; KIM-1, kidney injury marker-1; NGAL, neutrophil gelatinase-associated lipocalin. ***p<0.001; n.s. not significant.

This analysis of functional data suggests that WT-B6lpr mice until week 28 of life develop only mild renal injury without significant impairment of renal functional parameters. Unlike previous data obtained in the nephrotoxic serum nephritis model of immune complex glomerulonephritis [140] no increased functional renal impairment in Ackr2-deficient B6lpr mice could be detected.

To further investigate possible tubulointerstitial injury renal mRNA expression of the tubular injury markers KIM-1 and NGAL was measured. Compared with age-matched WT and Ackr2-/- control mice without lpr mutations higher renal mRNA expression of these tubular injury markers was present in WT-B6lpr and Ackr2-/-B6lpr mice at week 28 (Figure 10D). However, Ackr2 deficiency did not affect the degree of tubular injury in B6lpr mice, as evidenced by similar increases seen in renal mRNA expression of KIM-1 and NGAL in the WT- and Ackr2-/-B6lpr group.

Moreover, by 28 weeks of age WT-B6lpr mice developed diffuse proliferative glomerulonephritis with the presence of mesangial cell proliferation and glomerular hypercellularity, as revealed by histology of PAS-stained kidney sections (Figure 11A). Histology showed comparable glomerular injury between WT-B6lpr and Ackr2-/-B6lpr mice, as demonstrated by similar activity and chronicity indices for lupus nephritis after morphometrical assessment (Figure 11B). Similarly, glomerular deposition of murine IgG did not reveal significant differences in both genotypes while almost no IgG deposition was detected in the WT and Ackr2-/- control mice (Figure 12).

Taken together, these results demonstrate that B6lpr mice develop lupus nephritis with mild glomerular and tubular injury until week 28, but this renal injury is not altered by Ackr2 deficiency. In particular, unlike Ackr2-/- mice with nephrotoxic nephritis [140] Ackr2-deficient B6lpr mice do not present with exacerbated immune complex-mediated glomerulonephritis.

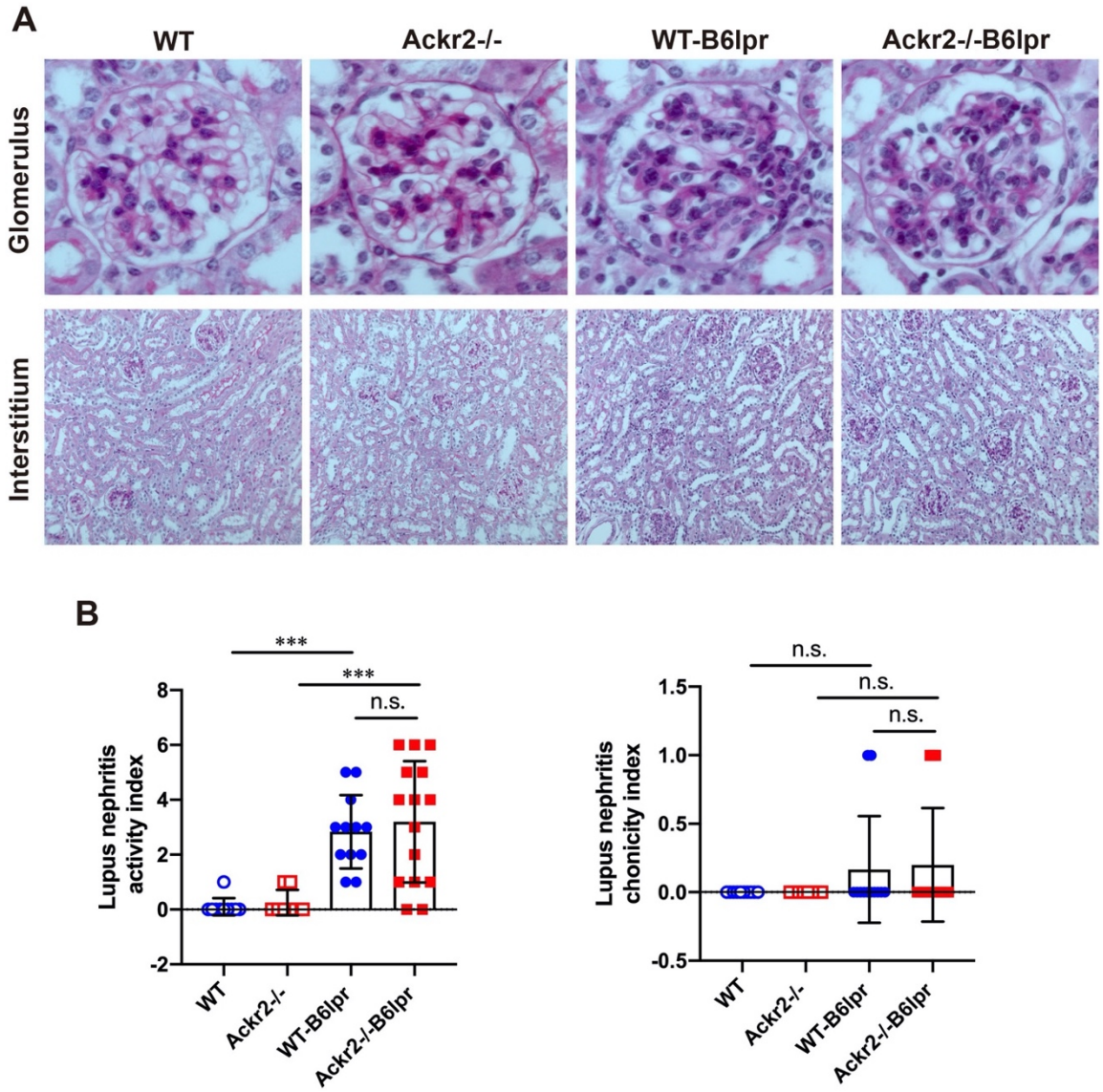

Figure 11: Effect of Ackr2 deficiency on renal histopathology of B6lpr mice. (A) Renal sections of 28 weeks old mice from all groups were stained with periodic acid-Schiff (PAS) reagent. Representative images of glomeruli (original magnification x400) and interstitium (original magnification x200) from wildtype (WT) and Ackr2-/- control mice, and WT-B6lpr and Ackr2-/-B6lpr mice are shown. (B) The lupus nephritis activity and chronicity indices were determined by semiquantitative scoring on PAS-stained sections from 28 weeks age old mice from all mice strains. ***p<0.001; n.s. not significant.

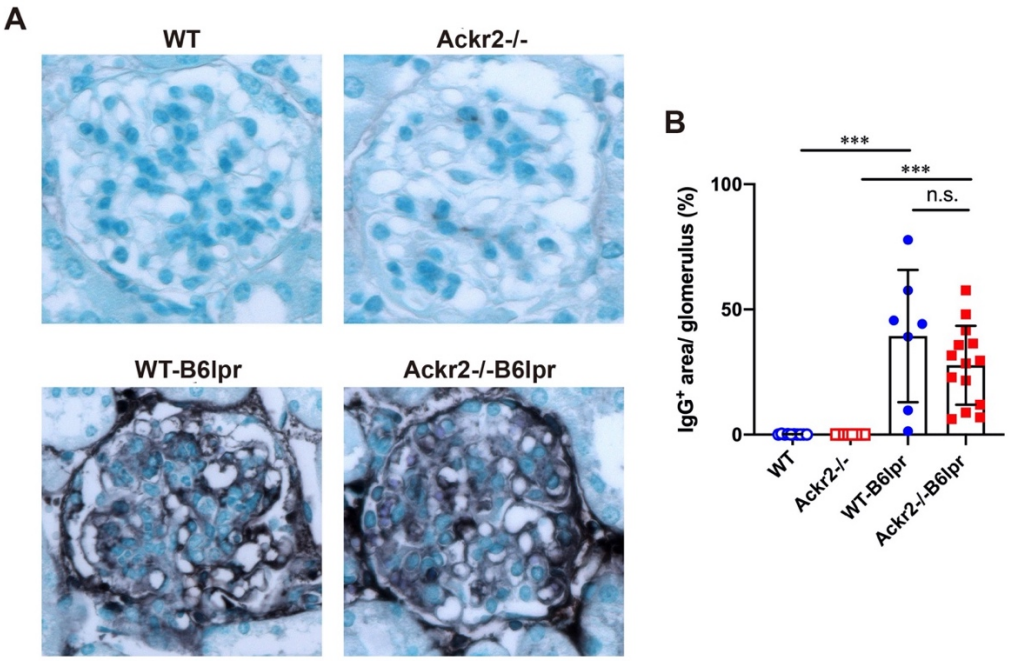

Figure 12: Effect of Ackr2 deficiency on glomerular IgG deposition. (A) Renal sections were stained for deposited murine IgG. Representative images of glomeruli from wildtype (WT) and Ackr2-/- control mice, and WT-B6lpr and Ackr2-/-B6lpr mice are shown. Original magnification x400. (B) Quantification of murine IgG deposition in glomeruli. Results were presented as the percentage of IgG positive area in relation to glomerular tuft area. ***p<0.001; n.s. not significant.

5.4 Effect of Ackr2 deficiency on renal leukocyte infiltration and inflammation

Immune cells infiltration exacerbates renal injury in lupus nephritis. Pro-inflammatory chemokines like CCL2, which may locally be scavenged and degraded by ACKR2, mediate the recruitment of leukocytes into nephritic kidneys, most prominently T cells and mononuclear phagocytes. To further investigate whether Ackr2 deficiency was correlated with increased renal inflammatory cell infiltrates in B6lpr mice, renal leukocyte subsets were quantified by flow cytometry in kidneys at week 28.

In comparison to WT and Ackr2-/- control mice B6lpr mice of both genotypes revealed increased renal leukocyte infiltrates (Figure 11). Moreover, Ackr2-deficient B6lpr mice showed significantly increased numbers of CD3+CD4+ T cells and CD19+ B cells, including the activated CD69+CD19+ B cell subset in the kidneys. In contrast, numbers in WT- and Ackr2-/-B6lpr mice were not different for CD11b+ mononuclear phagocytes, CD11b+Ly6G+ neutrophils, CD11b+Ly6C^{high} inflammatory macrophages, CD11b+CD11c+ DCs and CD3+CD4-CD8-autoreactive T cells (Figure 13).

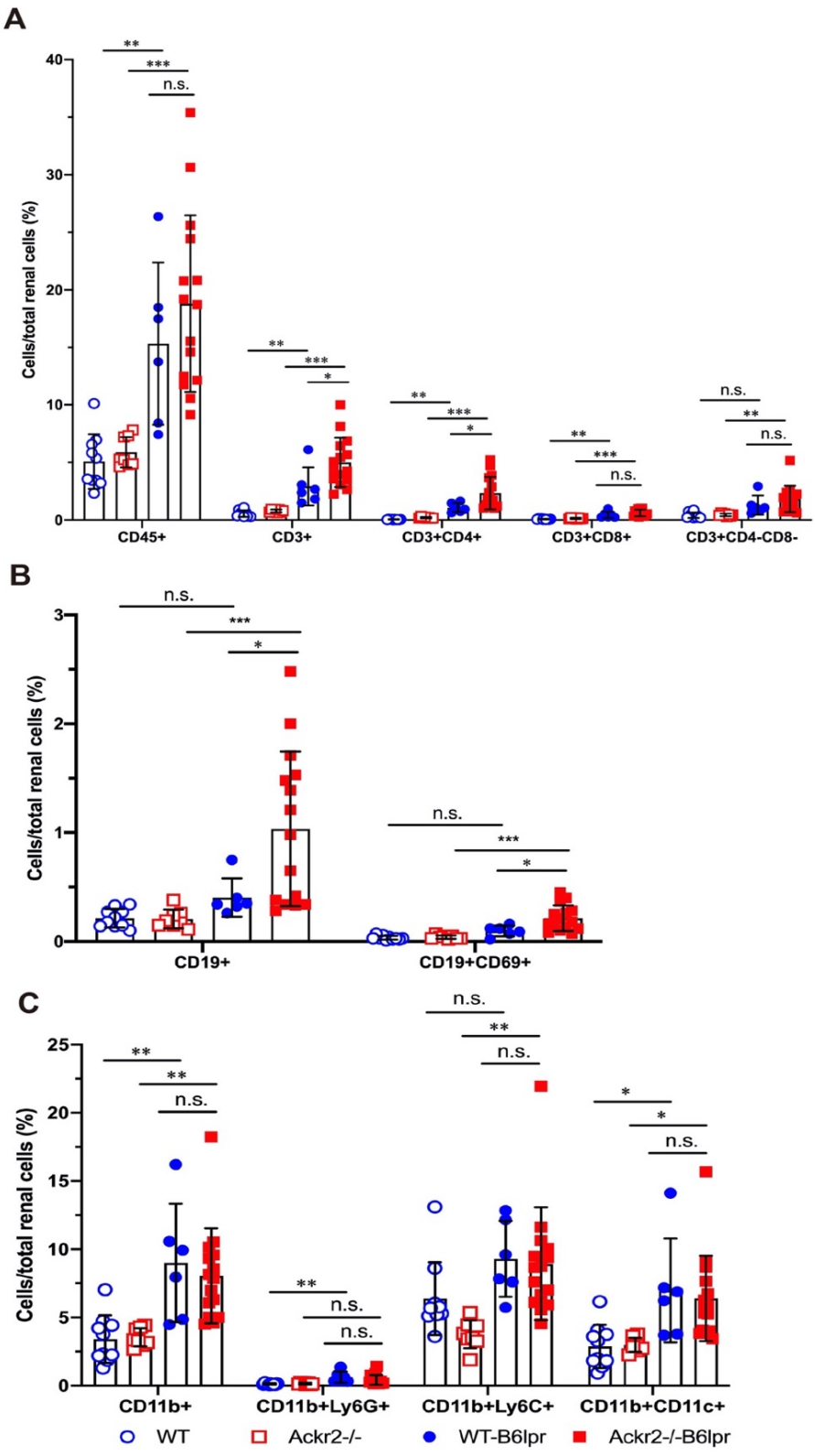

Figure 13: Effect of Ackr2 deficiency on renal leukocyte infiltrates in B6lpr mice at week 28 of lupus nephritis. Flow cytometry was applied to quantify (A) total leukocyte numbers and T cell subsets, (B) B cells, (C) mononuclear phagocytes, Ly6G+ granulocytes, Ly6C^{high} inflammatory macrophages, DCs in wildtype (WT) and Ackr2-/- control mice, and WT-B6lpr and Ackr2-/-B6lpr mice. *p<0.05; **p<0.01; ***p<0.001; n.s. not significant.

Flow cytometric analysis was confirmed by immunohistochemistry, which allowed for additional compartment-specific evaluation of renal leukocyte infiltration. Consistent to the flow cytometry results numbers of glomerular and tubulointerstitial CD3+ T cells and Ly6G+ neutrophils, as well as tubulointerstial ER-HR3+ or F4/80+ macrophages increased in WT- and Ackr2-/-B6lpr mice with lupus nephritis compared to respective controls without the lpr mutation (Figure 14). Moreover, a significant increase in tubulointerstitial, but not glomerular infiltration of CD3+ T cells was observed in Ackr2-/-B6lpr mice compared to WT-B6lpr littermates. In contrast, neutrophil and macrophage infiltrates were comparable between the two B6lpr groups as shown by flow cytometry (Figure 14).

Thus, Ackr2 deficiency in B6lpr mice increased tubulointerstitial T and B cells, but not neutrophil or macrophage infiltration into injured kidneys. However, this was not associated with more severe renal injury in Ackr2-/-B6lpr mice.

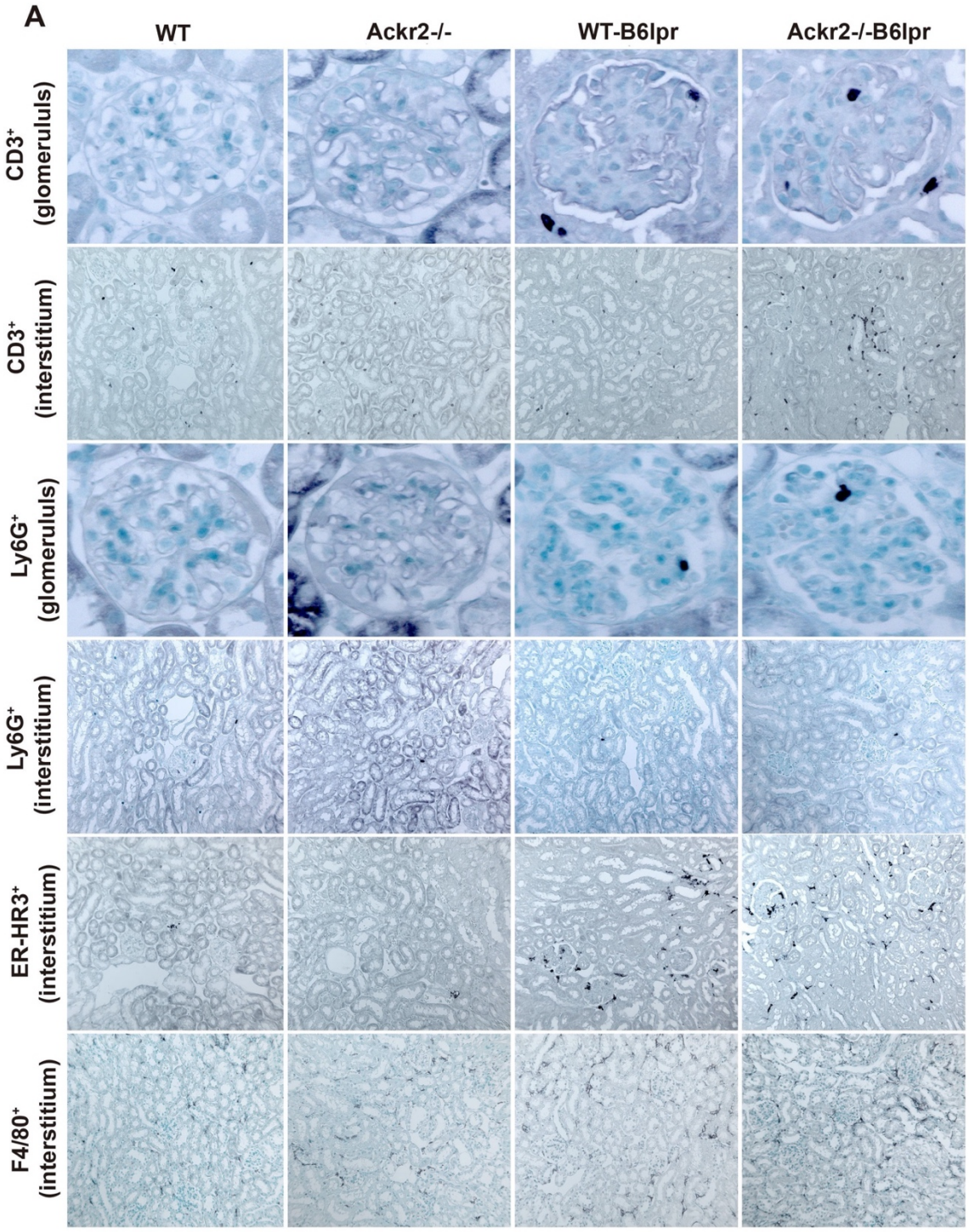
A
WT
Ackr2-/-
WT-B6lpr
Ackr2-/-B6lpr
CD3+ (glomerululs)
CD3+ (interstitium)
Ly6G+ (glomerululs)
Ly6G+ (interstitium)
ER-HR3+ (interstitium)
F4/80+ (interstitium)

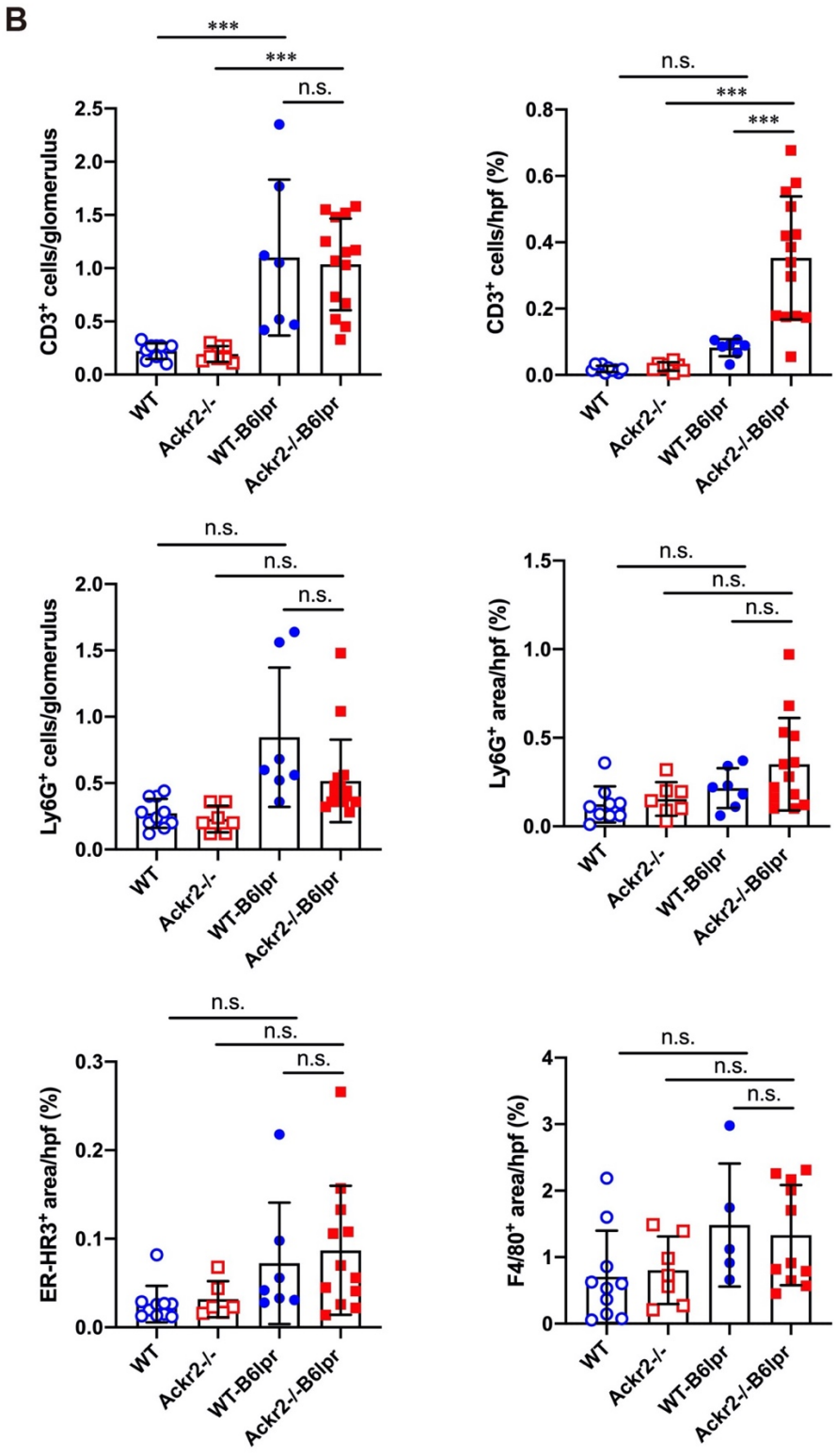

Figure 14: Compartment-specific analysis of renal leukocyte infiltration in B6lpr mice at week 28 of lupus nephritis. (A) Renal sections were stained with antibodies for CD3 (lymphocytes), Ly6G (granulocytes), and ER-HR3 and F4/80+ (macrophages). Representative images of glomeruli (original magnification x400) and interstitium (original magnification x200) from wildtype (WT) and Ackr2-/- control mice, and WT-B6lpr and Ackr2-/-B6lpr mice are shown. (B) Morphometric quantification of immunochemistry staining. ***p<0.001; n.s. not significant.

To analyze whether increased renal lymphocyte infiltrates in Ackr2-deficient B6lpr mice would correlate with more severe renal inflammation, renal expression of inflammatory mediators was investigated. First, renal CCL2 protein content was determined in WT and Ackr2-/- control mice, and in WT- and Ackr2-/-B6lpr mice at week 28 of age. Compared to WT-B6lpr mice a trend towards increased CCL2 protein levels in Ackr2-deficient B6lpr kidneys could be detected, although differences between analyzed groups did not reach statistical significance (Figure 15).

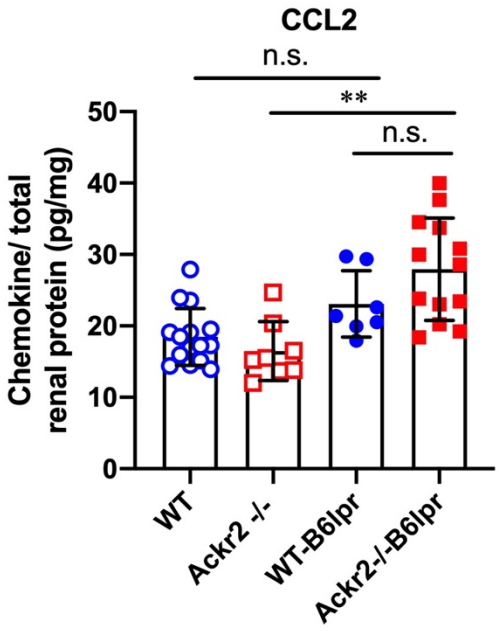

Figure 15: Renal CCL2 protein content in B6lpr mice at week 28 of lupus nephritis. Renal protein levels of CCL2 were determined in wildtype (WT) and Ackr2-/- control mice, and WT-B6lpr and Ackr2-/-lpr mice.

The mRNA expression of inflammatory chemokines, cytokines (Figure 16) as well as M1 and M2 macrophage markers (Figure 17) in healthy WT and Ackr2-/- control mice was comparable, but increased in B6lpr mice of both genotypes with lupus nephritis at week 28. However, all analyzed inflammatory mediators were similarly expressed in WT- and Ackr2-/-B6lpr mice, with the exception of a reduced expression of iNOS in Ackr2-deficient B6lpr kidneys (Figure 17).

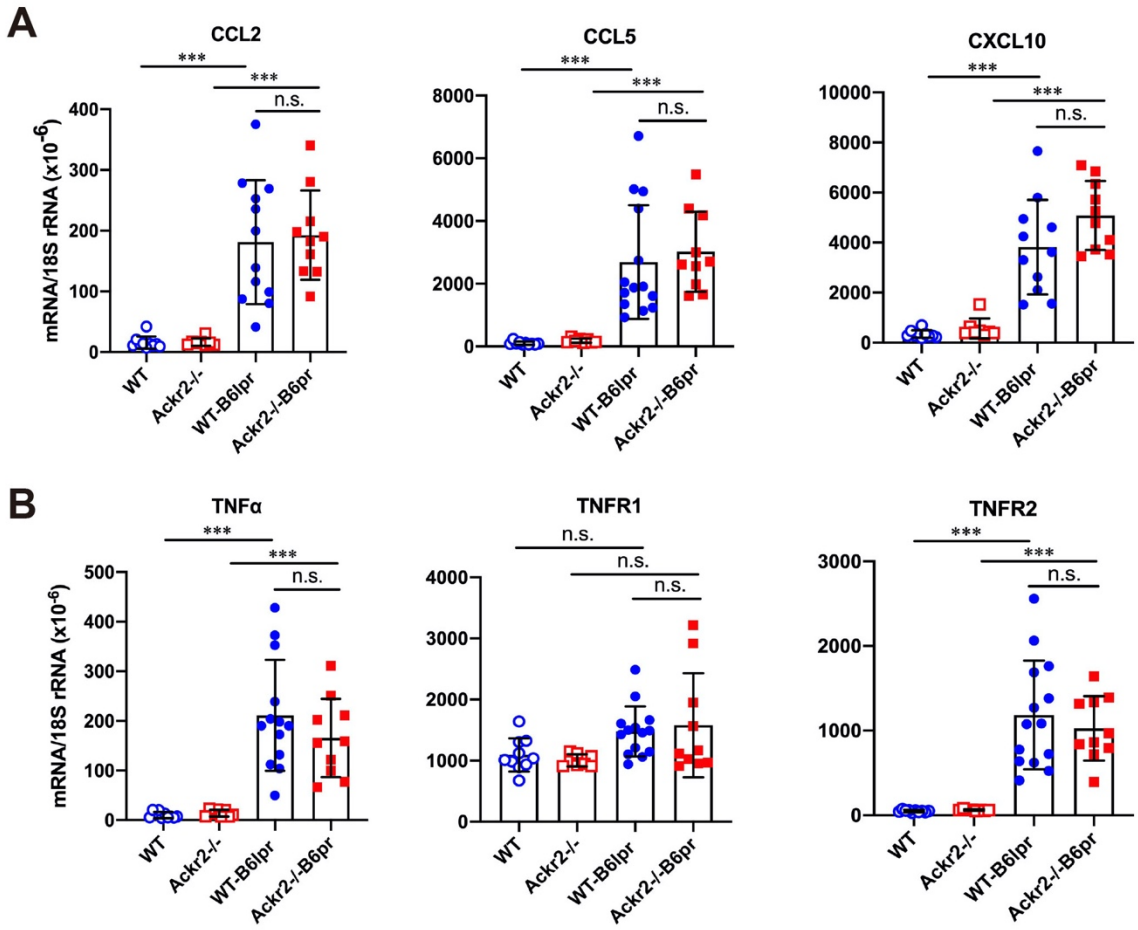

Figure 16: Effect of Ackr2 deficiency on renal mRNA expression of inflammatory markers in B6lpr mice at week 28 of lupus nephritis. Renal mRNA expression of (A) pro-inflammatory chemokines CCL2, CCL5 and CXCL10 and (B) the cytokine TNFα and its receptors TNFR1 and TNFR2 in wildtype (WT) and Ackr2-/- control mice, and WT-B6lpr and Ackr2-/-B6lpr mice. TNF, tumor necrosis factor. ***p<0.001; n.s. not significant.

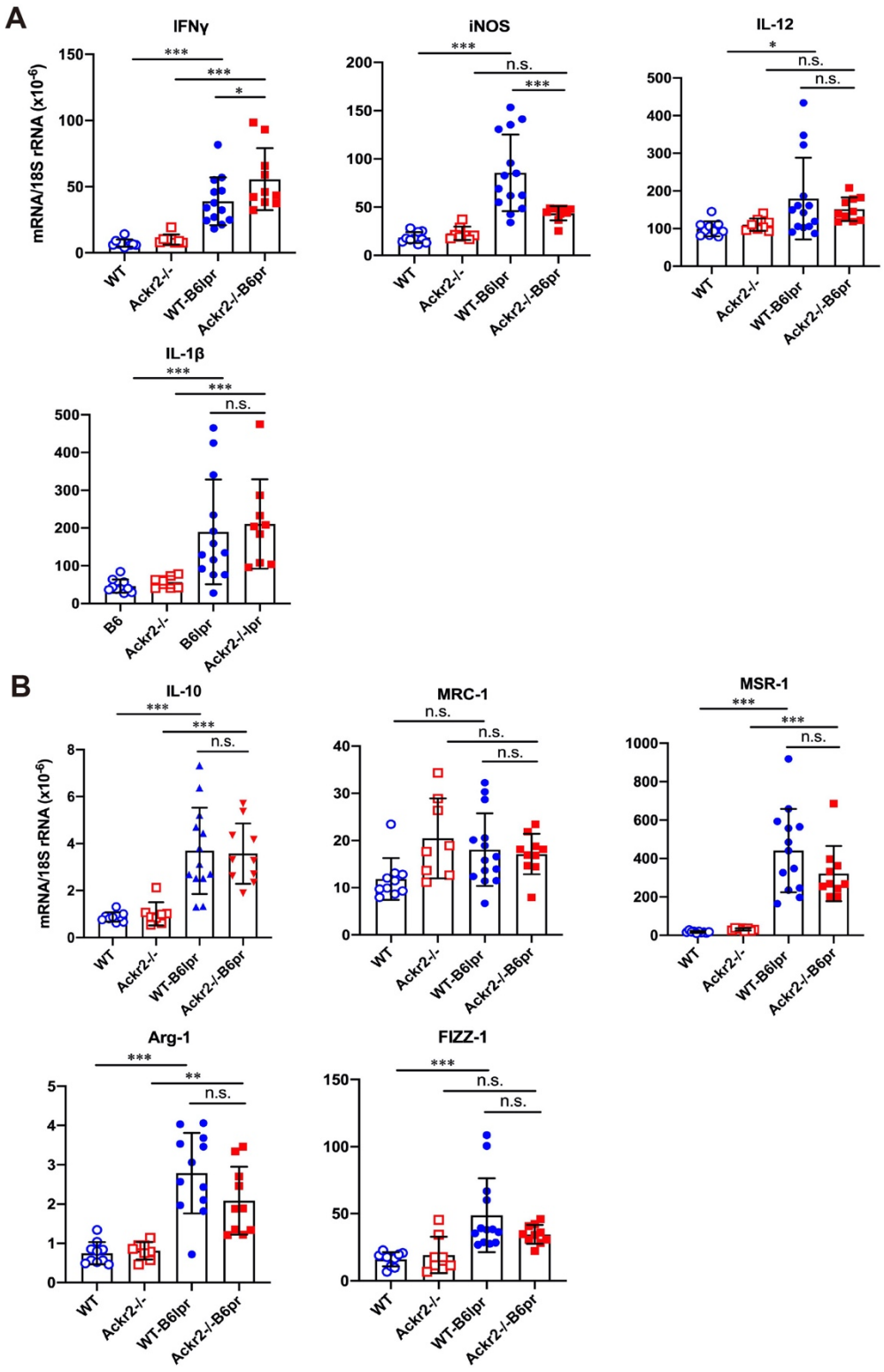

Figure 17: Effect of Ackr2 deficiency on renal mRNA expression of macrophage markers in B6lpr mice at week 28 of lupus nephritis. (A) Expression of M1 macrophage markers and (B) M2 macrophage markers in wildtype (WT) and Ackr2-/- control mice, and WT-B6lpr and Ackr2-/-B6lpr mice. IFN, interferon; iNOS, inducible nitric oxide synthase; IL, Interleukin; MSR, macrophage scavenger receptor; Arg, arginase; MRC, mannose receptor; FIZZ-1, resistin-like molecule α1. ***p<0.001; n.s. not significant.

In summary, these findings suggest that Ackr2 deficiency, despite promoting renal lymphocyte accumulation, did not lead to more severe renal inflammation in B6lpr mice. Furthermore, lack of Ackr2 did apparently not result in substantially reduced chemokine scavenging activity as CCL2 protein content was only non-significantly increased in kidneys of Ackr2-/-B6lpr mice. Apparently, loss of the chemokine scavenging activity of Ackr2 in kidneys of Ackr2-/-B6lpr mice could be compensated by alternative mechanisms, indicating a redundant role of Ackr2 in this lupus nephritis model.

5.5 Effect of Ackr2 deficiency on renal fibrosis

Persistent renal inflammation will lead to renal fibrosis, which is also a hallmark of lupus nephritis and an important prognostic marker for development of chronic renal functional impairment. An increased number of α-smooth muscle actin (SMA)-positive myofibroblasts contribute substantially to tissue fibrosis. Therefore, α-SMA staining was used to analyze the extent of kidney fibrosis. As shown in Figure 18A, in addition to physiological staining of arterial vessel walls α-SMA positive cells were mainly located in the tubulointerstitial area. However, α-SMA staining was comparable between healthy control and B6lpr mice and was not different in the respective Ackr2-deficient groups (Figure 18B). In contrast, compared to the WT and Ackr2-/- controls renal mRNA expression of extracellular matrix components and markers of fibrotic remodeling including procollagen 1, procollagen 4, fibronectin, laminin, transforming growth factor-β (TGF-β), connective tissue growth factor (CTGF), and the fibroblast marker α-SMA and the fibrosis-associated monocytic marker fibroblast-specific protein 1 (FSP-1) significantly increased in WT- and Ackr2-/-B6lpr mice, but was not different between these genotypes (Figure 18C).

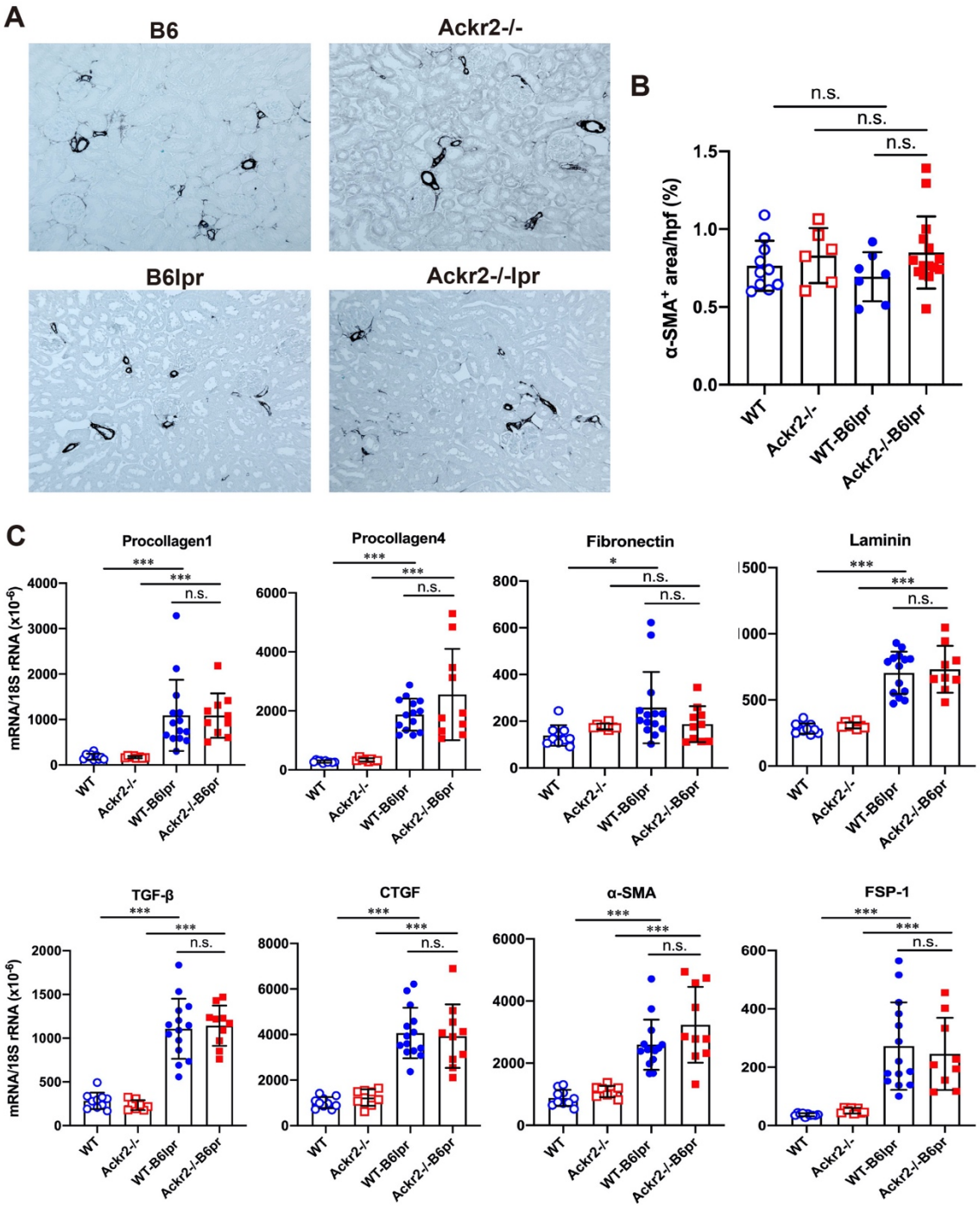

Figure 18: Effect of Ackr2 deficiency on markers of renal fibrosis in B6lpr mice at week 28 of lupus nephritis. (A) Renal accumulation of myofibroblasts was analyzed by α-SMA staining. Representative images of renal sections from wildtype (WT) and Ackr2-/- control mice, and WT-B6lpr and Ackr2-/-B6lpr mice are shown. Original magnification x200. (B) Morphometric quantification of α-SMA staining. Results are presented as the ratio of α-SMA positive area per total area of the renal section. (C) Renal mRNA expression of the fibrosis-associated markers procollagen 1, procollagen 4, fibronectin, laminin, TGF-β, CTGF, α-SMA, and FSP-1, and was analyzed in WT and Ackr2-/- healthy control and B6lpr mice. TGF-β, transferring growth factor; CTGF, connective tissue growth factor; α-SMA, α-smooth muscle actin; FSP-1, fibroblast-specific protein 1. *p<0.05; ***p<0.001; n.s. not significant.

Taken together, these results show that Ackr2 deficiency did not affect the extent of renal fibrosis in B6lpr mice with lupus nephritis at week 28, being consistent with comparable renal inflammation in WT- and Ackr2-/-B6lpr mice.

5.6 Effect of Ackr2 deficiency on autoimmune lung disease

Next to lupus nephritis SLE can lead to tissue injury in a variety of organs, and lung injury is one common manifestation in SLE. B6lpr mice developed significant autoimmune lung disease at week 28 of age, with marked peribronchial inflammation. Semiquantitative assessment of PAS-stained tissue sections demonstrated a significantly worsened lung injury score of 0.97±0.72 in Ackr2-/-B6lpr mice compared to 0.38±0.48 in WT-B6lpr mice, while lung pathology was absent in age-matched healthy WT and Ackr2-/- control mice (Figure 19). Of note, next to peribronchal T cell infiltrates no other parenchymal lung injury, e.g. alveolitis or interstitial fibrosis could be detected in WT- or Ackr2-/-B6lpr mice. Immunohistochemistry revealed significantly increased numbers of peribronchial and perivascular CD3 T cells infiltrates in Ackr2-/-B6lpr mice, whereas numbers of pulmonal granulocytes and ER-HR3 positive macrophages were comparable to WT-B6lpr mice (Figure 20).

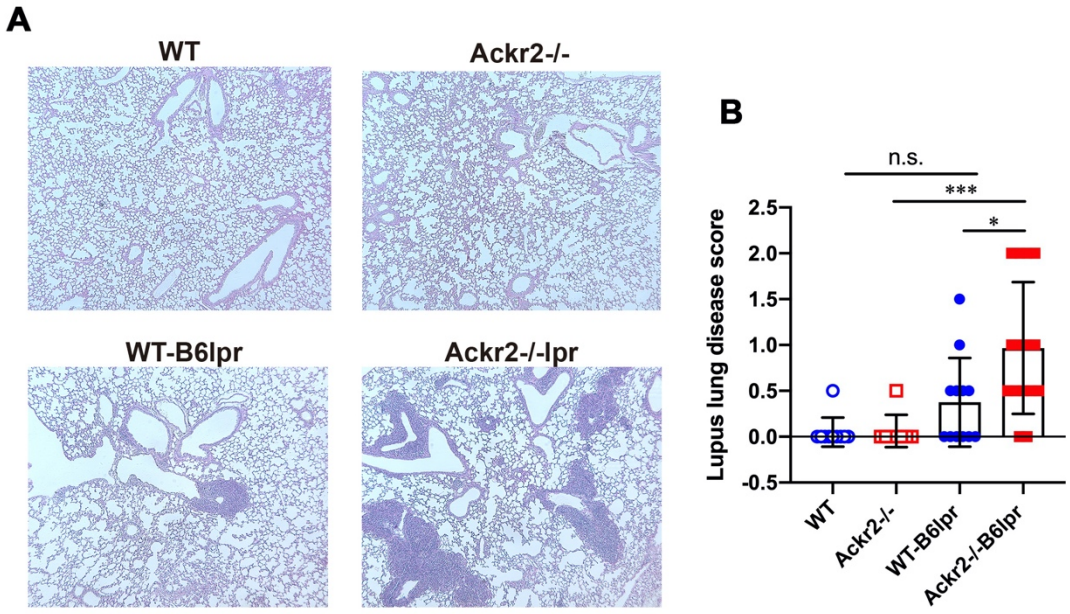

Figure 19: Effect of Ackr2 deficiency on autoimmune lung disease. (A) Representative images of PAS-stained lung sections from wildtype (WT) and Ackr2-/- control mice, and WT-B6lpr and Ackr2-/-B6lpr mice at 28 weeks are shown. Original magnification x50. (B) Lupus lung disease score as assessed by semiquantitative morphometric analysis. PAS, periodic acid-Schiff. *p<0.05; ***p<0.001; n.s. not significant.

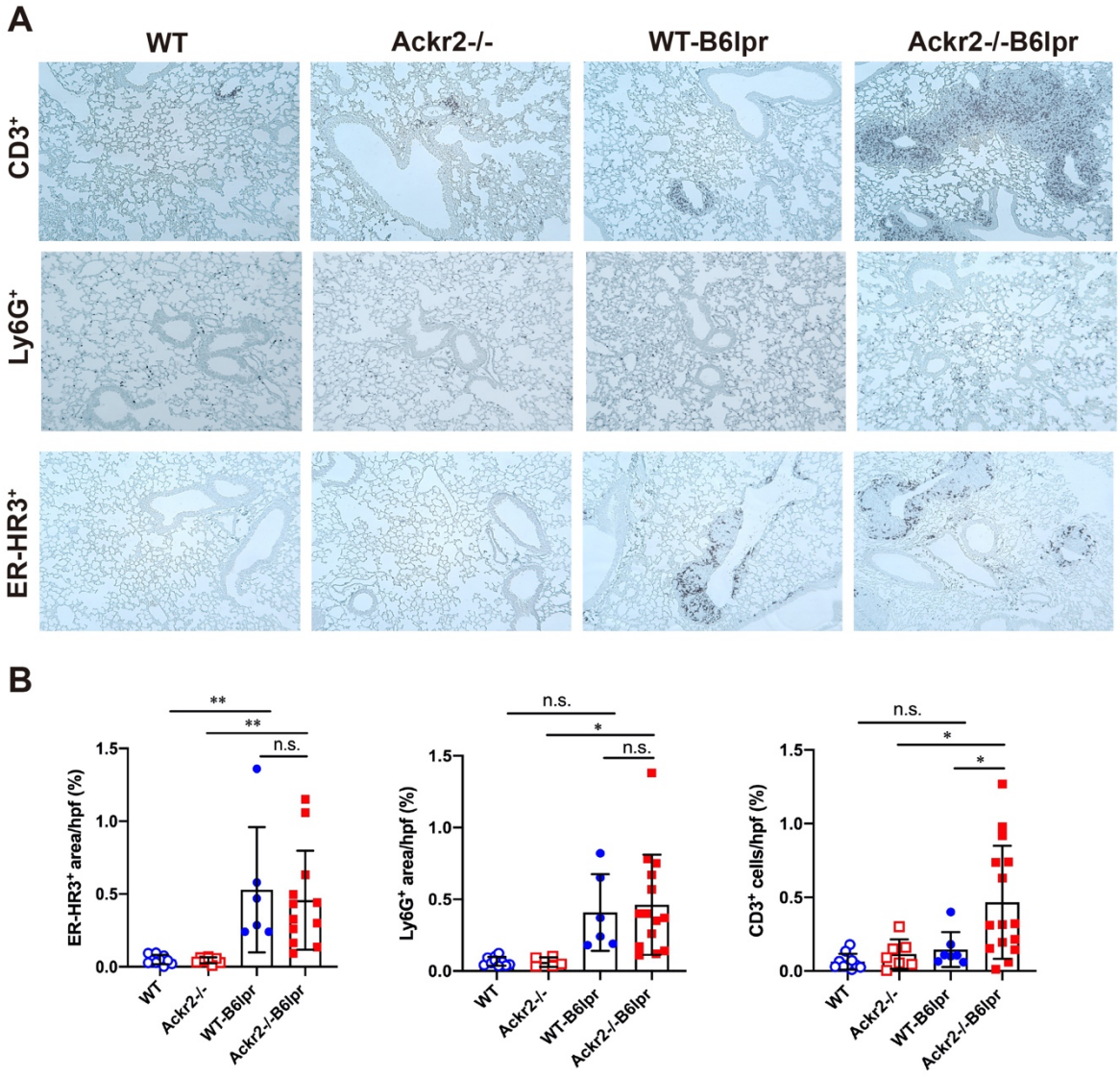

Figure 20: Effect of Ackr2 deficiency on lung leukocyte infiltration. Lung section of wildtype (WT) and Ackr2-/- control mice, and WT-B6lpr and Ackr2-/-B6lpr mice at 28 weeks were stained with antibodies for CD3 (lymphocytes), Ly6G (granulocytes), and ER-HR3 (macrophages), and Representative images of lung sections from each group are shown. Original magnification x200. (B) Quantification of immunochemistry staining. *p<0.05; **p<0.01; n.s. not significant.

As increased pulmonary T cell recruitment in Ackr2-deficient B6lpr mice may be mediated by reduced Ackr2-dependent chemokine scavenging and aggravated inflammation the extent of pulmonary inflammation in WT- and Ackr2-/-B6lpr mice was compared. However, pro-inflammatory chemokine CCL2 levels in lung tissue were not significantly different between the two genotypes, despite significantly induced mRNA expression of Ackr2 in WT-B6lpr mice compared to healthy WT controls (Figure 21). Moreover, mRNA expression of the chemokines CCL2, CCL5, CCL12, CXCL10 and the CCL2 receptor CCR2, inflammatory

cytokines like TNFα and its receptors (Figure 22) as well as M1 and M2 macrophage markers (Figure 23) were comparable between WT- and Ackr2-/-B6lpr mice, despite increased expression of several of these inflammatory mediators in B6lpr mice compared to their healthy counterparts, like CCL5, CCL2, CXCL10, CCR2, iNOS and MSR-1.

In summary, these results revealed that more severe autoimmune lung injury due to increased pulmonary T cell infiltrates is present in Ackr2-/- mice, although Ackr2 deficiency did not promote pulmonary accumulation of neutrophils or macrophages in B6lpr lupus mice. The latter correlated with comparable CCL2 tissue levels and expression of inflammatory mediators in WT- and B6lpr mice. Thus, similar to renal pathology, loss of the chemokine scavenging activity of Ackr2 in lungs of Ackr2-/-B6lpr mice model could be compensated by alternative mechanisms.

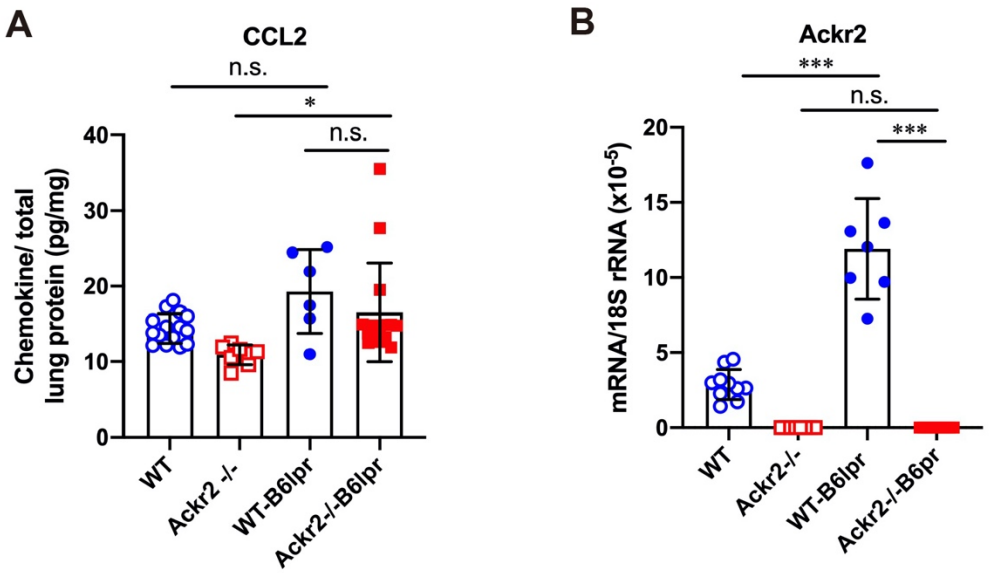

Figure 21: Pulmonary CCL2 protein content and Ackr2 mRNA expression in B6lpr mice at week 28 of age. (A) Lung protein levels of CCL2 were determined in wildtype (WT) and Ackr2-/- control mice, and WT-B6lpr and Ackr2-/-B6lpr mice. (B) Pulmonary Ackr2 mRNA expression in B6lpr mice at week 28. mRNA expression levels of Ackr2 were determined in WT and Ackr2-/- control mice, and WT-B6lpr and Ackr2-/-B6lpr mice. *p<0.05; ***p<0.001; n.s. not significant.

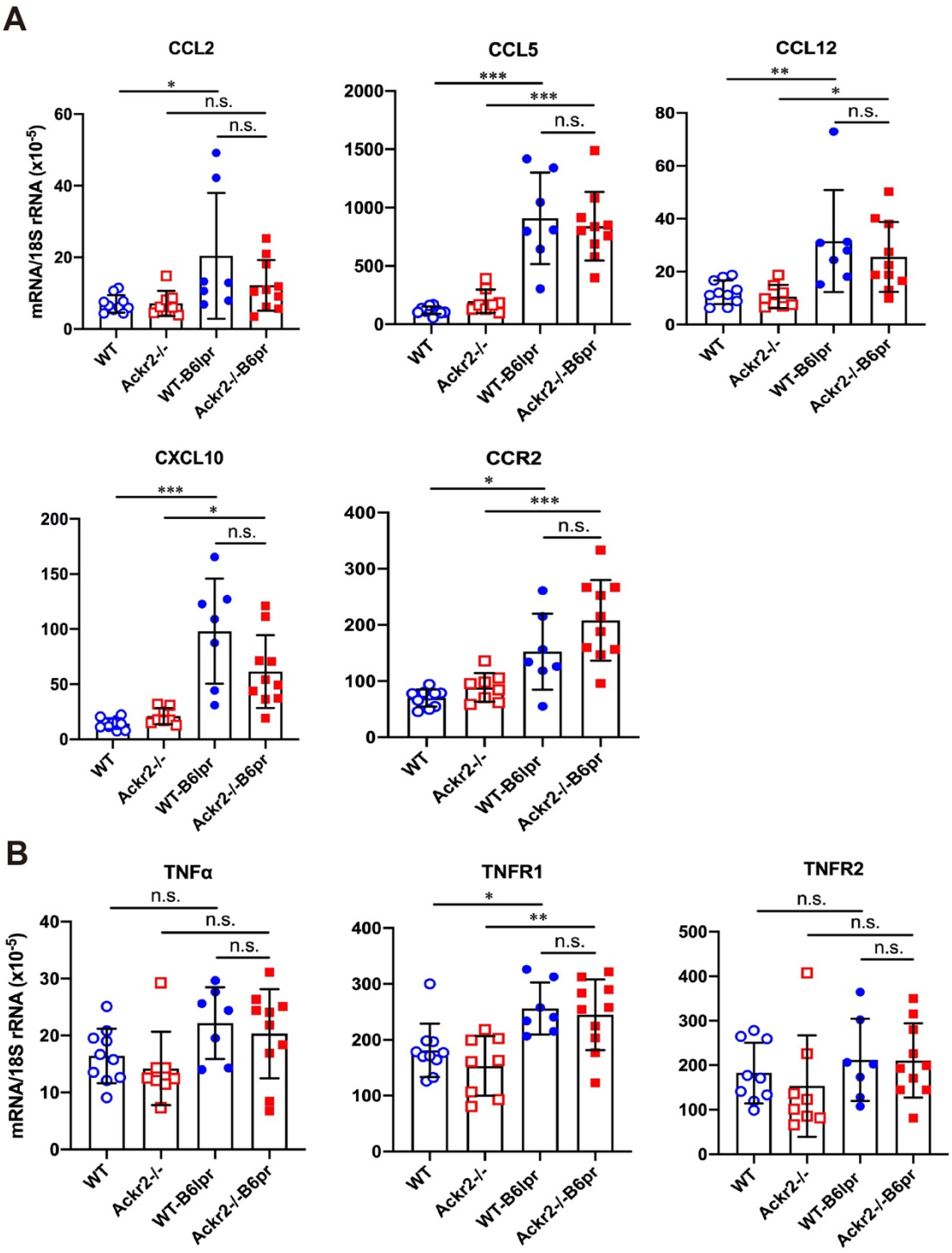

Figure 22: Effect of Ackr2 deficiency on pulmonary expression of inflammatory markers. (A) mRNA expression of pro-inflammatory chemokines CCL2, CCL5, CCL12，CXCL10 and chemokine receptor CCR2 and (B)TNFα and its receptors TNFR1 and TNFR2 in wildtype (WT) and Ackr2-/- control mice, and WT-B6lpr and Ackr2-/-B6lpr mice. *p<0.05; **p<0.01; ***p<0.001; n.s. not significant.

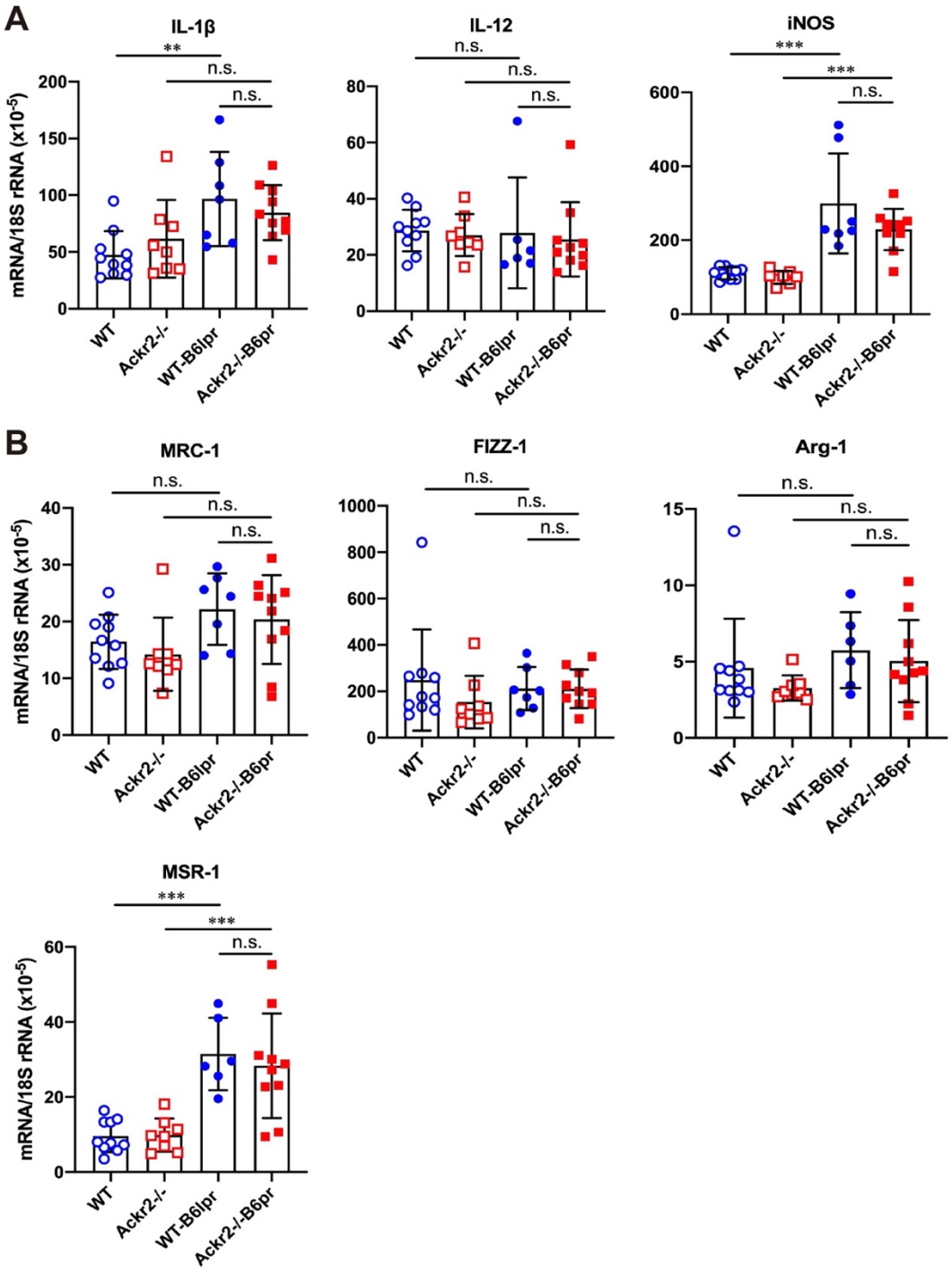

Figure 23: Effect of Ackr2 deficiency on pulmonary mRNA expression of macrophage markers in B6lpr mice at week 28 of age. (A) Expression of M1 macrophage markers and (B) expression of M2 macrophage markers was analysed in wildtype (WT) and Ackr2-/- control mice, and WT-B6lpr and Ackr2-/-B6lpr mice. IL, Interleukin; iNOS, inducible nitric oxide synthase; MRC, mannose receptor; FIZZ-1, resistin-like molecule α1; Arg, arginase; MSR, macrophage scavenger receptor. $^{**}p<0.01$; $^{***}p<0.001$; n.s. not significant.

5.7 Effect of Ackr2 deficiency on plasma CCL2 levels

To further investigated potential systemic effects of Ackr2 deficiency plasma CCL2 levels were determined in WT-B6lpr and Ackr2-/-B6lpr mice and compared to healthy controls at 28 weeks age. Plasma CCL2 concentration was significantly higher in Ackr2-/-B6lpr mice compared to Ackr2-/- control mice, and a similar trend was also observed for WT-B6lpr mice when compared to control WT mice (Figure 24). This is consistent with previous studies that reported a significant increase in CCL2 in lupus disease [162]. Moreover, CCL2 levels were significantly higher in Ackr2-/-B6lpr mice compared to WT-B6lpr littermates. Thus, this data suggests that increased T cells accumulation in kidneys and lungs could be mediated by elevated systemic level of CCL2 in Ackr2-/-lpr mice [122].

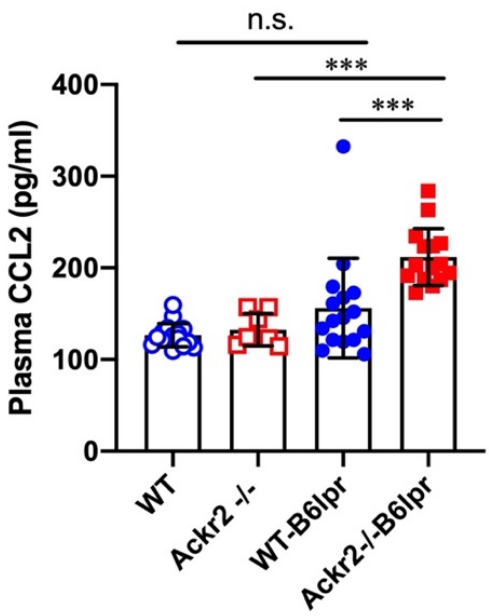

Figure 24: Plasma concentration of the pro-inflammatory chemokine CCL2. Plasma CCL2 levels were determined in wildtype (WT) and Ackr2-/- control mice, and WT-B6lpr and Ackr2-/-B6lpr mice at 28 weeks of age. ***$p<0.001$; n.s. not significant.

5.8 Effect of Ackr2 deficiency on splenomegaly and lymphadenopathy

Next, potential effects of Ackr2 deficiency on systemic autoimmune activity were investigated. Due to the lpr mutation a prominent clinical feature of lupus-like disease in B6lpr mice is a lymphoproliferative syndrome with splenomegaly and lymphadenopathy. Ackr2 mRNA expression levels in spleens were found to be significantly increased in WT-B6lpr mice with SLE compared to healthy control WT mice (Figure 25). Therefore, spleen size and total lymph node weight were analyzed in WT and Ackr2-/- control mice, and WT-B6lpr and Ackr2-/-lpr mice to detect any effect of Ackr2 deficiency on lymphroliferative disease in the B6lpr background. As shown in Figure 26A, female WT- and Ackr2-/-B6lpr mice both developed a lymphoproliferative syndrome characterized by significantly enlarged spleen and lymph nodes However, spleen weight and total lymph node weights were comparable in WT-B6lpr and Ackr2-/-B6lpr mice (Figure 26B-C). Thus, despite induced Ackr2 expression in B6lpr spleens Ackr2 deficiency did not affect the degree of lymphoproliferation in B6 lpr lupus mice.

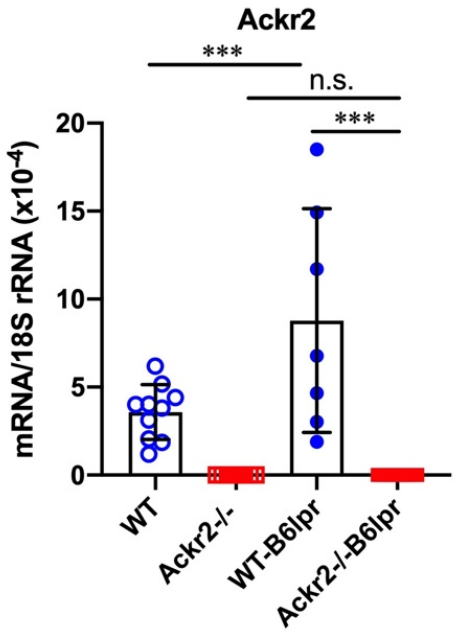

Figure 25: Spleen Ackr2 mRNA expression in B6lpr mice at week 28. mRNA expression levels of Ackr2 were determined in wildtype (WT) and Ackr2-/- control mice, and WT-B6lpr and Ackr2-/-B6lpr mice. ***p<0.001; n.s. not significant.

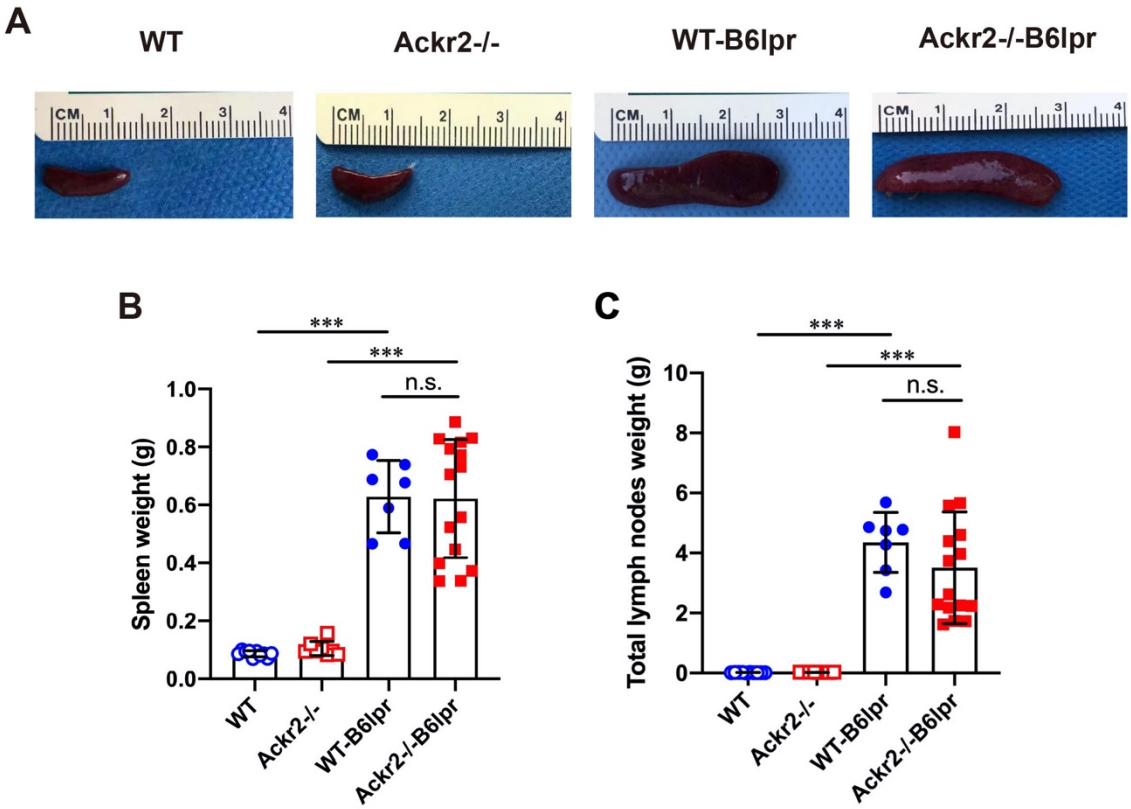

Figure 26: Effect of Ackr2 deficiency on lymphoproliferation. (A) Representative images of mice and spleens of wildtype (WT) and Ackr2-/- control mice, and WT-B6lpr and Ackr2-/-B6lpr mice at 28 weeks of age are shown. (B) Spleen and (C) total lymph node weights of all groups. ***p<0.001; n.s. not significant.

5.9 Effect of Ackr2 deficiency on lupus autoantibody levels and B cell expansion

The formation of anti-nuclear autoantibodies represents a crucial element in the pathogenesis of SLE and lupus nephritis. Therefore, the effect of the Ackr2 genotype on lupus autoantibody production was evaluated. At 28 weeks of age, plasma levels of total IgG and IgG1 isotype significantly increased in WT- and Ackr2-/-B6lpr mice compared to their respective healthy WT and Ackr2-/- controls. However, total IgG and all IgG isotype levels were comparable in WT- and Ackr2-/-B6lpr mice, demonstrating unaltered humoral immune activity in Ackr2-deficient B6lpr mice (Figure 27A). In regards to specific anti-nuclear autoantibodies, plasma levels of dsDNA autoantibodies, anti-histone antibodies, rheumatoid factor (RF) and Smith autoantibodies increased in B6lpr mice but were also comparable between WT- and Ackr2-/-B6lpr mice (Figure 27B).

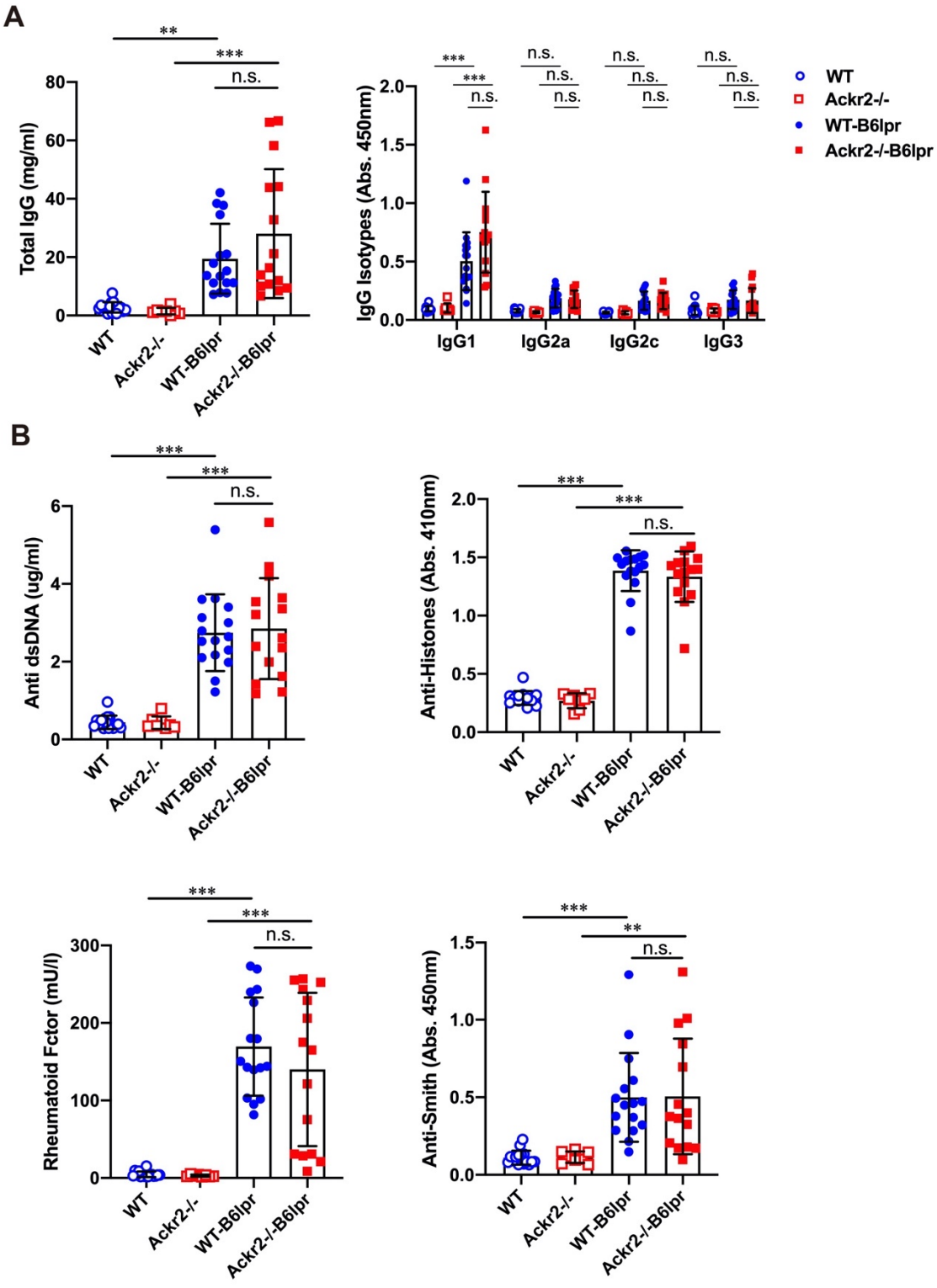

Figure 27: Effect of Ackr2 deficiency on plasma levels of total IgG, IgG isotypes and lupus autoantibody production. Wildtype (WT) and Ackr2-/- control mice, and WT and Ackr2-/- B6lpr mice were bled at the end point of the study to determine plasma levels of (A) total IgG and IgG isotypes and (B) various lupus autoantibodies including dsDNA autoantibodies, anti-histone antibodies, rheumatoid factor, and anti-Smith antibody by ELISA. **p<0.01; ***p<0.001; n.s., not significant.

Consistent with the similar levels of circulating lupus autoantibodies, flow cytometry did not reveal any differences in total numbers of various B cell subsets and plasma cells in spleens of WT-B6lpr and Ackr2-/-B6lpr mice, although most of these cells were increased in both B6lpr genotypes compared to healthy controls (Figure 28A). Leukocyte subtypes investigated included total number of B cells, transitional B cells, mature B cells, follicular B cells, marginal zone B cells, and plasma cells. Similar results were obtained when the total number of B cells and plasma cells was determined in lymph node tissue, with the exception of significantly lower numbers of plasma cells in lymph nodes of Ackr2-/- B6lpr mice (Figure 28B).

Together, this data suggests that Ackr2-deficiency in B6lpr mice did not substantially alter systemic humoral autoimmune responses indicated by comparable SLE autoantibody levels in WT- and Ackr2-/-B6lpr mice. In addition, B cell numbers were not significantly affected, although in lymph nodes plasma cells significantly decreased in the Ackr2-/-B6lpr group. However, with comparable plasma cell numbers in spleens the latter did apparently not affect systemic humoral autoimmune activity and the production of autoantibodies that cause immune complex glomerulonephritis in SLE.

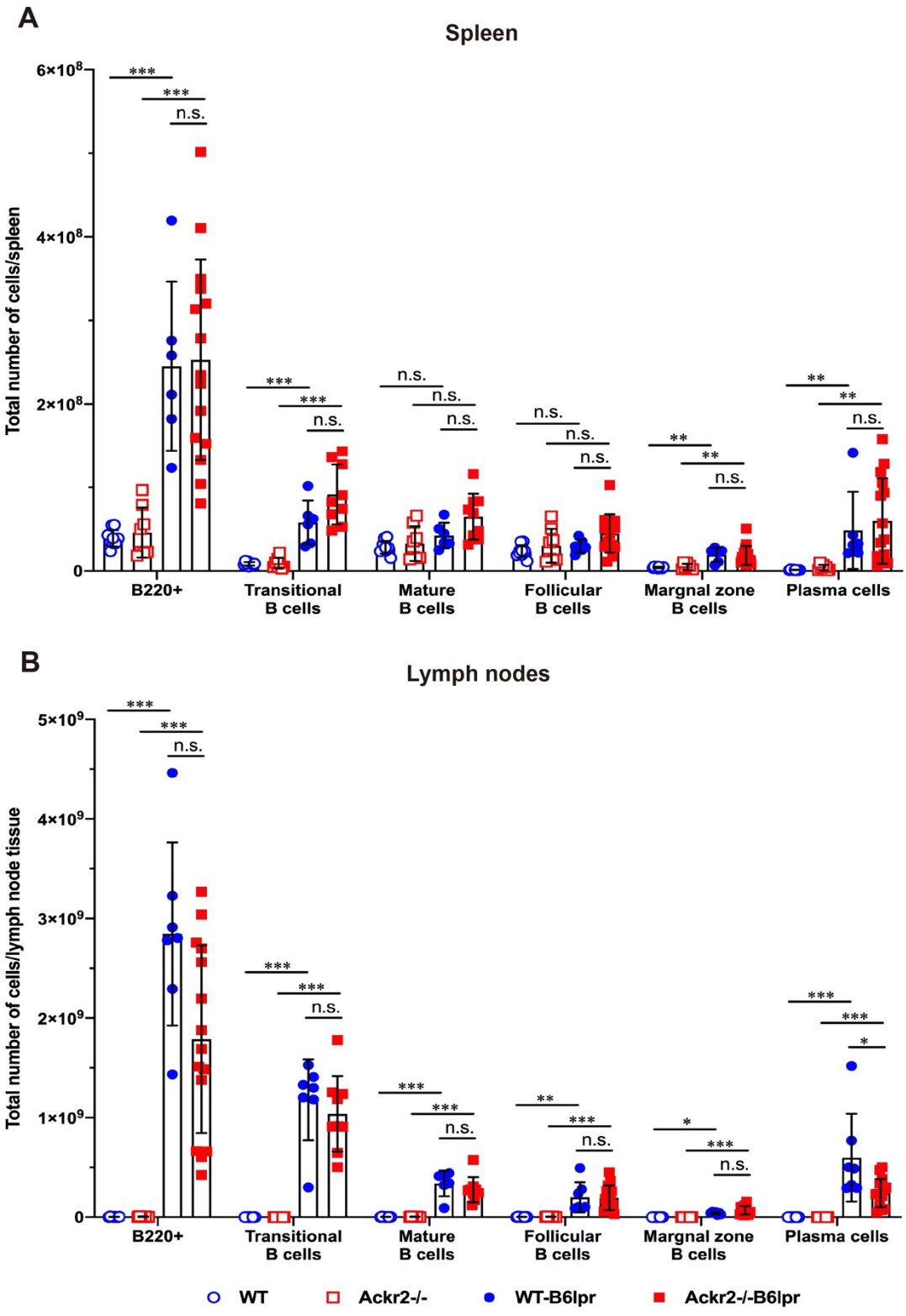

Figure 28: Effect of Ackr2 deficiency on numbers of B cell subsets in spleen and lymph nodes. (A) Spleen B cell subsets and (B) lymph node B cell subsets were quantitated by flow cytometry identifying B220+ IgM+ transitional B cells, B220+ IgM+ IgD+ mature B cells, B220+ CD21^{high} CD23^{low} marginal zone B cells, B220+ CD21^{low} CD23^{high} follicular B cells, and B220+ CD138+ plasma cells. *p<0.05; **p<0.01; ***p<0.001; n.s., not significant.

5.10 Effect of Ackr2 deficiency on the accumulation and activation of dendritic cells and macrophages

ACKR2 has been described to facilitate the migration of antigen-presenting cells to draining lymph nodes for effective T cell priming by reducing pro-inflammatory chemokine concentrations in draining lymphatic capillaries [163]. Therefore, flow cytometry was performed to quantify DC subsets and characterize their activation state in spleens and lymph nodes harvested from WT and Ackr2-/- control mice, WT-B6lpr mice, and Ackr2-/-B6lpr mice at 28 weeks of age. Total numbers of DCs and several DC subsets were significantly higher in WT- and Ackr2-/-B6lpr spleens compared to respective healthy control mice, but were not significantly different (Figure 29A). Consistent with this finding mRNA expression of the DC-related IFN-dependent genes Ifit1, TLR7 and TLR9 were comparable in spleens of both strains (Figure 29C). Total DC numbers in lymph nodes were similarly increased in B6lpr mice of both genotypes compared to WT and Ackr2-/- control mice. However, in lymph node tissue Ackr2-/-B6lpr mice showed significantly lower numbers of CD11c+MHCII+ DCs, CD11c+CD4+ DCs, and CD11c+CD40+ activated DCs in comparison to WT-B6lpr littermates (Figure 29B).

Analysis of macrophage accumulation revealed that numbers of both CD11b+ myeloid leukocytes and CD11b+ F4/80+ MHCII+ macrophages were elevated in spleens and lymph nodes of WT- and Ackr2-/-B6lpr mice compared with healthy control mice, but were comparable in the two B6lpr groups (Figure 30).

In summary, these results indicate that consistent with earlier reports [140] [163] Ackr2 deficiency reduced numbers of activated DCs in lymph nodes of B6lpr mice, possibly due to impaired influx from peripheral tissues due to less chemokine scavenging in draining lymphatics. This may also contribute to reduced generation of plasma cells, which were also found to be reduced in lymph nodes of Ackr2-/-B6lpr mice. However, Ackr2 deficiency did not alter numbers of DCs in spleens, which may explain overall comparable systemic autoimmune activity in WT- and Ackr2-/-B6lpr mice.

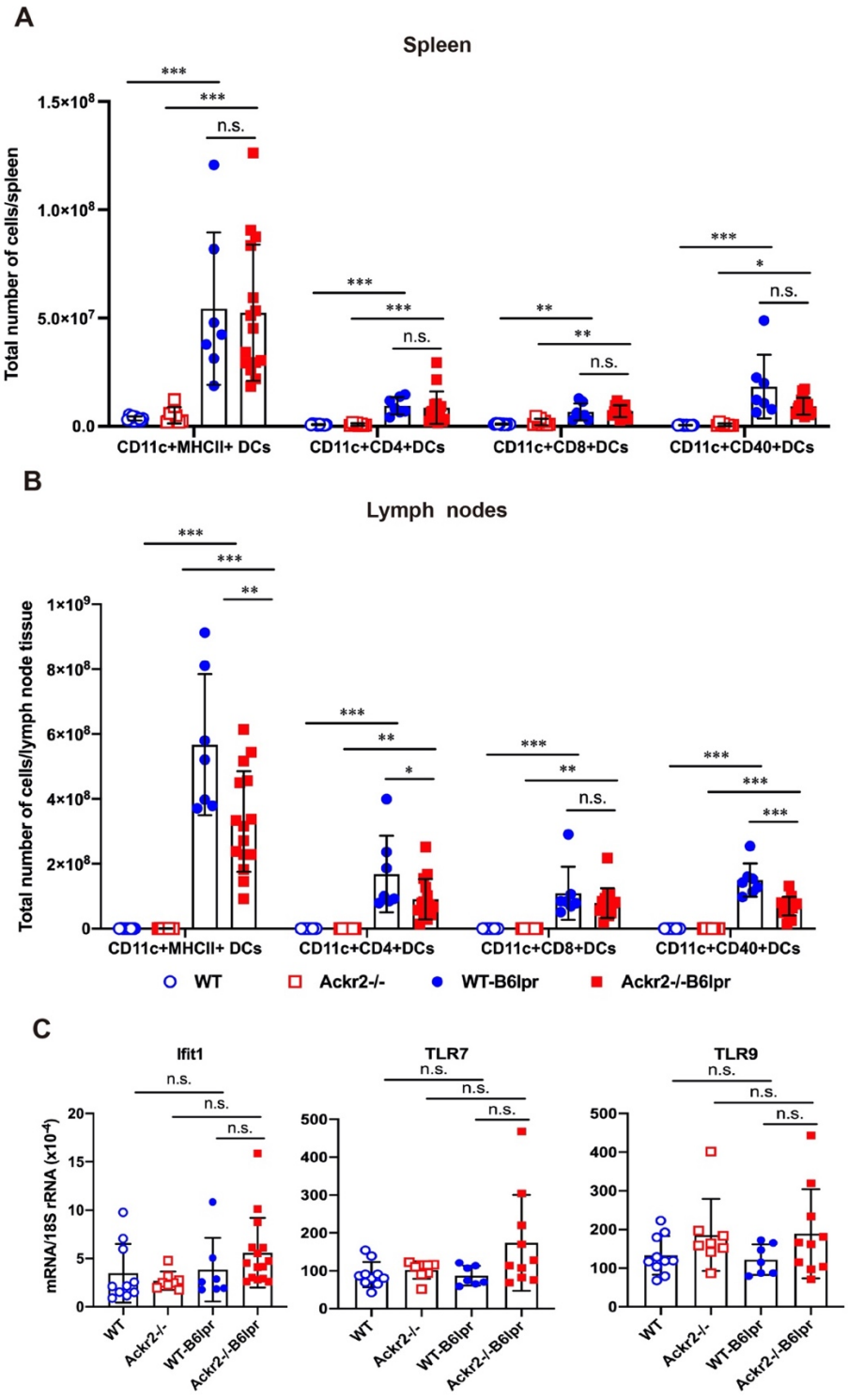

Figure 29: Effect of Ackr2 deficiency on dendritic cells in spleens and lymph nodes of B6lpr mice. (A) Dendritic cell (DC) subsets in spleen and (B) lymph nodes from wildtype (WT) and Ackr2-/- control mice, and WT-B6lpr and Ackr2-/-B6lpr mice were quantified by flow cytometry. (C) mRNA expression levels of the IFNα-dependent genes Ifit1, TLR7, and TLR9 in splenocytes were determined by real-time quantitative PCR. MHCII, major histocompatibility complex II; Ifit, interferon-induced protein with tetratricopeptide repeats; TLR, toll like receptor. *p<0.05; **p<0.01; ***p<0.001; n.s., not significant.

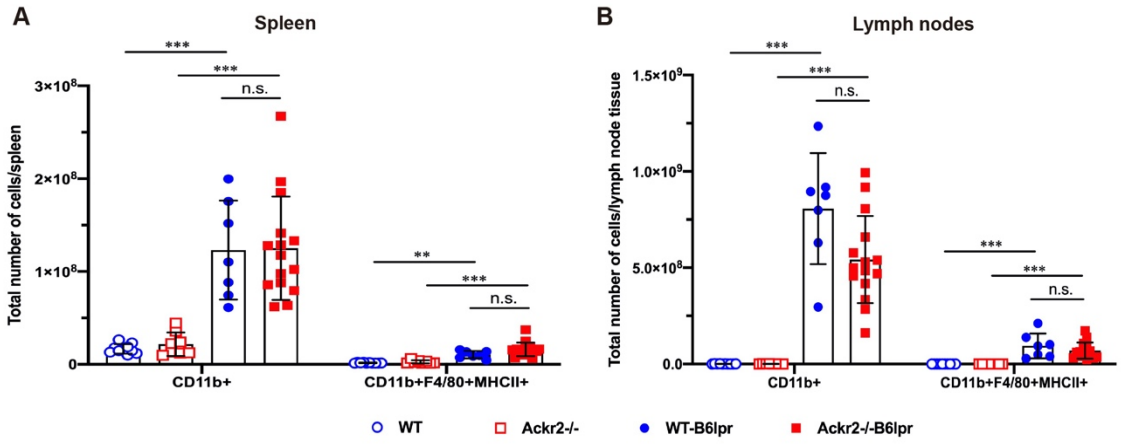

Figure 30: Effect of Ackr2 deficiency on numbers of myeloid leukocytes and macrophages. (A) Spleen and (B) lymph node cells from wildtype (WT) and Ackr2-/- control mice, and WT-B6lpr and Ackr2-/-B6lpr mice were quantified by flow cytometry Myeloid cells and Macrophages were identified as CD11b+ and CD11b+F4/80+MHCII+ leukocytes, respectively. $^{**}p<0.01$; $^{***}p<0.001$; n.s., not significant.

5.11 Effect of Ackr2 deficiency on the expansion of T cells

To further investigate whether altered DC numbers and activation in lymph nodes of Ackr2-/-B6lpr mice affected systemic activation of T cells, various T cell subsets were quantified in spleens and lymph nodes of mice at 28 weeks of age by flow cytometry. The results indicated that total number of CD3+CD4+ T cells, activated CD69+ CD3+CD4+ T cells, and CD4+CD25+ regulatory T cells in spleens were significantly increased in Ackr2-/-B6lpr compared to WT-B6lpr mice, whereas T cell numbers in spleens of WT and Ackr2-/- control mice were low (Figure 31). In contrast, numbers of CD3+CD8+ T cells and autoreactive CD3+CD4-CD8-/- were similar in WT- and Ackr2-/-B6lpr spleens.

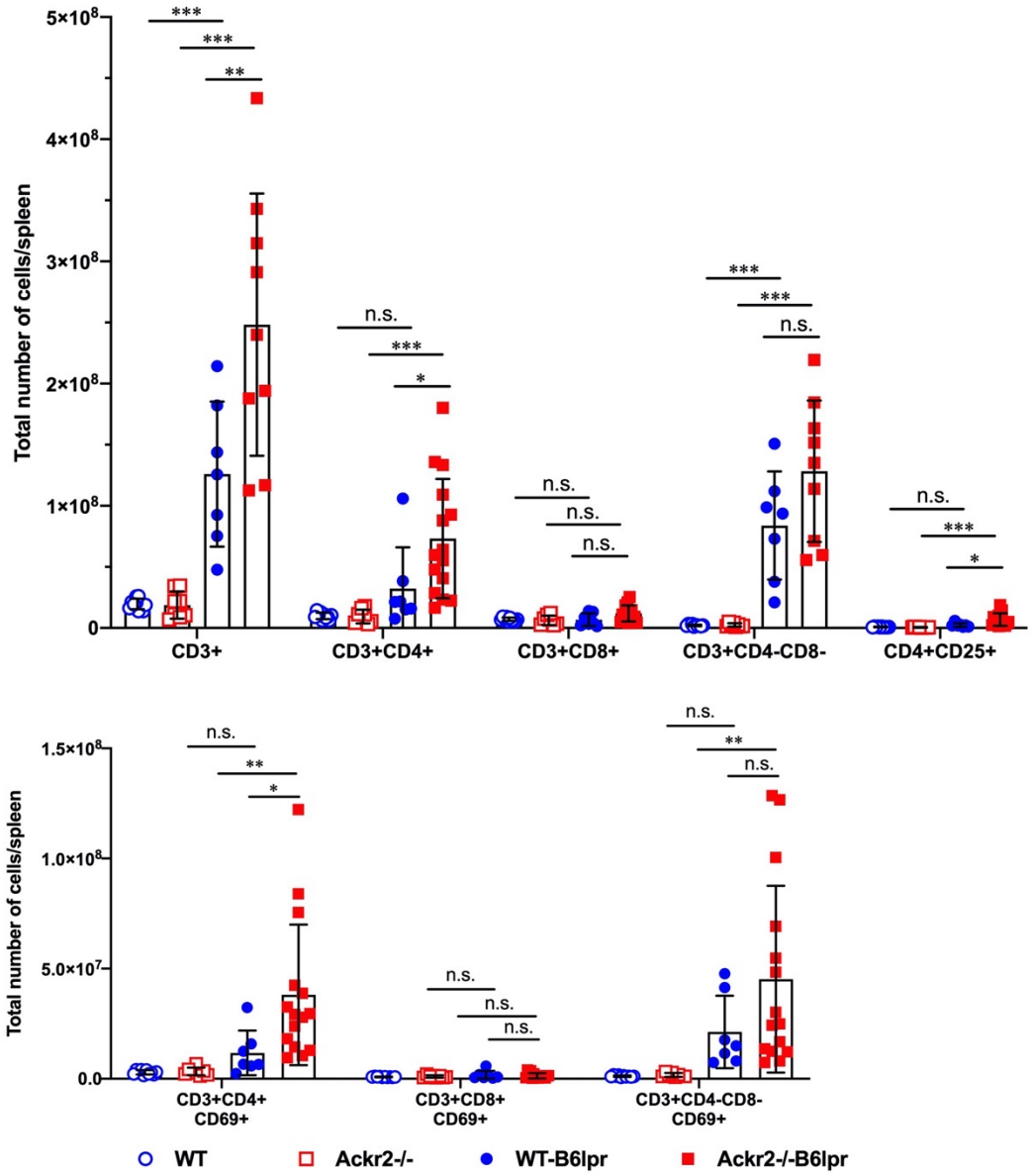

Figure 31: Effect of Ackr2 deficiency on T cell numbers and activation in spleens. T cells subsets and the number of CD69+ activated T cells were determined by flow cytometric analysis of spleens from wildtype (WT) and Ackr2-/- control mice, and WT-B6lpr and Ackr2-/-B6lpr mice at week 28 of age. *p<0.05; **p<0.01; ***p<0.001; n.s., not significant.

Moreover, despite reduced accumulation of activated DCs in Ackr2-/-B6lpr lymph nodes T cell numbers and activation in lymph nodes was comparable between WT-B6lpr and Ackr2-/-B6lpr mice (Figure 32).

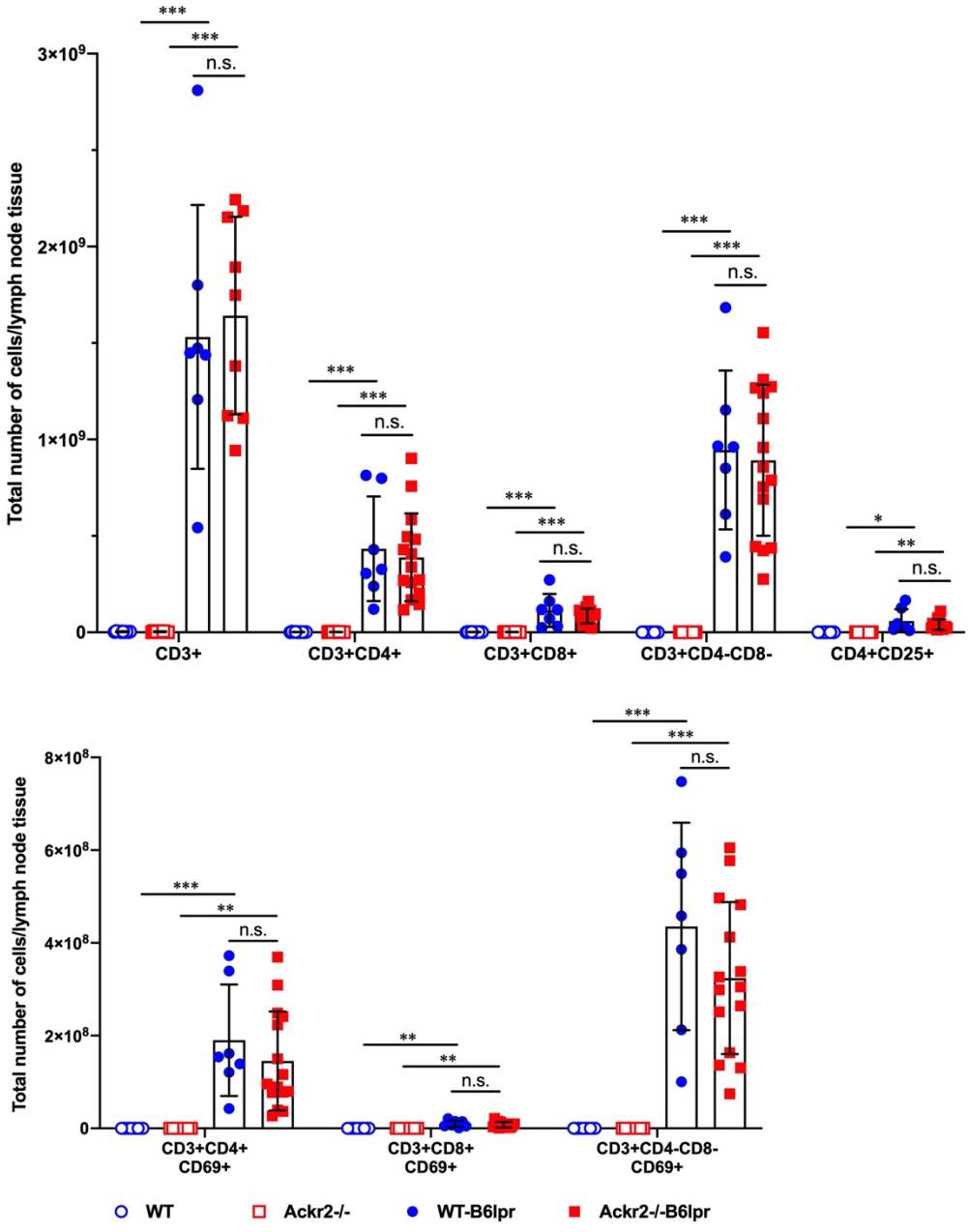

Figure 32: Effect of Ackr2 deficiency on T cell numbers and activation in lymph nodes. T cells subsets and the number of CD69+ activated T cells were determined by flow cytometric analysis of lymph nodes from wildtype (WT) and Ackr2-/- control mice, and WT-B6lpr and Ackr2-/-B6lpr mice at week 28 of age. *p<0.05; **p<0.01; ***p<0.001; n.s., not significant.

Therefore, Ackr2 deficiency promoted CD4+ T cell accumulation including regulatory T cell subsets in spleens of B6lpr mice, similarly to increased T cell infiltrates in affected organs of Ackr2-/-B6lpr mice like kidney and lung. Instead, reduced numbers of activated DCs in lymph nodes of Ackr2-deficient B6lpr mice did not translate into reduced T cell activation in this compartment. Higher levels of plasma CCL2 levels in Ackr2-/-B6lpr mice suggest that increased mobilization of T cells from bone marrow may contribute to their increased infiltration into solid organs like spleen, kidney, and lung.

6. Discussion

The ACKR family currently consists of four members, which are mainly expressed by cell types other than leukocytes, such as erythrocytes and lymphatic and vascular endothelial cells. However, ACKR2 expression has also been detected in leukocyte subtypes, such as DCs, T cells and macrophages [122]. Previous studies have demonstrated that ACKR2 is a key regulator of lymphatic biology, including lymphatic vessel function and density [164,165]. Moreover, due to its chemokine scavenging function ACKR2 is also involved in limiting inflammatory processes and leads to the resolution of inflammation, including *Mycobacterium tuberculosis* infection [166], skin inflammation [167] and cardiac remodeling [168]. However, the lack of Ackr2 in mice can also lead to the improvement of autoimmune disease such as EAE due to impaired T cell priming in draining lymph nodes and reduced encephalitogenic responses [128]. It was postulated that ACKR2 expression by lymphatic endothelial cells reduced local chemokine concentrations which allows migration of activated DCs into regional lymph nodes [163]. Since all of these functions play a critical role in the pathogenesis of autoimmune diseases and resulting tissue damage, it was assumed that ACKR2 may have a decisive influence on systemic autoimmunity and autoimmune organ injury. ACKR2 could either augment autoimmunity by facilitating adaptive immune responses or may inhibit the development of autoimmunity and reduce tissue injury due to its anti-inflammatory effects.

To investigate this hypothesis, Ackr2-/- mice were crossed with Fas-mutated (lpr) mice to generate Ackr2-/-B6lpr mice and WT-B6lpr littermate controls. B6lpr mice develop an autoimmune disease that is comparable to human SLE.

The results of this study revealed that systemic cellular and humoral autoimmune activity was not substantially altered in Ackr2-deficient B6lpr mice. Some distinct effects of Ackr2 deficiency could be seen, including reduced accumulation of activated DCs in lymph nodes and increased activation of splenic C4+ T cells, including regulatory CD4 T cell subsets. These pro- and anti-inflammatory effects, however, may balance each other leading to a grossly unaffected systemic autoimmune response in Ackr2-/-B6lpr mice. Thus, the extent of splenomegaly and lymphadenopathy was comparable between WT- and Ackr2-/-B6lpr mice, as were levels of circulating lupus autoantibodies and the extent of glomerular IgG deposition. Consistently, Ackr2 deficiency did not affect numbers of effector leukocyte subsets like neutrophils and macrophages systemically in spleen and lymph nodes nor locally in injured kidneys and lungs.

Moreover, tissue levels of the ACKR2 ligand CCL2 did not increase in diseased kidneys and lungs of Ackr2-/-B6lpr mice compared to WT littermates, indicating a redundant role of Ackr2 in controlling local chemokine levels in this SLE model. Apparently, loss of the chemokine scavenging activity of Ackr2 in injured organs could be compensated by alternative mechanisms.

Despite this, lymphocyte infiltrates including CD4+ T cells and B cells were increased in Ackr2-/-B6lpr kidneys, as was peribronchial T cell infiltration in lungs. This expansion of tertiary lymphoid tissue may be mediated by increased plasma levels of CCL2 facilitating mobilization of lymphocytes, e.g. from the bone marrow.

Together, sufficient autoimmune responses with increased systemic chemokine levels in the circulation, but persevered chemokine scavenging activity in kidneys and lungs of Ackr2-deficient B6lpr mice lead to increased lymphocyte infiltration into these organs without affecting accumulation of effector leukocyte subsets, local inflammation or clinical significant organ injury.

6.1 Ackr2 scavenges pro-inflammatory chemokines in tubulointerstitial tissue of B6lpr mice in vitro and limits accumulation of lymphocytes in parenchymal organs of B6lpr mice with SLE in vivo

The initial *in vitro* experiments performed in this work revealed higher CCL2 chemokine levels in supernatants of TNFα-stimulated tubulointerstitial tissue, but not glomeruli isolated from Ackr2-/-B6lpr mice compared to WT-B6lpr littermates. Due to the analysis of isolated renal tissue *in vitro*, increased chemokine production was independent of potentially altered renal leukocyte infiltration. These results were consistent with previously reported similar findings in WT and Ackr2-/- C57Bl/6 mice without the lpr mutation [140]. They demonstrate Ackr2-dependent chemokine scavenging activity in the renal tubulointerstitial compartment and correlate with the known renal expression of Ackr2 in lymphatic endothelial cells [136,140], which are present in the tubulointerstitium, but not in glomeruli. Moreover, mRNA expression analysis showed induced expression of Ackr2 in WT-B6lpr mice at week 28 of age compared to healthy control mice. Together, these data supported the hypothesis of this work suggesting a potential anti-inflammatory role of ACKR2 in lupus nephritis by limiting local availability of pro-inflammatory chemokines.

Reduced capability of Ackr2-deficient B6lpr mice to down-regulate pro-inflammatory chemokines in inflamed kidneys may facilitate renal leukocyte recruitment. Increased renal leukocyte infiltration was present in Ackr2-/-B6lpr kidneys compared to kidneys of WT-B6lpr littermates. Flow cytometry revealed that the individual leukocyte populations which were significantly increased were primarily CD4+ T cells and B cells, but not granulocytes, macrophages or DCs. Increased renal T cell infiltration in Ackr2-/-B6lpr mice was also confirmed by immunochemistry staining and evaluated specifically for the glomerular and tubulointerstitial compartments. In contrast to increased tubulointerstitial accumulation of T cells in Ackr2-deficient B6lpr kidneys, the number of glomerular T cells was comparable between WT- and Ackr2-/-B6lpr mice. This data is consistent with a reduced ability of Ackr2-deficient tubulointerstitial tissue for chemokine scavenging in inflamed kidneys with lupus nephritis, most likely due to absent Ackr2 expression in interstitial lymphatic endothelium.

When investigating lung pathology in B6lpr mice similar results could be found. Pulmonary Ackr2 mRNA expression was induced in WT-B6lpr mice compared to healthy WT controls, and peribronchial T cell infiltration significantly increased in Ackr2-deficient B6lpr mice in comparison to the WT-B6lpr group.

T cells from lupus-prone mice and SLE patients are aberrantly activated and thus contribute to induction and progression of SLE and tissue injury [169-171]. Previous studies in other disease models also demonstrated that exacerbated tissue injury was paralleled by increased T cell infiltration in Ackr2-deficient mice. For example, in T-helper 2 (Th2) cell-dependent ovalbumin-induced asthma, a significantly higher number of T cells was observed in the lung parenchyma of Ackr2-/- mice [148]. Additionally, in a mouse model of psoriasis, Ackr2-deficient mice displayed a notably exacerbated inflammatory pathology, characterized by increased epidermal T cells [167]. Importantly, previous studies of our laboratory also found increased CD4+ T cell infiltration into kidneys of Ackr2-/-mice in the NTN model of immune complex-mediated glomerulonephritis [140], which is in line with the findings reported here. Together, this data suggested that reduced tubulointerstitial and pulmonary chemokine scavenging in Ackr2-/-B6lpr mice could indeed facilitate local infiltration of pathogenic T cells, potentially leading to increased tissue inflammation and injury in kidney and lung.

6.2 Ackr2 does not limit organ-specific tissue damage in lupus-prone B6lpr mice

However, in kidney and lung of WT- and Ackr2-/-B6lpr mice numbers of infiltrating neutrophils and mononuclear phagocytes, including inflammatory macrophages and DCs were similar in the two groups. Correlating with equal accumulation of these effector leukocyte subsets in injured organs renal and pulmonary mRNA expression of inflammatory mediators was comparable in the two genotypes, despite increased T and B cell infiltrates. Moreover, parenchymal tissue injury in kidneys and lungs on WT-B6lpr and Ackr2-/-B6lpr mice was similar. Of note, significant renal functional impairment and overt proteinuria was absent in WT-B6lpr mice at week 28 of age. This is consistent with the known development of mild glomerulonephritis in B6lpr mice in comparison to lupus-prone mouse strains with other genetic backgrounds like MRLlpr mice. Nevertheless, WT-B6lpr mice developed renal injury, as revealed by glomerular IgG deposition, an increased lupus nephritis activity index assessed in PAS-stained kidney sections, and increased expression of the tubular injury markers KIM-1 and NGAL. Importantly, proteinuria, plasma creatinine and BUN values were not increased in Ack2-deficient B6lpr mice compared to WT littermates, and the extent of glomerular IgG deposition, the lupus nephritis activity index, and the expression of tubular injury markers were comparable between the two genotypes. Moreover, fibrotic remodeling of B6lpr kidneys was not exacerbated in Ackr2-/-B6lpr mice, as indicated by comparable numbers of α-SMA+ myofibroblasts and similar renal mRNA expression of extracellular matrix components and pro-fibrotic mediators in WT- and Ackr2-/-B6lpr mice.

Thus, accumulation of renal neutrophils, macrophages and DCs as well as renal injury, inflammation and fibrosis was not affected by Ackr2 deficiency in B6lpr mice. This is in contrast to findings in other disease models which report more severe renal functional impairment, injury, and fibrotic remodeling in Ackr2-deficient mice with immune complex-mediated glomerulonephritis due to NTN [140] or following renal IRI [136].

6.3 Ackr2 has no essential role in parenchymal chemokine scavenging in B6lpr mice with lupus-like disease

Importantly, Ackr2 deficiency did not significantly increase CCL2 protein levels in kidneys of Ackr2-/-B6lpr mice compared to WT-B6lpr littermates *in vivo*. Similar to kidneys, CCL2 protein content in pulmonary tissue was comparable between WT- and Ackr2-/-B6lpr mice. This finding is in contrast to previous work of our laboratory that found higher CCL2

concentrations in renal tissue of Ackr2-deficient mice with NTN [140] or in mice with chronic renal injury following IRI [136], which correlated with more severe renal inflammation, injury, and fibrosis in both models.

This data demonstrates that in lupus-like disease of B6lpr mice the chemokine scavenging function of Ackr2 in parenchymal tissue is redundant and compensatory mechanisms for degradation must exist which prevent excessive accumulation of chemokines in inflamed tissue of Ackr2-deficient B6lpr mice. Indeed, binding of pro-inflammatory chemokines to their canonical receptors may not only activate target cells but also leads to internalization of bound ligands. For example, some cells like Ly6C^{high} monocytes can express both ACKR2 and CCR2, which results in markedly strong CCL2 scavenging activity *in vitro* and *in vivo*, with CCR2 scavenging CCL2 much more effectively than ACKR2 [172].

One can speculate that these compensatory mechanisms are sufficient to control local chemokine levels in chronic, slowly progressive disease, like autoimmune renal and pulmonary injury developing in B6lpr mice until week 28 of age. In contrast, Ackr2-dependent chemokine clearance is apparently essential in down-regulating chemokine levels during the regeneration phase following severe initial injury, as demonstrated in the NTN model after acute glomerular deposition of nephritogenic antibodies, after severe IRI or in chronic kidney injury induced by earlier exposure to aristolochic acid [136,140]. An ongoing progressive injury without phases of regeneration, but continuous exposure to the tissue damaging insult may also limit the ability of Ackr2 to sufficiently degrade pro-inflammatory chemokines. This is illustrated by comparable renal chemokine levels and renal injury in WT and Ackr2-/- mice following irreversible UUO, which leads to progressive tubular injury, inflammation and fibrotic remodeling [136].

6.4 Systemic anti-inflammatory effects of Ackr2 in B6lpr mice

Despite comparable local chemokine levels in kidney and lung of WT- and Ackr2-/-B6lpr mice lymphocyte infiltrates were increased in these organs when Ackr2 was lacking. Numbers of CD4+ T cells were also higher in spleens of Ackr2-deficient B6lpr mice. The reason for this enhanced accumulation of T and B cells is not entirely clear. However, systemic plasma CCL2 levels were increased in Ackr2-/-B6lpr mice compared to the WT-B6lpr group. Elevated plasma CCL2 levels in Ackr2-deficient mice have been reported in previous studies, and these may facilitate mobilization of leukocytes including T cells from the bone marrow into the

circulation and peripheral tissue [129,136,140]. Consistently, mice deficient for the CCL2 receptor CCR2 showed an opposite phenotype, with reduced CCR2-mediated leukocyte emigration from the bone marrow into blood [173]. An alternative mechanism promoting tissue infiltration of lymphocytes in Ackr2-deficient B6lpr mice may be the loss of chemokine scavenging by cell-autonomous lymphocyte-expressed Ackr2 that would facilitate their activation by pro-inflammatory chemokines [120,122]. Ackr2 may be less prominently expressed by neutrophils, macrophages and DCs, which may explain unaltered organ infiltration of these leukocyte subtypes into organs of Ackr2-/- deficient B6lpr mice. To further investigate these mechanisms leukocyte-specific Ackr2 knockout mice need to be investigated after cross-breeding with lupus-prone mouse strains.

6.5 Effects of Ackr2 on systemic autoimmune activity in B6lpr mice

The expression of ACKR2 on lymphatic endothelial cells affects innate and adaptive immunity. Ackr2 plays a crucial role in scavenging pro-inflammatory chemokines on lymphatic endothelial surfaces and facilitating the migration of antigen-presenting cells to regional lymph nodes, guaranteeing effective adaptive immune responses [163,177]. Liu et al. [128] reported that Ackr2-deficient mice were protected in the EAE model, which contradicted previous studies that described increased inflammatory activity in the Ackr2-/- genotype. The unexpected observation could be explained due to impaired T-cell priming resulting from reduced migration of activated DCs to draining lymph nodes caused by uncontrolled inflammation at the immunization site of Ackr2-deficient mice. However, Ackr2 deficient mice were recently associated also with a deteriorated EAE phenotype when mice were immunized with entire protein instead of encephalitogenic peptide. This suggested that Ackr2 may also be a potential regulator in T cell polarization [130]. Nevertheless, reduced accumulation of activated DCs with subsequently impaired T cell priming in draining lymph nodes has also been reported in other disease models, including previous work from the own group in the NTN model [140,163]. In line with this data the current study demonstrated reduced numbers of DCs, including activated DCs in lymph node tissue, but not the spleen of Ackr2-/-B6lpr mice compared to WT-B6lpr mice. The number of activated lymph node T cells was not different in both genotypes, but in spleen CD3+CD4+ T cells, their activated fraction and CD25+ regulatory CD3+CD4+ T cells significantly increased. Thus, as in other models Ackr2-deficiency reduced DC accumulation and blunted T cell activation in lymph node tissue in B6lpr mice, without affecting leukocyte numbers in spleen. However, with apparently intact

systemic autoimmune activity in spleens the extent of lymphoproliferation was not different in WT- and Ackr2-/-B6lpr mice, as evidenced by comparable splenomegaly and total lymph node weight in both genotypes. Consistently, the systemic humoral immune response was similar in Ackr2-/-B6lpr mice as compared to WT-B6lpr mice with comparable circulating autoantibody levels and glomerular deposition of IgG-containing immune complexes. Thus, systemic cellular and humoral autoimmune activity was not substantially altered in Ackr2-deficient B6lpr mice, leading to comparable immune-mediated kidney injury in WT- and Ackr2-/-B6lpr mice.

6.6 Limitations of the study

There are several limitations of this study. Firstly, the pathophysiology of SLE is complex and none of the current mouse models can be completely representative of human lupus, both in clinical manifestations, underlying pathogenesis, and genetics. Thus, B6lpr mice model mechanisms that may be present in a limited subset of human lupus patients.

Secondly, SLE is thought to be a multi-genetic disorder. There is not a single genetic defect for SLE that is present in all lupus patients and one individual gene is not sufficient to exacerbate or improve disease severity.

Third, SLE can be associated with little or fatal autoimmune tissue damage [178]. However, B6lpr mice do not develop major tissue injury and only mild glomerulonephritis until 24 weeks of age, despite significant lymphoproliferation leading to splenomegaly and prominent lymph node enlargement [179]. Due to the progressive lymphadenopathy duration of our observation was limited to 28 weeks. This could possibly mask further long-term effects, such as glomerulosclerosis and more severe tubulointerstitial fibrosis, which were not evident at the endpoint of this study. For this, other lupus-prone mouse strains with more severe organ injury like MRLlpr mice should be investigated, but this would require crossbreeding of Ackr2-/- mice on the respective genetic background for several generations.

Forth, group sizes of mice in this study were limited. Individual lupus mice vary from each other significantly, resulting in less power to determine differences between groups despite some high trends in individual mice.

Fifth, global Ackr2 knockout mice were used in this study. This did not allow for tissue or cell-specific investigation of Ackr2 functions in SLE and lupus nephritis. Studies with Ackr2-deficient B6lpr bone marrow chimeras could have possibly identified parenchymal (e.g. lymphatic endothelial cell-mediated) and leukocyte-dependent Ackr2 functions. Moreover, leukocyte subtype-specific Ackr2 deletion, e.g. in macrophages, DCs, T or B cells could show specific roles of Ackr2 in these cell populations.

Finally, it would be interesting to further investigate whether a loss-of-function mutation of the Ackr2 gene is a genetic risk factor for lung involvement in SLE. Pulmonary function tests, which are feasible in mice [175], could be performed to investigate any association of reduced pulmonary function with increased peribronchial lymphocyte infiltrates seen in Ackr2-deficient B6lpr mice. If this was true, SLE-associated lung injury could be improved by the administration of recombinant Ackr2 or other Ackr2 agonists.

7. Conclusions

The results of the presented study provide limited evidence for a potential immune suppressive role of Ackr2 in SLE or a nephroprotective function for this atypical chemokine receptor in lupus nephritis. Importantly, the data reveal that chemokine scavenging activity of Ackr2 is redundant in kidney and lung tissue of lupus-prone B6lpr mice. Unaltered pro-inflammatory chemokine levels in these organs suggest compensatory mechanisms that sufficiently limit local chemokine concentrations in Ackr2-deficient B6lpr mice. This is in contrast to the presented *in vitro* findings that demonstrate impaired chemokine clearance by tubulointerstitial tissue from Ackr2-/-B6lp mice upon acute stimulation with TNFα, and to previously reported *in vivo* data that revealed increased parenchymal chemokine levels in Ackr2-deficient mice with exacerbated nephrotoxic nephritis and IRI. In contrast to the continuous, slowly progressive autoimmune injury in B6lpr mice these models are characterized by acute injury which induces renal disease. Therefore, Ackr2-dependent chemokine scavenging activity may be critical to down-regulate inflammation in the regeneration phase after more severe acute injury, but can be sufficiently compensated by alternative mechanisms in chronic disease with ongoing low-grade inflammation as it is present in lupus-like disease in B6lpr mice. Therefore, Ackr2-deficiency did not result in increased inflammation and organ injury in B6lpr mice.

Of note, Ackr2 deficiency did alter some aspects of systemic inflammatory and autoimmune activity in B6lpr mice. As in other disease models, CCL2 plasma concentrations increased in Ackr2-/-B6lpr mice suggesting a lack of systemic chemokine scavenging activity. This can facilitate mobilization of leukocytes, including T cells, from the bone marrow into the circulation and peripheral tissue and may contribute to the increased accumulation of T cells observed in Ackr2-deficient B6lpr kidneys and lungs. Although not investigated in this study, cell-autonomous regulation of lymphocyte infiltration due to lack of T cell-expressed Ackr2 may also enhance tissue accumulation of these cells. With the absence of increased organ infiltration by other effector leukocyte subsets like neutrophils, macrophages, and DCs this did, however, not lead to more severe inflammation and tissue injury.

In addition, Ackr2 may facilitate efflux of activated DCs into regional lymph nodes and subsequent T cell activation, as suggested by decreased numbers of DCs in lymph node tissue of Ackr2-/-B6lpr mice. Instead, abundance of DCs in spleens was comparable in both genotypes. This correlated with blunted T cell activation in lymph node tissue, as numbers of activated CD4+ T cells were similar in lymph nodes, but significantly increased in spleens of

Ackr2-deficient B6lpr mice. However, cellular and humoral autoimmune activity was not compromised in Ackr2-/-B6lpr mice, as indicated by increased numbers of T cells in spleen, greater accumulation of lymphocytes in kidney and lung, and comparable circulating autoantibody levels.

In conclusion, this study suggests that ACKR2 has no major role in controlling autoimmune activity or inflammatory tissue injury including lupus nephritis in lupus-prone B6lpr mice. Thus, in contrast to previous work that identified AKCR2 as a potential target for agonistic therapies to limit renal disease following acute episodes of injury its therapeutic potential in chronic autoimmune disease is limited.

8. References

1. Stojan G, Petri M. Epidemiology of systemic lupus erythematosus: an update. Curr Opin Rheumatol. 2018 Mar;30(2):144-150.
2. Perl A, Fernandez DR, Telarico T, Doherty E, Francis L, Phillips PE. T-cell and B-cell signaling biomarkers and treatment targets in lupus. Curr Opin Rheumatol. 2009;21(5):454-64.
3. Sawada T, Fujimori D, Yamamoto Y. Systemic lupus erythematosus and immunodeficiency. Immunol Med. 2019 Mar;42(1):1-9.
4. Tsokos GC. Systemic lupus erythematosus. N Engl J Med. 2011 Dec 1;365(22):2110-21.
5. Sozzani S, Del Prete A, Bosisio D. Dendritic cell recruitment and activation in autoimmunity. J Autoimmun. 2017 Dec;85:126-140.
6. Soni C, Perez OA, Voss WN, Pucella JN, Serpas L, Mehl J, Ching KL, Goike J, Georgiou G, Ippolito GC, Sisirak V, Reizis B. Plasmacytoid Dendritic Cells and Type I Interferon Promote Extrafollicular B Cell Responses to Extracellular Self-DNA. Immunity. 2020 Jun 16;52(6):1022-1038 e7.
7. Leylek R, Idoyaga J. The versatile plasmacytoid dendritic cell: Function, heterogeneity, and plasticity. Int Rev Cell Mol Biol. 2019;349:177-211.
8. Bijl M, Reefman E, Horst G, Limburg PC, Kallenberg CG. Reduced uptake of apoptotic cells by macrophages in systemic lupus erythematosus: correlates with decreased serum levels of complement. Ann Rheum Dis. 2006 Jan;65(1):57-63.
9. Li F, Yang Y, Zhu X, Huang L, Xu J. Macrophage Polarization Modulates Development of Systemic Lupus Erythematosus. Cell Physiol Biochem. 2015;37(4):1279-88.
10. Iwata Y, Bostrom EA, Menke J, Rabacal WA, Morel L, Wada T, Kelley VR. Aberrant macrophages mediate defective kidney repair that triggers nephritis in lupus-susceptible mice. J Immunol. 2012 May 1;188(9):4568-80.
11. Nemazee D. Mechanisms of central tolerance for B cells. Nat Rev Immunol. 2017 May;17(5):281-294.
12. Jacobi AM, Zhang J, Mackay M, Aranow C, Diamond B. Phenotypic characterization of autoreactive B cells--checkpoints of B cell tolerance in patients with systemic lupus erythematosus. PLoS One. 2009 Jun 2;4(6):e5776.
13. Mackay F, Schneider P. Cracking the BAFF code. Nat Rev Immunol. 2009 Jul;9(7):491-502.
14. Suarez-Fueyo A, Bradley SJ, Tsokos GC. T cells in Systemic Lupus Erythematosus. Curr Opin Immunol. 2016 Dec;43:32-38.
15. Katsuyama T, Tsokos GC, Moulton VR. Aberrant T Cell Signaling and Subsets in Systemic Lupus Erythematosus. Front Immunol. 2018;9:1088.
16. Linterman MA, Rigby RJ, Wong RK, Yu D, Brink R, Cannons JL, Schwartzberg PL, Cook MC, Walters GD, Vinuesa CG. Follicular helper T cells are required for systemic autoimmunity. J Exp Med. 2009 Mar 16;206(3):561-76.
17. Simpson N, Gatenby PA, Wilson A, Malik S, Fulcher DA, Tangye SG, Manku H, Vyse TJ, Roncador G, Huttley GA, Goodnow CC, Vinuesa CG, Cook MC. Expansion of circulating T cells resembling follicular helper T cells is a fixed phenotype that identifies

a subset of severe systemic lupus erythematosus. Arthritis Rheum. 2010 Jan;62(1):234-44.

18. Albert D, Dunham J, Khan S, Stansberry J, Kolasinski S, Tsai D, Pullman-Mooar S, Barnack F, Striebich C, Looney RJ, Prak ET, Kimberly R, Zhang Y, Eisenberg R. Variability in the biological response to anti-CD20 B cell depletion in systemic lupus erythaematosus. Ann Rheum Dis. 2008 Dec;67(12):1724-31.
19. Mok CC. Current role of rituximab in systemic lupus erythematosus. Int J Rheum Dis. 2015 Feb;18(2):154-63.
20. Arbuckle MR, McClain MT, Rubertone MV, Scofield RH, Dennis GJ, James JA, Harley JB. Development of autoantibodies before the clinical onset of systemic lupus erythematosus. N Engl J Med. 2003 Oct 16;349(16):1526-33.
21. Li X, Ptacek TS, Brown EE, Edberg JC. Fcgamma receptors: structure, function and role as genetic risk factors in SLE. Genes Immun. 2009 Jul;10(5):380-9.
22. Hom G, Graham RR, Modrek B, Taylor KE, Ortmann W, Garnier S, Lee AT, Chung SA, Ferreira RC, Pant PV, Ballinger DG, Kosoy R, Demirci FY, Kamboh MI, Kao AH, Tian C, Gunnarsson I, Bengtsson AA, Rantapaa-Dahlqvist S, Petri M, Manzi S, Seldin MF, Ronnblom L, Syvanen AC, Criswell LA, Gregersen PK, Behrens TW. Association of systemic lupus erythematosus with C8orf13-BLK and ITGAM-ITGAX. N Engl J Med. 2008 Feb 28;358(9):900-9.
23. Parikh SV, Almaani S, Brodsky S, Rovin BH. Update on Lupus Nephritis: Core Curriculum 2020. Am J Kidney Dis. 2020 Aug;76(2):265-281.
24. Elliott MK, Jarmi T, Ruiz P, Xu Y, Holers VM, Gilkeson GS. Effects of complement factor D deficiency on the renal disease of MRL/lpr mice. Kidney Int. 2004 Jan;65(1):129-38.
25. Watanabe H, Garnier G, Circolo A, Wetsel RA, Ruiz P, Holers VM, Boackle SA, Colten HR, Gilkeson GS. Modulation of renal disease in MRL/lpr mice genetically deficient in the alternative complement pathway factor B. J Immunol. 2000 Jan 15;164(2):786-94.
26. De Rosa M, Azzato F, Toblli JE, De Rosa G, Fuentes F, Nagaraja HN, Nash R, Rovin BH. A prospective observational cohort study highlights kidney biopsy findings of lupus nephritis patients in remission who flare following withdrawal of maintenance therapy. Kidney Int. 2018 Oct;94(4):788-794.
27. Malvar A, Pirruccio P, Alberton V, Lococo B, Recalde C, Fazini B, Nagaraja H, Indrakanti D, Rovin BH. Histologic versus clinical remission in proliferative lupus nephritis. Nephrol Dial Transplant. 2017 Aug 1;32(8):1338-1344.
28. Arazi A, Rao DA, Berthier CC, Davidson A, Liu Y, Hoover PJ, Chicoine A, Eisenhaure TM, Jonsson AH, Li S, Lieb DJ, Zhang F, Slowikowski K, Browne EP, Noma A, Sutherby D, Steelman S, Smilek DE, Tosta P, Apruzzese W, Massarotti E, Dall'Era M, Park M, Kamen DL, Furie RA, Payan-Schober F, Pendergraft WF, 3rd, McInnis EA, Buyon JP, Petri MA, Putterman C, Kalunian KC, Woodle ES, Lederer JA, Hildeman DA, Nusbaum C, Raychaudhuri S, Kretzler M, Anolik JH, Brenner MB, Wofsy D, Hacohen N, Diamond B, Accelerating Medicines Partnership in SLEn. The immune cell landscape in kidneys of patients with lupus nephritis. Nat Immunol. 2019 Jul;20(7):902-914.
29. Hahn BH, McMahon MA, Wilkinson A, Wallace WD, Daikh DI, Fitzgerald JD, Karpouzas GA, Merrill JT, Wallace DJ, Yazdany J, Ramsey-Goldman R, Singh K,

Khalighi M, Choi SI, Gogia M, Kafaja S, Kamgar M, Lau C, Martin WJ, Parikh S, Peng J, Rastogi A, Chen W, Grossman JM, American College of R. American College of Rheumatology guidelines for screening, treatment, and management of lupus nephritis. Arthritis Care Res (Hoboken). 2012 Jun;64(6):797-808.

30. Constantin A, Nastase D, Tulba D, Balanescu P, Baicus C. Immunosuppressive therapy of systemic lupus erythematosus associated peripheral neuropathy: A systematic review. Lupus. 2020 Oct;29(12):1509-1519.
31. Weening JJ, D'Agati VD, Schwartz MM, Seshan SV, Alpers CE, Appel GB, Balow JE, Bruijn JA, Cook T, Ferrario F, Fogo AB, Ginzler EM, Hebert L, Hill G, Hill P, Jennette JC, Kong NC, Lesavre P, Lockshin M, Looi LM, Makino H, Moura LA, Nagata M, International Society of Nephrology Working Group on the Classification of Lupus N, Renal Pathology Society Working Group on the Classification of Lupus N. The classification of glomerulonephritis in systemic lupus erythematosus revisited. Kidney Int. 2004 Feb;65(2):521-30.
32. Nadeau JH. Maps of linkage and synteny homologies between mouse and man. Trends Genet. 1989 Mar;5(3):82-6.
33. Mestas J, Hughes CC. Of mice and not men: differences between mouse and human immunology. J Immunol. 2004 Mar 1;172(5):2731-8.
34. Bonecchi R, Galliera E, Borroni EM, Corsi MM, Locati M, Mantovani A. Chemokines and chemokine receptors: an overview. Front Biosci (Landmark Ed). 2009 Jan 1;14(2):540-51.
35. Lopez-Cotarelo P, Gomez-Moreira C, Criado-Garcia O, Sanchez L, Rodriguez-Fernandez JL. Beyond Chemoattraction: Multifunctionality of Chemokine Receptors in Leukocytes. Trends Immunol. 2017 Dec;38(12):927-941.
36. Dyer DP. Understanding the mechanisms that facilitate specificity, not redundancy, of chemokine-mediated leukocyte recruitment. Immunology. 2020 Aug;160(4):336-344.
37. David BA, Kubes P. Exploring the complex role of chemokines and chemoattractants in vivo on leukocyte dynamics. Immunol Rev. 2019 May;289(1):9-30.
38. Wolf M, Moser B. Antimicrobial activities of chemokines: not just a side-effect? Front Immunol. 2012;3:213.
39. Ladikou EE, Chevassut T, Pepper CJ, Pepper AG. Dissecting the role of the CXCL12/CXCR4 axis in acute myeloid leukaemia. Br J Haematol. 2020 Jun;189(5):815-825.
40. Stone MJ, Hayward JA, Huang C, Z EH, Sanchez J. Mechanisms of Regulation of the Chemokine-Receptor Network. Int J Mol Sci. 2017 Feb 7;18(2).
41. Liu H, Cheng Q, Xu DS, Wang W, Fang Z, Xue DD, Zheng Y, Chang AH, Lei YJ. Overexpression of CXCR7 accelerates tumor growth and metastasis of lung cancer cells. Respir Res. 2020 Oct 31;21(1):287.
42. Morein D, Erlichman N, Ben-Baruch A. Beyond Cell Motility: The Expanding Roles of Chemokines and Their Receptors in Malignancy. Front Immunol. 2020;11:952.
43. Dimberg A. Chemokines in angiogenesis. Curr Top Microbiol Immunol. 2010;341:59-80.
44. Ridiandries A, Tan JTM, Bursill CA. The Role of Chemokines in Wound Healing. Int J Mol Sci. 2018 Oct 18;19(10).

45. Mollica Poeta V, Massara M, Capucetti A, Bonecchi R. Chemokines and Chemokine Receptors: New Targets for Cancer Immunotherapy. Front Immunol. 2019;10:379.
46. Lombardi L, Tavano F, Morelli F, Latiano TP, Di Sebastiano P, Maiello E. Chemokine receptor CXCR4: role in gastrointestinal cancer. Crit Rev Oncol Hematol. 2013 Dec;88(3):696-705.
47. Teicher BA, Fricker SP. CXCL12 (SDF-1)/CXCR4 pathway in cancer. Clin Cancer Res. 2010 Jun 1;16(11):2927-31.
48. Liu Q, Li A, Tian Y, Wu JD, Liu Y, Li T, Chen Y, Han X, Wu K. The CXCL8-CXCR1/2 pathways in cancer. Cytokine Growth Factor Rev. 2016 Oct;31:61-71.
49. Zlotnik A, Burkhardt AM, Homey B. Homeostatic chemokine receptors and organ-specific metastasis. Nat Rev Immunol. 2011 Aug 25;11(9):597-606.
50. Muller A, Homey B, Soto H, Ge N, Catron D, Buchanan ME, McClanahan T, Murphy E, Yuan W, Wagner SN, Barrera JL, Mohar A, Verastegui E, Zlotnik A. Involvement of chemokine receptors in breast cancer metastasis. Nature. 2001 Mar 1;410(6824):50-6.
51. Anders HJ, Belemezova E, Eis V, Segerer S, Vielhauer V, Perez de Lema G, Kretzler M, Cohen CD, Frink M, Horuk R, Hudkins KL, Alpers CE, Mampaso F, Schlondorff D. Late onset of treatment with a chemokine receptor CCR1 antagonist prevents progression of lupus nephritis in MRL-Fas(lpr) mice. J Am Soc Nephrol. 2004 Jun;15(6):1504-13.
52. Bignon A, Gaudin F, Hemon P, Tharinger H, Mayol K, Walzer T, Loetscher P, Peuchmaur M, Berrebi D, Balabanian K. CCR1 inhibition ameliorates the progression of lupus nephritis in NZB/W mice. J Immunol. 2014 Feb 1;192(3):886-96.
53. Tesch GH, Maifert S, Schwarting A, Rollins BJ, Kelley VR. Monocyte chemoattractant protein 1-dependent leukocytic infiltrates are responsible for autoimmune disease in MRL-Fas(lpr) mice. J Exp Med. 1999 Dec 20;190(12):1813-24.
54. Vielhauer V, Anders HJ, Perez de Lema G, Luckow B, Schlondorff D, Mack M. Phenotyping renal leukocyte subsets by four-color flow cytometry: characterization of chemokine receptor expression. Nephron Exp Nephrol. 2003;93(2):e63.
55. Zoja C, Liu XH, Donadelli R, Abbate M, Testa D, Corna D, Taraboletti G, Vecchi A, Dong QG, Rollins BJ, Bertani T, Remuzzi G. Renal expression of monocyte chemoattractant protein-1 in lupus autoimmune mice. J Am Soc Nephrol. 1997 May;8(5):720-9.
56. Perez de Lema G, Maier H, Franz TJ, Escribese M, Chilla S, Segerer S, Camarasa N, Schmid H, Banas B, Kalaydjiev S, Busch DH, Pfeffer K, Mampaso F, Schlondorff D, Luckow B. Chemokine receptor Ccr2 deficiency reduces renal disease and prolongs survival in MRL/lpr lupus-prone mice. J Am Soc Nephrol. 2005 Dec;16(12):3592-601.
57. Chow FY, Nikolic-Paterson DJ, Ma FY, Ozols E, Rollins BJ, Tesch GH. Monocyte chemoattractant protein-1-induced tissue inflammation is critical for the development of renal injury but not type 2 diabetes in obese db/db mice. Diabetologia. 2007 Feb;50(2):471-80.
58. Wilkening A, Krappe J, Muhe AM, Lindenmeyer MT, Eltrich N, Luckow B, Vielhauer V. C-C chemokine receptor type 2 mediates glomerular injury and interstitial fibrosis in focal segmental glomerulosclerosis. Nephrol Dial Transplant. 2020 Feb 1;35(2):227-239.

59. Cassini MF, Kakade VR, Kurtz E, Sulkowski P, Glazer P, Torres R, Somlo S, Cantley LG. Mcp1 Promotes Macrophage-Dependent Cyst Expansion in Autosomal Dominant Polycystic Kidney Disease. J Am Soc Nephrol. 2018 Oct;29(10):2471-2481.
60. Nakashima H, Akahoshi M, Shimizu S, Inoue Y, Miyake K, Ninomiya I, Igawa T, Sadanaga A, Otsuka T, Harada M. Absence of association between the MCP-1 gene polymorphism and histological phenotype of lupus nephritis. Lupus. 2004;13(3):165-7.
61. Kulkarni O, Pawar RD, Purschke W, Eulberg D, Selve N, Buchner K, Ninichuk V, Segerer S, Vielhauer V, Klussmann S, Anders HJ. Spiegelmer inhibition of CCL2/MCP-1 ameliorates lupus nephritis in MRL-(Fas)lpr mice. J Am Soc Nephrol. 2007 Aug;18(8):2350-8.
62. Hasegawa H, Kohno M, Sasaki M, Inoue A, Ito MR, Terada M, Hieshima K, Maruyama H, Miyazaki J, Yoshie O, Nose M, Fujita S. Antagonist of monocyte chemoattractant protein 1 ameliorates the initiation and progression of lupus nephritis and renal vasculitis in MRL/lpr mice. Arthritis Rheum. 2003 Sep;48(9):2555-66.
63. Shimizu S, Nakashima H, Masutani K, Inoue Y, Miyake K, Akahoshi M, Tanaka Y, Egashira K, Hirakata H, Otsuka T, Harada M. Anti-monocyte chemoattractant protein-1 gene therapy attenuates nephritis in MRL/lpr mice. Rheumatology (Oxford). 2004 Sep;43(9):1121-8.
64. Balabanian K, Couderc J, Bouchet-Delbos L, Amara A, Berrebi D, Foussat A, Baleux F, Portier A, Durand-Gasselin I, Coffman RL, Galanaud P, Peuchmaur M, Emilie D. Role of the chemokine stromal cell-derived factor 1 in autoantibody production and nephritis in murine lupus. J Immunol. 2003 Mar 15;170(6):3392-400.
65. Jin O, Zhang H, Gu Z, Zhao S, Xu T, Zhou K, Jiang B, Wang J, Zeng X, Sun L. A pilot study of the therapeutic efficacy and mechanism of artesunate in the MRL/lpr murine model of systemic lupus erythematosus. Cell Mol Immunol. 2009 Dec;6(6):461-7.
66. Richard ML, Gilkeson G. Mouse models of lupus: what they tell us and what they don't. Lupus Sci Med. 2018;5(1):e000199.
67. Menke J, Zeller GC, Kikawada E, Means TK, Huang XR, Lan HY, Lu B, Farber J, Luster AD, Kelley VR. CXCL9, but not CXCL10, promotes CXCR3-dependent immune-mediated kidney disease. J Am Soc Nephrol. 2008 Jun;19(6):1177-89.
68. Michael R, Piper K. Non-inpatient costing study. Aust Health Rev. 1991;14(2):127-36.
69. Horuk R. Chemokine receptor antagonists: overcoming developmental hurdles. Nat Rev Drug Discov. 2009 Jan;8(1):23-33.
70. Solari R, Pease JE, Begg M. "Chemokine receptors as therapeutic targets: Why aren't there more drugs?". Eur J Pharmacol. 2015 Jan 5;746:363-7.
71. Proudfoot AE, Bonvin P, Power CA. Targeting chemokines: Pathogens can, why can't we? Cytokine. 2015 Aug;74(2):259-67.
72. Schioppa T, Sozio F, Barbazza I, Scutera S, Bosisio D, Sozzani S, Del Prete A. Molecular Basis for CCRL2 Regulation of Leukocyte Migration. Front Cell Dev Biol. 2020;8:615031.
73. Kohn L, Kohl S, Bowne SJ, Sullivan LS, Kellner U, Daiger SP, Sandgren O, Golovleva I. PITPNM3 is an uncommon cause of cone and cone-rod dystrophies. Ophthalmic Genet. 2010 Sep;31(3):139-40.
74. Novitzky-Basso I, Rot A. Duffy antigen receptor for chemokines and its involvement in patterning and control of inflammatory chemokines. Front Immunol. 2012;3:266.

75. Lu ZH, Wang ZX, Horuk R, Hesselgesser J, Lou YC, Hadley TJ, Peiper SC. The promiscuous chemokine binding profile of the Duffy antigen/receptor for chemokines is primarily localized to sequences in the amino-terminal domain. J Biol Chem. 1995 Nov 3;270(44):26239-45.
76. Rot A. Contribution of Duffy antigen to chemokine function. Cytokine Growth Factor Rev. 2005 Dec;16(6):687-94.
77. Zarbock A, Bishop J, Muller H, Schmolke M, Buschmann K, Van Aken H, Singbartl K. Chemokine homeostasis vs. chemokine presentation during severe acute lung injury: the other side of the Duffy antigen receptor for chemokines. Am J Physiol Lung Cell Mol Physiol. 2010 Mar;298(3):L462-71.
78. Zarbock A, Schmolke M, Bockhorn SG, Scharte M, Buschmann K, Ley K, Singbartl K. The Duffy antigen receptor for chemokines in acute renal failure: A facilitator of renal chemokine presentation. Crit Care Med. 2007 Sep;35(9):2156-63.
79. Rundle CH, Mohan S, Edderkaoui B. Duffy antigen receptor for chemokines regulates post-fracture inflammation. PLoS One. 2013;8(10):e77362.
80. Wan W, Liu Q, Lionakis MS, Marino AP, Anderson SA, Swamydas M, Murphy PM. Atypical chemokine receptor 1 deficiency reduces atherogenesis in ApoE-knockout mice. Cardiovasc Res. 2015 Jun 1;106(3):478-87.
81. Zimmerman PA, Ferreira MU, Howes RE, Mercereau-Puijalon O. Red blood cell polymorphism and susceptibility to Plasmodium vivax. Adv Parasitol. 2013;81:27-76.
82. Smith E, McGettrick HM, Stone MA, Shaw JS, Middleton J, Nash GB, Buckley CD, Ed Rainger G. Duffy antigen receptor for chemokines and CXCL5 are essential for the recruitment of neutrophils in a multicellular model of rheumatoid arthritis synovium. Arthritis Rheum. 2008 Jul;58(7):1968-73.
83. Jenkins BD, Martini RN, Hire R, Brown A, Bennett B, Brown I, Howerth EW, Egan M, Hodgson J, Yates C, Kittles R, Chitale D, Ali H, Nathanson D, Nikolinakos P, Newman L, Monteil M, Davis MB. Atypical Chemokine Receptor 1 (DARC/ACKR1) in Breast Tumors Is Associated with Survival, Circulating Chemokines, Tumor-Infiltrating Immune Cells, and African Ancestry. Cancer Epidemiol Biomarkers Prev. 2019 Apr;28(4):690-700.
84. Maeda S, Kuboki S, Nojima H, Shimizu H, Yoshitomi H, Furukawa K, Miyazaki M, Ohtsuka M. Duffy antigen receptor for chemokines (DARC) expressing in cancer cells inhibits tumor progression by suppressing CXCR2 signaling in human pancreatic ductal adenocarcinoma. Cytokine. 2017 Jul;95:12-21.
85. Wang J, Ou ZL, Hou YF, Luo JM, Shen ZZ, Ding J, Shao ZM. Enhanced expression of Duffy antigen receptor for chemokines by breast cancer cells attenuates growth and metastasis potential. Oncogene. 2006 Nov 16;25(54):7201-11.
86. Zhu Q, Jiang L, Wang X. The expression of Duffy antigen receptor for chemokines by epithelial ovarian cancer decreases growth potential. Oncol Lett. 2017 Jun;13(6):4302-4306.
87. Heesen M, Berman MA, Charest A, Housman D, Gerard C, Dorf ME. Cloning and chromosomal mapping of an orphan chemokine receptor: mouse RDC1. Immunogenetics. 1998 Apr;47(5):364-70.
88. Cancellieri C, Vacchini A, Locati M, Bonecchi R, Borroni EM. Atypical chemokine receptors: from silence to sound. Biochem Soc Trans. 2013 Feb 1;41(1):231-6.

89. Gustavsson M, Wang L, van Gils N, Stephens BS, Zhang P, Schall TJ, Yang S, Abagyan R, Chance MR, Kufareva I, Handel TM. Structural basis of ligand interaction with atypical chemokine receptor 3. Nat Commun. 2017 Jan 18;8:14135.
90. Levoye A, Balabanian K, Baleux F, Bachelerie F, Lagane B. CXCR7 heterodimerizes with CXCR4 and regulates CXCL12-mediated G protein signaling. Blood. 2009 Jun 11;113(24):6085-93.
91. Rajagopal S, Kim J, Ahn S, Craig S, Lam CM, Gerard NP, Gerard C, Lefkowitz RJ. Beta-arrestin- but not G protein-mediated signaling by the "decoy" receptor CXCR7. Proc Natl Acad Sci U S A. 2010 Jan 12;107(2):628-32.
92. Naumann U, Cameroni E, Pruenster M, Mahabaleshwar H, Raz E, Zerwes HG, Rot A, Thelen M. CXCR7 functions as a scavenger for CXCL12 and CXCL11. PLoS One. 2010 Feb 11;5(2):e9175.
93. Streichan SJ, Valentin G, Gilmour D, Hufnagel L. Collective cell migration guided by dynamically maintained gradients. Phys Biol. 2011 Aug;8(4):045004.
94. Sierro F, Biben C, Martinez-Munoz L, Mellado M, Ransohoff RM, Li M, Woehl B, Leung H, Groom J, Batten M, Harvey RP, Martinez AC, Mackay CR, Mackay F. Disrupted cardiac development but normal hematopoiesis in mice deficient in the second CXCL12/SDF-1 receptor, CXCR7. Proc Natl Acad Sci U S A. 2007 Sep 11;104(37):14759-64.
95. Quinn KE, Mackie DI, Caron KM. Emerging roles of atypical chemokine receptor 3 (ACKR3) in normal development and physiology. Cytokine. 2018 Sep;109:17-23.
96. Hao H, Hu S, Chen H, Bu D, Zhu L, Xu C, Chu F, Huo X, Tang Y, Sun X, Ding BS, Liu DP, Hu S, Wang M. Loss of Endothelial CXCR7 Impairs Vascular Homeostasis and Cardiac Remodeling After Myocardial Infarction: Implications for Cardiovascular Drug Discovery. Circulation. 2017 Mar 28;135(13):1253-1264.
97. Ngamsri KC, Muller A, Bosmuller H, Gamper-Tsigaras J, Reutershan J, Konrad FM. The Pivotal Role of CXCR7 in Stabilization of the Pulmonary Epithelial Barrier in Acute Pulmonary Inflammation. J Immunol. 2017 Mar 15;198(6):2403-2413.
98. Banisadr G, Podojil JR, Miller SD, Miller RJ. Pattern of CXCR7 Gene Expression in Mouse Brain Under Normal and Inflammatory Conditions. J Neuroimmune Pharmacol. 2016 Mar;11(1):26-35.
99. Odemis V, Lipfert J, Kraft R, Hajek P, Abraham G, Hattermann K, Mentlein R, Engele J. The presumed atypical chemokine receptor CXCR7 signals through G(i/o) proteins in primary rodent astrocytes and human glioma cells. Glia. 2012 Mar;60(3):372-81.
100. Mazzinghi B, Ronconi E, Lazzeri E, Sagrinati C, Ballerini L, Angelotti ML, Parente E, Mancina R, Netti GS, Becherucci F, Gacci M, Carini M, Gesualdo L, Rotondi M, Maggi E, Lasagni L, Serio M, Romagnani S, Romagnani P. Essential but differential role for CXCR4 and CXCR7 in the therapeutic homing of human renal progenitor cells. J Exp Med. 2008 Feb 18;205(2):479-90.
101. Li S, Fong KW, Gritsina G, Zhang A, Zhao JC, Kim J, Sharp A, Yuan W, Aversa C, Yang XJ, Nelson PS, Feng FY, Chinnaiyan AM, de Bono JS, Morrissey C, Rettig MB, Yu J. Activation of MAPK Signaling by CXCR7 Leads to Enzalutamide Resistance in Prostate Cancer. Cancer Res. 2019 May 15;79(10):2580-2592.

102. Liu K, Wu L, Yuan S, Wu M, Xu Y, Sun Q, Li S, Zhao S, Hua T, Liu ZJ. Structural basis of CXC chemokine receptor 2 activation and signalling. Nature. 2020 Sep;585(7823):135-140.
103. Shi Y, Riese DJ, 2nd, Shen J. The Role of the CXCL12/CXCR4/CXCR7 Chemokine Axis in Cancer. Front Pharmacol. 2020;11:574667.
104. Watanabe K, Penfold ME, Matsuda A, Ohyanagi N, Kaneko K, Miyabe Y, Matsumoto K, Schall TJ, Miyasaka N, Nanki T. Pathogenic role of CXCR7 in rheumatoid arthritis. Arthritis Rheum. 2010 Nov;62(11):3211-20.
105. Cruz-Orengo L, Holman DW, Dorsey D, Zhou L, Zhang P, Wright M, McCandless EE, Patel JR, Luker GD, Littman DR, Russell JH, Klein RS. CXCR7 influences leukocyte entry into the CNS parenchyma by controlling abluminal CXCL12 abundance during autoimmunity. J Exp Med. 2011 Feb 14;208(2):327-39.
106. Meyrath M, Reynders N, Uchanski T, Chevigne A, Szpakowska M. Systematic reassessment of chemokine-receptor pairings confirms CCL20 but not CXCL13 and extends the spectrum of ACKR4 agonists to CCL22. J Leukoc Biol. 2021 Feb;109(2):373-376.
107. Comerford I, Milasta S, Morrow V, Milligan G, Nibbs R. The chemokine receptor CCX-CKR mediates effective scavenging of CCL19 in vitro. Eur J Immunol. 2006 Jul;36(7):1904-16.
108. Lucas B, White AJ, Ulvmar MH, Nibbs RJ, Sitnik KM, Agace WW, Jenkinson WE, Anderson G, Rot A. CCRL1/ACKR4 is expressed in key thymic microenvironments but is dispensable for T lymphopoiesis at steady state in adult mice. Eur J Immunol. 2015 Feb;45(2):574-83.
109. Bryce SA, Wilson RA, Tiplady EM, Asquith DL, Bromley SK, Luster AD, Graham GJ, Nibbs RJ. ACKR4 on Stromal Cells Scavenges CCL19 To Enable CCR7-Dependent Trafficking of APCs from Inflamed Skin to Lymph Nodes. J Immunol. 2016 Apr 15;196(8):3341-53.
110. Ulvmar MH, Werth K, Braun A, Kelay P, Hub E, Eller K, Chan L, Lucas B, Novitzky-Basso I, Nakamura K, Rulicke T, Nibbs RJ, Worbs T, Forster R, Rot A. The atypical chemokine receptor CCRL1 shapes functional CCL21 gradients in lymph nodes. Nat Immunol. 2014 Jul;15(7):623-30.
111. Kara EE, Bastow CR, McKenzie DR, Gregor CE, Fenix KA, Babb R, Norton TS, Zotos D, Rodda LB, Hermes JR, Bourne K, Gilchrist DS, Nibbs RJ, Alsharifi M, Vinuesa CG, Tarlinton DM, Brink R, Hill GR, Cyster JG, Comerford I, McColl SR. Atypical chemokine receptor 4 shapes activated B cell fate. J Exp Med. 2018 Mar 5;215(3):801-813.
112. Whyte CE, Osman M, Kara EE, Abbott C, Foeng J, McKenzie DR, Fenix KA, Harata-Lee Y, Foyle KL, Boyle ST, Kochetkova M, Aguilera AR, Hou J, Li XY, Armstrong MA, Pederson SM, Comerford I, Smyth MJ, McColl SR. ACKR4 restrains antitumor immunity by regulating CCL21. J Exp Med. 2020 Jun 1;217(6).
113. Lokeshwar BL, Kallifatidis G, Hoy JJ. Atypical chemokine receptors in tumor cell growth and metastasis. Adv Cancer Res. 2020;145:1-27.
114. Sjoberg E, Meyrath M, Chevigne A, Ostman A, Augsten M, Szpakowska M. The diverse and complex roles of atypical chemokine receptors in cancer: From molecular biology to clinical relevance and therapy. Adv Cancer Res. 2020;145:99-138.

115. Harata-Lee Y, Turvey ME, Brazzatti JA, Gregor CE, Brown MP, Smyth MJ, Comerford I, McColl SR. The atypical chemokine receptor CCX-CKR regulates metastasis of mammary carcinoma via an effect on EMT. Immunol Cell Biol. 2014 Nov;92(10):815-24.
116. Comerford I, Nibbs RJ, Litchfield W, Bunting M, Harata-Lee Y, Haylock-Jacobs S, Forrow S, Korner H, McColl SR. The atypical chemokine receptor CCX-CKR scavenges homeostatic chemokines in circulation and tissues and suppresses Th17 responses. Blood. 2010 Nov 18;116(20):4130-40.
117. Daiyasu H, Nemoto W, Toh H. Evolutionary Analysis of Functional Divergence among Chemokine Receptors, Decoy Receptors, and Viral Receptors. Front Microbiol. 2012;3:264.
118. Blackburn PE, Simpson CV, Nibbs RJ, O'Hara M, Booth R, Poulos J, Isaacs NW, Graham GJ. Purification and biochemical characterization of the D6 chemokine receptor. Biochem J. 2004 Apr 15;379(Pt 2):263-72.
119. Martinez de la Torre Y, Buracchi C, Borroni EM, Dupor J, Bonecchi R, Nebuloni M, Pasqualini F, Doni A, Lauri E, Agostinis C, Bulla R, Cook DN, Haribabu B, Meroni P, Rukavina D, Vago L, Tedesco F, Vecchi A, Lira SA, Locati M, Mantovani A. Protection against inflammation- and autoantibody-caused fetal loss by the chemokine decoy receptor D6. Proc Natl Acad Sci U S A. 2007 Feb 13;104(7):2319-24.
120. Hansell CA, Schiering C, Kinstrie R, Ford L, Bordon Y, McInnes IB, Goodyear CS, Nibbs RJ. Universal expression and dual function of the atypical chemokine receptor D6 on innate-like B cells in mice. Blood. 2011 May 19;117(20):5413-24.
121. Bordon Y, Hansell CA, Sester DP, Clarke M, Mowat AM, Nibbs RJ. The atypical chemokine receptor D6 contributes to the development of experimental colitis. J Immunol. 2009 Apr 15;182(8):5032-40.
122. McKimmie CS, Fraser AR, Hansell C, Gutierrez L, Philipsen S, Connell L, Rot A, Kurowska-Stolarska M, Carreno P, Pruenster M, Chu CC, Lombardi G, Halsey C, McInnes IB, Liew FY, Nibbs RJ, Graham GJ. Hemopoietic cell expression of the chemokine decoy receptor D6 is dynamic and regulated by GATA1. J Immunol. 2008 Dec 1;181(11):8171-81.
123. Bazzan E, Saetta M, Turato G, Borroni EM, Cancellieri C, Baraldo S, Savino B, Calabrese F, Ballarin A, Balestro E, Mantovani A, Cosio MG, Bonecchi R, Locati M. Expression of the atypical chemokine receptor D6 in human alveolar macrophages in COPD. Chest. 2013 Jan;143(1):98-106.
124. Bonavita O, Mollica Poeta V, Setten E, Massara M, Bonecchi R. ACKR2: An Atypical Chemokine Receptor Regulating Lymphatic Biology. Front Immunol. 2016;7:691.
125. Blanton RA, Perez-Reyes N, Merrick DT, McDougall JK. Epithelial cells immortalized by human papillomaviruses have premalignant characteristics in organotypic culture. Am J Pathol. 1991 Mar;138(3):673-85.
126. Borroni EM, Cancellieri C, Vacchini A, Benureau Y, Lagane B, Bachelerie F, Arenzana-Seisdedos F, Mizuno K, Mantovani A, Bonecchi R, Locati M. beta-arrestin-dependent activation of the cofilin pathway is required for the scavenging activity of the atypical chemokine receptor D6. Sci Signal. 2013 Apr 30;6(273):ra30 1-11, S1-3.
127. Graham GJ, Locati M. Regulation of the immune and inflammatory responses by the 'atypical' chemokine receptor D6. J Pathol. 2013 Jan;229(2):168-75.

128. Liu L, Graham GJ, Damodaran A, Hu T, Lira SA, Sasse M, Canasto-Chibuque C, Cook DN, Ransohoff RM. Cutting edge: the silent chemokine receptor D6 is required for generating T cell responses that mediate experimental autoimmune encephalomyelitis. J Immunol. 2006 Jul 1;177(1):17-21.
129. Savino B, Castor MG, Caronni N, Sarukhan A, Anselmo A, Buracchi C, Benvenuti F, Pinho V, Teixeira MM, Mantovani A, Locati M, Bonecchi R. Control of murine Ly6C(high) monocyte traffic and immunosuppressive activities by atypical chemokine receptor D6. Blood. 2012 May 31;119(22):5250-60.
130. Hansell CA, MacLellan LM, Oldham RS, Doonan J, Chapple KJ, Anderson EJ, Linington C, McInnes IB, Nibbs RJ, Goodyear CS. The atypical chemokine receptor ACKR2 suppresses Th17 responses to protein autoantigens. Immunol Cell Biol. 2015 Feb;93(2):167-76.
131. Vetrano S, Borroni EM, Sarukhan A, Savino B, Bonecchi R, Correale C, Arena V, Fantini M, Roncalli M, Malesci A, Mantovani A, Locati M, Danese S. The lymphatic system controls intestinal inflammation and inflammation-associated Colon Cancer through the chemokine decoy receptor D6. Gut. 2010 Feb;59(2):197-206.
132. Sjoberg E, Meyrath M, Milde L, Herrera M, Lovrot J, Hagerstrand D, Frings O, Bartish M, Rolny C, Sonnhammer E, Chevigne A, Augsten M, Ostman A. A Novel ACKR2-Dependent Role of Fibroblast-Derived CXCL14 in Epithelial-to-Mesenchymal Transition and Metastasis of Breast Cancer. Clin Cancer Res. 2019 Jun 15;25(12):3702-3717.
133. Hansell CAH, Fraser AR, Hayes AJ, Pingen M, Burt CL, Lee KM, Medina-Ruiz L, Brownlie D, Macleod MKL, Burgoyne P, Wilson GJ, Nibbs RJB, Graham GJ. The Atypical Chemokine Receptor Ackr2 Constrains NK Cell Migratory Activity and Promotes Metastasis. J Immunol. 2018 Oct 15;201(8):2510-2519.
134. Bonventre JV, Yang L. Cellular pathophysiology of ischemic acute kidney injury. J Clin Invest. 2011 Nov;121(11):4210-21.
135. Lovisa S, Zeisberg M, Kalluri R. Partial Epithelial-to-Mesenchymal Transition and Other New Mechanisms of Kidney Fibrosis. Trends Endocrinol Metab. 2016 Oct;27(10):681-695.
136. Lux M, Blaut A, Eltrich N, Bideak A, Muller MB, Hoppe JM, Grone HJ, Locati M, Vielhauer V. The Atypical Chemokine Receptor 2 Limits Progressive Fibrosis after Acute Ischemic Kidney Injury. Am J Pathol. 2019 Feb;189(2):231-247.
137. Anders HJ, Vielhauer V, Kretzler M, Cohen CD, Segerer S, Luckow B, Weller L, Grone HJ, Schlondorff D. Chemokine and chemokine receptor expression during initiation and resolution of immune complex glomerulonephritis. J Am Soc Nephrol. 2001 May;12(5):919-31.
138. Eller K, Rosenkranz AR. Atypical chemokine receptors-"chemokine PACMANs" as new therapeutic targets in glomerulonephritis. Kidney Int. 2018 Apr;93(4):774-775.
139. Rovin BH, Doe N, Tan LC. Monocyte chemoattractant protein-1 levels in patients with glomerular disease. Am J Kidney Dis. 1996 May;27(5):640-6.
140. Bideak A, Blaut A, Hoppe JM, Muller MB, Federico G, Eltrich N, Grone HJ, Locati M, Vielhauer V. The atypical chemokine receptor 2 limits renal inflammation and fibrosis in murine progressive immune complex glomerulonephritis. Kidney Int. 2018 Apr;93(4):826-841.

141. Donate-Correa J, Luis-Rodriguez D, Martin-Nunez E, Tagua VG, Hernandez-Carballo C, Ferri C, Rodriguez-Rodriguez AE, Mora-Fernandez C, Navarro-Gonzalez JF. Inflammatory Targets in Diabetic Nephropathy. J Clin Med. 2020 Feb 7;9(2).
142. Navarro-Gonzalez JF, Mora-Fernandez C, Muros de Fuentes M, Garcia-Perez J. Inflammatory molecules and pathways in the pathogenesis of diabetic nephropathy. Nat Rev Nephrol. 2011 Jun;7(6):327-40.
143. Tesch GH, Pullen N, Jesson MI, Schlerman FJ, Nikolic-Paterson DJ. Combined inhibition of CCR2 and ACE provides added protection against progression of diabetic nephropathy in Nos3-deficient mice. Am J Physiol Renal Physiol. 2019 Dec 1;317(6):F1439-F1449.
144. Lee CP, Nithiyanantham S, Hsu HT, Yeh KT, Kuo TM, Ko YC. ALPK1 regulates streptozotocin-induced nephropathy through CCL2 and CCL5 expressions. J Cell Mol Med. 2019 Nov;23(11):7699-7708.
145. Montalvany-Antonucci CC, Zicker MC, Ferreira AVM, Macari S, Ramos-Junior ES, Gomez RS, Pereira TSF, Madeira MFM, Fukada SY, Andrade I, Jr., Silva TA. High-fat diet disrupts bone remodeling by inducing local and systemic alterations. J Nutr Biochem. 2018 Sep;59:93-103.
146. Fioravante M, Bombassaro B, Ramalho AF, de Moura RF, Haddad-Tovolli R, Solon C, Dragano NR, Vettorazzi JF, Gaspar RS, Ropelle ER, Carneiro EM, Morari J, Velloso LA. Hypothalamic expression of the atypical chemokine receptor ACKR2 is involved in the systemic regulation of glucose tolerance. Biochim Biophys Acta Mol Basis Dis. 2019 Jun 1;1865(6):1126-1137.
147. Zheng S, Coventry S, Cai L, Powell DW, Jala VR, Haribabu B, Epstein PN. Renal Protection by Genetic Deletion of the Atypical Chemokine Receptor ACKR2 in Diabetic OVE Mice. J Diabetes Res. 2016;2016:5362506.
148. Whitehead GS, Wang T, DeGraff LM, Card JW, Lira SA, Graham GJ, Cook DN. The chemokine receptor D6 has opposing effects on allergic inflammation and airway reactivity. Am J Respir Crit Care Med. 2007 Feb 1;175(3):243-9.
149. Honarpisheh M, Foresto-Neto O, Steiger S, Kraft F, Koehler P, von Rauchhaupt E, Potempa J, Adamowicz K, Koziel J, Lech M. Aristolochic acid I determine the phenotype and activation of macrophages in acute and chronic kidney disease. Sci Rep. 2018 Aug 15;8(1):12169.
150. Novitskaya T, McDermott L, Zhang KX, Chiba T, Paueksakon P, Hukriede NA, de Caestecker MP. A PTBA small molecule enhances recovery and reduces postinjury fibrosis after aristolochic acid-induced kidney injury. Am J Physiol Renal Physiol. 2014 Mar 1;306(5):F496-504.
151. Pozdzik AA, Salmon IJ, Debelle FD, Decaestecker C, Van den Branden C, Verbeelen D, Deschodt-Lanckman MM, Vanherweghem JL, Nortier JL. Aristolochic acid induces proximal tubule apoptosis and epithelial to mesenchymal transformation. Kidney Int. 2008 Mar;73(5):595-607.
152. Reich B, Schmidbauer K, Rodriguez Gomez M, Johannes Hermann F, Gobel N, Bruhl H, Ketelsen I, Talke Y, Mack M. Fibrocytes develop outside the kidney but contribute to renal fibrosis in a mouse model. Kidney Int. 2013 Jul;84(1):78-89.
153. Braga TT, Correa-Costa M, Silva RC, Cruz MC, Hiyane MI, da Silva JS, Perez KR, Cuccovia IM, Camara NOS. CCR2 contributes to the recruitment of monocytes and

leads to kidney inflammation and fibrosis development. Inflammopharmacology. 2018 Apr;26(2):403-411.

154. Smirnov A, Pohlmann S, Nehring M, Ali S, Mann-Nuttel R, Scheu S, Antoni AC, Hansen W, Buettner M, Gardiasch MJ, Westendorf AM, Wirsdorfer F, Pastille E, Dudda M, Flohe SB. Sphingosine 1-Phosphate- and C-C Chemokine Receptor 2-Dependent Activation of CD4(+) Plasmacytoid Dendritic Cells in the Bone Marrow Contributes to Signs of Sepsis-Induced Immunosuppression. Front Immunol. 2017;8:1622.
155. Winter C, Herbold W, Maus R, Langer F, Briles DE, Paton JC, Welte T, Maus UA. Important role for CC chemokine ligand 2-dependent lung mononuclear phagocyte recruitment to inhibit sepsis in mice infected with Streptococcus pneumoniae. J Immunol. 2009 Apr 15;182(8):4931-7.
156. Graham GJ. D6 and the atypical chemokine receptor family: novel regulators of immune and inflammatory processes. Eur J Immunol. 2009 Feb;39(2):342-51.
157. Nibbs RJ, Gilchrist DS, King V, Ferra A, Forrow S, Hunter KD, Graham GJ. The atypical chemokine receptor D6 suppresses the development of chemically induced skin tumors. J Clin Invest. 2007 Jul;117(7):1884-92.
158. Castanheira F, Borges V, Sonego F, Kanashiro A, Donate PB, Melo PH, Pallas K, Russo RC, Amaral FA, Teixeira MM, Ramalho FS, Cunha TM, Liew FY, Alves-Filho JC, Graham GJ, Cunha FQ. The Atypical Chemokine Receptor ACKR2 is Protective Against Sepsis. Shock. 2018 Jun;49(6):682-689.
159. Austin HA, 3rd, Muenz LR, Joyce KM, Antonovych TT, Balow JE. Diffuse proliferative lupus nephritis: identification of specific pathologic features affecting renal outcome. Kidney Int. 1984 Apr;25(4):689-95.
160. Sadanaga A, Nakashima H, Akahoshi M, Masutani K, Miyake K, Igawa T, Sugiyama N, Niiro H, Harada M. Protection against autoimmune nephritis in MyD88-deficient MRL/lpr mice. Arthritis Rheum. 2007 May;56(5):1618-28.
161. Takemoto M, Asker N, Gerhardt H, Lundkvist A, Johansson BR, Saito Y, Betsholtz C. A new method for large scale isolation of kidney glomeruli from mice. Am J Pathol. 2002 Sep;161(3):799-805.
162. Abozaid MA, Ahmed GH, Tawfik NM, Sayed SK, Ghandour AM, Madkour RA. Serum and Urine Monocyte Chemoattractant Protein-1 as A Markers for Lupus Nephritis. Egypt J Immunol. 2020 Jan;27(1):97-107.
163. Lee KM, McKimmie CS, Gilchrist DS, Pallas KJ, Nibbs RJ, Garside P, McDonald V, Jenkins C, Ransohoff R, Liu L, Milling S, Cerovic V, Graham GJ. D6 facilitates cellular migration and fluid flow to lymph nodes by suppressing lymphatic congestion. Blood. 2011 Dec 1;118(23):6220-9.
164. McKimmie CS, Singh MD, Hewit K, Lopez-Franco O, Le Brocq M, Rose-John S, Lee KM, Baker AH, Wheat R, Blackbourn DJ, Nibbs RJ, Graham GJ. An analysis of the function and expression of D6 on lymphatic endothelial cells. Blood. 2013 May 2;121(18):3768-77.
165. Lee KM, Danuser R, Stein JV, Graham D, Nibbs RJ, Graham GJ. The chemokine receptors ACKR2 and CCR2 reciprocally regulate lymphatic vessel density. EMBO J. 2014 Nov 3;33(21):2564-80.

166. Di Liberto D, Locati M, Caccamo N, Vecchi A, Meraviglia S, Salerno A, Sireci G, Nebuloni M, Caceres N, Cardona PJ, Dieli F, Mantovani A. Role of the chemokine decoy receptor D6 in balancing inflammation, immune activation, and antimicrobial resistance in Mycobacterium tuberculosis infection. J Exp Med. 2008 Sep 1;205(9):2075-84.
167. Jamieson T, Cook DN, Nibbs RJ, Rot A, Nixon C, McLean P, Alcami A, Lira SA, Wiekowski M, Graham GJ. The chemokine receptor D6 limits the inflammatory response in vivo. Nat Immunol. 2005 Apr;6(4):403-11.
168. Cochain C, Auvynet C, Poupel L, Vilar J, Dumeau E, Richart A, Recalde A, Zouggari Y, Yin KY, Bruneval P, Renault G, Marchiol C, Bonnin P, Levy B, Bonecchi R, Locati M, Combadiere C, Silvestre JS. The chemokine decoy receptor D6 prevents excessive inflammation and adverse ventricular remodeling after myocardial infarction. Arterioscler Thromb Vasc Biol. 2012 Sep;32(9):2206-13.
169. Moulton VR, Tsokos GC. T cell signaling abnormalities contribute to aberrant immune cell function and autoimmunity. J Clin Invest. 2015 Jun;125(6):2220-7.
170. Wahl DR, Petersen B, Warner R, Richardson BC, Glick GD, Opipari AW. Characterization of the metabolic phenotype of chronically activated lymphocytes. Lupus. 2010 Nov;19(13):1492-501.
171. Gergely P, Jr., Grossman C, Niland B, Puskas F, Neupane H, Allam F, Banki K, Phillips PE, Perl A. Mitochondrial hyperpolarization and ATP depletion in patients with systemic lupus erythematosus. Arthritis Rheum. 2002 Jan;46(1):175-90.
172. Ford LB, Cerovic V, Milling SW, Graham GJ, Hansell CA, Nibbs RJ. Characterization of conventional and atypical receptors for the chemokine CCL2 on mouse leukocytes. J Immunol. 2014 Jul 1;193(1):400-11.
173. Fujimura N, Xu B, Dalman J, Deng H, Aoyama K, Dalman RL. CCR2 inhibition sequesters multiple subsets of leukocytes in the bone marrow. Sci Rep. 2015 Jul 24;5:11664.
174. Kulkarni O, Anders HJ. Chemokines in lupus nephritis. Front Biosci. 2008 May 1;13:3312-20.
175. Tavares LP, Garcia CC, Goncalves APF, Kraemer LR, Melo EM, Oliveira FMS, Freitas CS, Lopes GAO, Reis DC, Cassali GD, Machado AM, Mantovani A, Locati M, Teixeira MM, Russo RC. ACKR2 contributes to pulmonary dysfunction by shaping CCL5:CCR5-dependent recruitment of lymphocytes during influenza A infection in mice. Am J Physiol Lung Cell Mol Physiol. 2020 Apr 1;318(4):L655-L670.
176. Russo RC, Savino B, Mirolo M, Buracchi C, Germano G, Anselmo A, Zammataro L, Pasqualini F, Mantovani A, Locati M, Teixeira MM. The atypical chemokine receptor ACKR2 drives pulmonary fibrosis by tuning influx of CCR2(+) and CCR5(+) IFNgamma-producing gammadeltaT cells in mice. Am J Physiol Lung Cell Mol Physiol. 2018 Jun 1;314(6):L1010-L1025.
177. Lee KM, Nibbs RJ, Graham GJ. D6: the 'crowd controller' at the immune gateway. Trends Immunol. 2013 Jan;34(1):7-12.
178. Macy DW, Ensley BA, Gillette EL. In vitro susceptibility of canine tumor stem cells to doxorubicin. Am J Vet Res. 1988 Nov;49(11):1903-5.
179. Cohen PL, Eisenberg RA. Lpr and gld: single gene models of systemic autoimmunity and lymphoproliferative disease. Annu Rev Immunol. 1991;9:243-69.

9. Abbreviations

ACKR	Atypical chemokine receptors
AAN	Aristolochic acid nephropathy
BUN	Blood urea nitrogen
CCL	Chemokine ligand
CCR	Chemokine receptor
CD	Cluster of differentiation
cDNA	Complementary DNA
CKD	Chronic kidney disease
CLP	Cecal ligation and puncture
CXCL	C-X-C motif chemokine ligand
CTGF	Connective tissue growth factor
DN	Diabetic nephropathy
NTN	Nephrotoxic serum nephritis
DNA	Deoxyribonucleic acid
dsDNA	Double stranded DNA
EAE	Experimental autoimmune encephalomyelitis
FSP-1	fibroblast-specific protein-1
GPCR	G protein–coupled receptors
IRI	Ischemic reperfusion injury
IHC	Immunohistochemistry staining
IL	Interleukin
kDa	Kilo Dalton
Kim-1	Kidney Injury Molecule-1
LN	Lupus nephritis
mRNA	Messenger RNA
NGAL	Neutrophil gelatinase-associated lipocalin
PAS	Periodic acid-Schiff
PCR	Polymerase chain reaction
RF	Rheumatoid factors
RNA	Ribonucleic acid
RNP	ribonucleoprotein
RT-PCR	Real-time polymerase chain reaction
SLE	Systemic lupus erythematodes
Sm	Smith antigen
TGF	transforming growth factor
TLR	Toll like receptor
TNF-α	Tumor necrosis factor-alpha
UACR	Urinary albumin-creatinine ratio
UUO	Unilateral ureteral obstruction
WT	Wildtype
α-SMA	Alpha smooth muscle actin

10. List of tables

11. List of figures

12. Acknowledgements

There are many colleagues who have helped and inspired me during my doctoral study. I would like to convey my sincere gratitude to all of them.

First and foremost, I would like to express my gratitude and appreciation to my supervisor Prof. Dr. Volker Vielhauer. Thank you very much for giving me the opportunity to study and work at Medizinische Klinik und Poliklinik IV, Nephrologisches Zentrum, LMU Munich. Thank you for providing careful guidance, constructive suggestion, professional vision for me to proceed through the doctoral program. I would also thank Prof. Dr. Maciej Lech. Thank you for your excellent work in lab organization and management, sharing knowledge and experience to complete my thesis.

I would also express my special thanks to Nuru Eltrich for teaching me skilful technology step by step from the beginning. I thank Dr. Stefanie Steiger and Dr. Julian Marschner for their encouragement of my researcher work. I thank Yvonne Minor, Kerstin Zehentbauer and Michele Wettstein for taking care of my animals. Many thanks to Janina Mandelbaum and Anna Anfimiadou for their technical support on animal histology. And thanks to Sylke Rohrer and Sofia Andrea for providing chemical reagent and technique support. I also thank Thi Dolidze for her attentive secretary work.

I would like to express my sincere thanks to my lab members. I thank Yutian, Qiuyue, Yao, Manga, Meisi, Zhibo, Chenyu, Danyang, Moritz, Nils, Gergana, Lyuben, Lucas, Sophie and others for their help, love and support. Thank you all for creating a friendly and scientific environment，your enthusiasm and kindness motivated me to embrace life.

I would like to thank the CSC-LMU scholarship for the finical support and for giving me the precise opportunity to study abroad.

I would like to thank all of my friends for their support in my daily life.

Special thanks to my parents for their endless love and support throughout my life. I owe my deepest gratitude and apologize to my maternal grandparents for not being with them, how I wish you were here to witness my doctoral graduation.

13. Affidavit

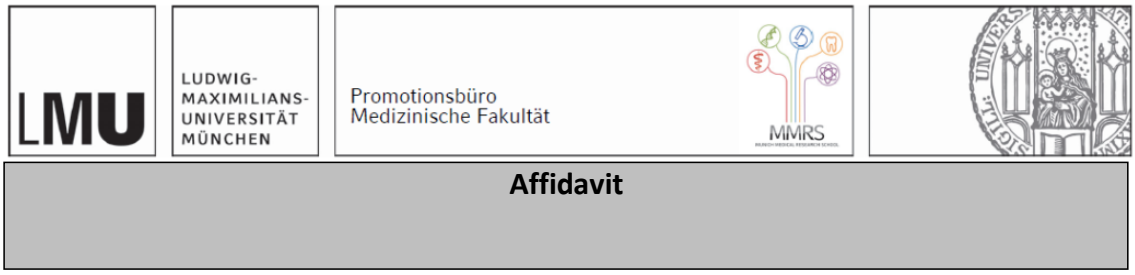

Affidavit

Xia, Wenkai

Surname, first name

Josef-Wirth-Weg-21

Street

80939, Munich, Germany

Zip code, town, country

I hereby declare, that the submitted thesis entitled:

Role of Atypical Chemokine Receptor 2 in Systemic Lupus Erythematous and Lupus Nephritis

is my own work. I have only used the sources indicated and have not made unauthorized use of services of a third party. Where the work of others has been quoted or reproduced, the source is always given.

I further declare that the dissertation presented here has not been submitted in the same or similar form to any other institution for the purpose of obtaining an academic degree.

Munich, 31.Jan.2023 — Place, date

Wenkai Xia — Signature doctoral candidate

14. Publication list

1. **Xia W**, Kuang M, Li C, Yao X, Chen Y, Lin J, Hu H. Prognostic Significance of the Albumin to Fibrinogen Ratio in Peritoneal Dialysis Patients. Front Med (accepted). https://doi.org/10.3389/fmed.2022.820281.
2. **Xia W**, Zhao D, Li C, Xu L, Yao X, Hu H. Prognostic significance of albumin to alkaline phosphatase ratio in critically ill patients with acute kidney injury. (accepted)
3. **Xia W**, Li C, Yao X, Chen Y, Zhang Y, Hu H. Prognostic value of fibrinogen to albumin ratios among critically ill patients with acute kidney injury. Intern Emerg Med. 2021;30:doi:10.1007/s11739-021-02898-3.
4. **Xia W**, Yao X, Chen Y, Lin J, Vielhauer V, Hu H. Elevated TG/HDL-C and non-HDL-C/HDL-C ratios predict mortality in peritoneal dialysis patients. BMC Nephrol. 2020;21(1):324.
5. **Xia WK**, Lin QF, Shen D, Liu ZL, Su J, Mao WD. Clinical implication of long noncoding RNA 91H expression profile in osteosarcoma patients. Onco Targets Ther. 2016;9:4645-52.
6. **Xia WK**, Liu ZL, Shen D, Lin QF, Su J, Mao WD. Prognostic performance of pre-treatment NLR and PLR in patients suffering from osteosarcoma. World J Surg Oncol. 2016;14:127.
7. **Xia WK**, Wu X, Yu TH, Wu Y, Yao XJ, Hu H. Prognostic significance of lymphocyte-to-monocyte ratio and CRP in patients with nonmetastatic clear cell renal cell carcinoma: a retrospective multicenter analysis. Onco Targets Ther. 2016;9:2759-67.
8. **Xia WK**, Lin QF, Shen D, Liu ZL, Su J, Mao WD. Prognostic significance of lymphocyte-to-monocyte ratio in diffuse large B-cell lymphoma: a systematic review and meta-analysis. FEBS Open Bio. 2016;6(6):558-65.
9. **Xia WK**, Wang T, Sun D, Mao W, Xie X. Association of estrogen receptor-beta (ESR2) polymorphism and cancer risk: a meta-analysis. Eur J Gynaecol Oncol. 2016;37(4):530-8.
10. Wan X, **Xia W**, Gendoo Y, Chen W, Sun W, Sun D, Cao C. Upregulation of stromal cell-derived factor 1 (SDF-1) is associated with macrophage infiltration in renal ischemia-reperfusion injury. PLoS One. 2014;9(12):e114564.
11. Xie X, **Xia W**, Fei X, Xu Q, Yang X, Qiu D, Wang M. Relaxin Inhibits High Glucose-Induced Matrix Accumulation in Human Mesangial Cells by Interfering with TGF-beta1 Production and Mesangial Cells Phenotypic Transition. Biol Pharm Bull 2015;38(10):1464-9.